August 2013
Doctorate Thesis

August 2013

Doctorate Thesis

A Study on the Variation of Heavy Snowfall Intensity Associated with the Interaction between Atmosphere and Ocean Surface

A Study on the Variation of Heavy Snowfall Intensity Associated with the Interaction between Atmosphere and Ocean Surface

Graduate School of Chosun University

Department of Atmospheric Sciences

Park, Geon-Young

G.-Y. Park

A Study on the Variation of Heavy Snowfall Intensity Associated with the Interaction between Atmosphere and Ocean Surface

대기-해양 상호작용과 관련된 대설 강도에 관한 연구

23 August, 2013

Graduate School of Chosun University

Department of Atmospheric Sciences

Park, Geon-Young

A Study on the Variation of Heavy Snowfall Intensity Associated with the Interaction between Atmosphere and Ocean Surface

Advisor : Prof. Ryu, Chan-Su, Ph.D.

This thesis submitted in partial fulfillment of
the requirements for the degree of Doctor of Philosophy.

April 2013

Graduate School of Chosun University

Department of Atmospheric Sciences

Park, Geon-Young

박근영의 박사학위 논문을 인준함

위원장 국가태풍센터 센 터 장 이 종 호 (인)

위 원 국립기상연구소 과 장 김 백 조 (인)

위 원 부산대학교 교 수 이 순 환 (인)

위 원 조선대학교 교 수 정 효 상 (인)

위 원 조선대학교 교 수 류 찬 수 (인)

2013년 6월

조선대학교 대학원

CONTENTS

LIST OF TABLES

LIST OF FIGURES

ABSTRACT

A Study on the Variation of Heavy Snowfall Intensity Associated with the Interaction between Atmosphere and Ocean Surface

Geon-young, Park

Advisor : Prof. Ryu, Chan-Su, Ph.D.

Department of Atmospheric Sciences,

Graduate School of Chosun University

With the increase in the sea surface temperature (SST) all over the world and around the Korean Peninsula, the atmosphere-ocean interaction in winter is causing frequent heavy snows along the west and south coasts of Korea. The drop in the number of disasters in winter caused by dangerous meteorological phenomena requires forecasting technology based on the synoptic meteorological analysis and meso-scale numerical simulation model.

In this study, three recent heavy snow cases in the west and south coasts (continental polar air mass, migratory anticyclone and middle latitude cyclone) were analyzed in view of synoptic meteorology, and three types of SST (NCEP/NCAR SST, RTG SST and OSTIA) sensitivity tests were conducted based on weather research and forecasting (WRF) to interpret the influence of the atmosphere-ocean interaction on the snowfall intensity.

The results of the synoptic meteorological analysis showed that when the cold and dry continental high pressure was extended, heavy snow occurred at dawn when the upper atmosphere cooled. In particular, when the continental high pressure was extended and the upper pressure trough passed through, heavy snow occurred due to the convergence region formed in the west coast area, sometimes in the inland of the Honam area. In addition, it was verified that the changes in the humidity coefficients in the upper and lower layers are important data for the determination of the probability, start/end and intensity of heavy snow. However, when the area was

influenced by the middle-latitude low pressure, the heavy snow was influenced by the wind in the lower layer (925 hPa and 850 hPa), the equivalent potential temperature, the convergence field, the moisture convergence and the topography.

SST sensitivity tests were conducted for the two cases of heavy snow in the west and south coasts of Korea (Extension of continental high pressure, 30 December 2010, Case 2010; and Effect of migratory low pressure, 28 December 2012, Case 2012). The results showed that NCEP/NCAR SST was generally balanced by latitude, but OSTIA and RTG SST were distributed along the coastline. Because NCEP/NCAR SST was excessive simulated for the west coast area prior to the SST sensitivity test, the snowfall was also excessive simulated.

In Case 2010 (30 December 2010), OSTIA had the best numerical simulation with diverse atmospheric conditions, and the maximum difference in the numerically simulated snowfall between NCEP/NCAR SST and OSTIA was 20 cm. Although there was a regional difference in the snowfall according to the difference in the SST in the OSTIA and RTG SST numerical tests, it was not as significant as in the previous results. A higher SST led to the numerical simulation of larger snowfall, and the difference was greatest near Buan in the west coast area.

Case 2012 (28 December 2012) had a smaller difference in snowfall according to the SST than Case 2010. However, the numerically simulated snowfall based on NCEP/NCAR SST and OSTIA significantly differed near Jiri Mountain due to the topographical effect, and the difference was 1-2 cm in other areas. In addition, in the sensitivity test with OSTIA and RTG SST, the spatial difference of the snowfall was less than 1 cm. When the low pressure that developed in the south sea passed the Korean Peninsula, it passed through the warm south sea and caused precipitation rather than snowfall, and it did not significantly influence the snowfall after it reached the land. Its influence was also limited to the coastline in the west sea.

Thus, SST was found to be a very important factor of the heavy snowfall in the west and south coasts. In the case of snowfall due to a low atmospheric pressure, it is expected that the snowfall development mechanism will be identified while considering not only the two-dimensional SST distribution but also the topographical factors and the types of precipitation.

CHAPTER Ⅰ. INTRODUCTION

A. Background

Among various types of precipitation in winter, 'rain' type precipitation does not lead to huge damages, while 'snow' type precipitation usually causes tremendous damages especially over eastern part of the Korean Peninsula. Generally, heavy snowfall is defined over 1~3 cm per hour or 5~20cm of snow within 24 hours.

Above heavy snow fall often causes serious trafficway damages on the land, air, and sea, In addition, most damages tends to be concentrated on the urban areas because the facilities and people are densely aggregated in the cities. And its amount of economical and human injuries induced by heavy snowfall tends to increase gradually during this decade (National Institute of Meteorological Research, 2006).

Because, Jeonlla and Chungcheong provinces are situated close to the Yellow Sea and the alteration of cold air mass is often occurred over warm yellow sea, heavy snow fall events are observed frequently.

General heavy snowfall is also associated with the temperature difference between the continent and the ocean, water vapor supply from the sea, orographic effect, and synoptic wind field. Especially, since the Korean Peninsula is surrounded by ocean on three side, snowfall can be formed by various factors such as synoptic wind field, moisture environment, and air-sea interaction.

The 'lake effect' has originally defined by Barny Wiggin who was working in an affiliate laboratory of the National Weather Service in Bufallo city, New York, U.S.A.

According to the observational results of the meteorological phenomenon appeared in the adjacent region of the 5 Great Lakes during winter time, they figured out the mechanism to different snowfall pattern between north and south region of Great Lake. They called the lake effect

was defined as follows: "phenomenon of forming snowfall when the cold and stable air mass passes the relatively warm surface of the sea throughout late autumn through winter".

Almost same snowfall phenomena are also observed at Northern part of Japan and the Chesapeake and the Massachusetts in USA. the snowfall effect between interaction air and sea in Japan and southern USA are called as "ocean effect" and "bay effect", respectively.

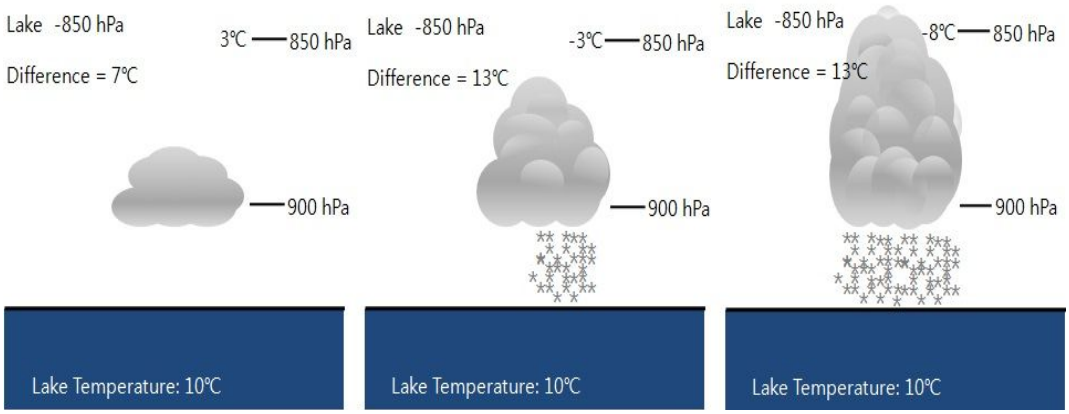

Fig. 1.1. Schematic diagram of snowfall occurrence caused by lake effect.

Same phenomena called as "black stream phenomenon" also occur around the Korean Peninsula. The occurrence of phenomena is mainly caused by the difference between the air temperature and the ocean surface temperature.

Although the Kuroshio Current affects little impacts on the Yellow Sea during winter time, the phenomena often develops by itself to change the weather of the west coast of the Korean Peninsula. Kuroshio Current is relevant to the west boundary current of subtropical circulation at middle-latitude of North Pacific and is a warm current which moves from the low latitude toward high latitude.

Since the color of the seawater is blackish blue, it is said to be called, "Black Stream (Kuroshio)". When the sea color becomes darker and

warmer in the west coast affected by the Kuroshio warm current during the winter time, the temperature difference between the west sea and Siberia air mass becomes larger and lots of heavy snowfall have occurred in the south and west coast in Korean peninsula due to this phenomenon.

The repetition rate and the occurrence amount of the fresh snow cover was shown in Fig. 1.2 ~ Fig. 1.4 for the past 30 years (1981~ 2010).

The snowfall repetition rate showed to be high in 1985 and 2005 in the Korean Peninsula. The snowfall has showed to be large quantity especially in 2005 and the damages due to heavy snowfall also appeared in a large quantity. With the interval of 5~6 years for the past 30 years, the frequency of the snowfall and the amount of the snowfall appeared in a repetitive pattern (Fig. 1.2).

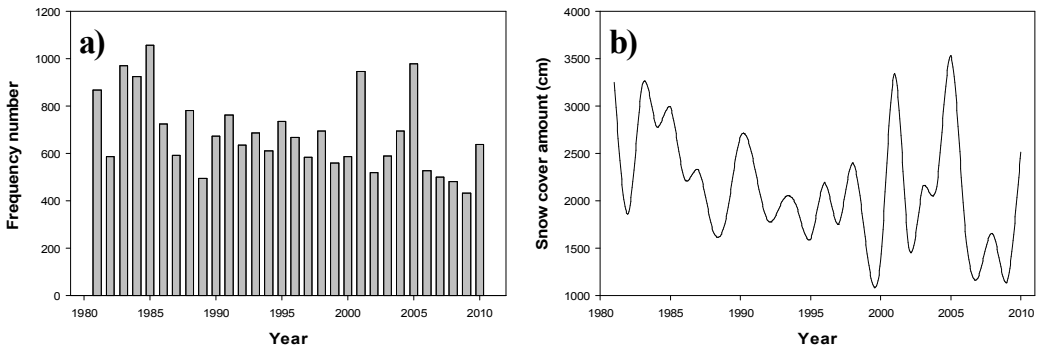

Fig. 1.2. Interannual variations of a) the fresh snowfall frequency and b) amount in Korea based at 59 stations.

According to the research results on the monthly snowfall frequency and snowfall amount, they appeared in a large quantity in January and December when the high atmospheric pressure of Siberia is strong and the southwest sea region is relatively low temperature and thus is much different from the water temperature of the west sea (Kim, 2013).

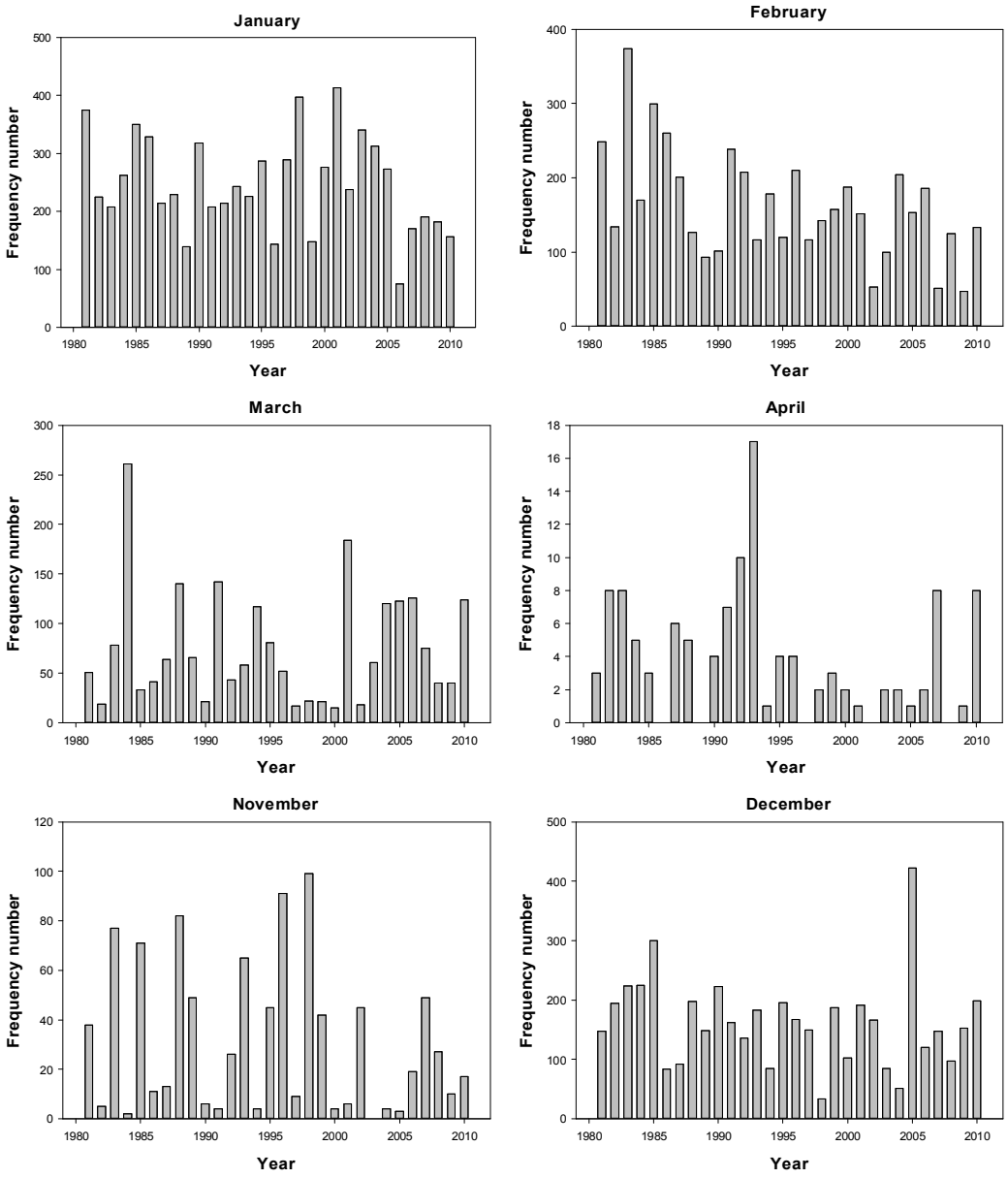

Fig. 1.3. Interannual variations of monthly frequency of fresh snowfall in Korea from January to April and November to December.

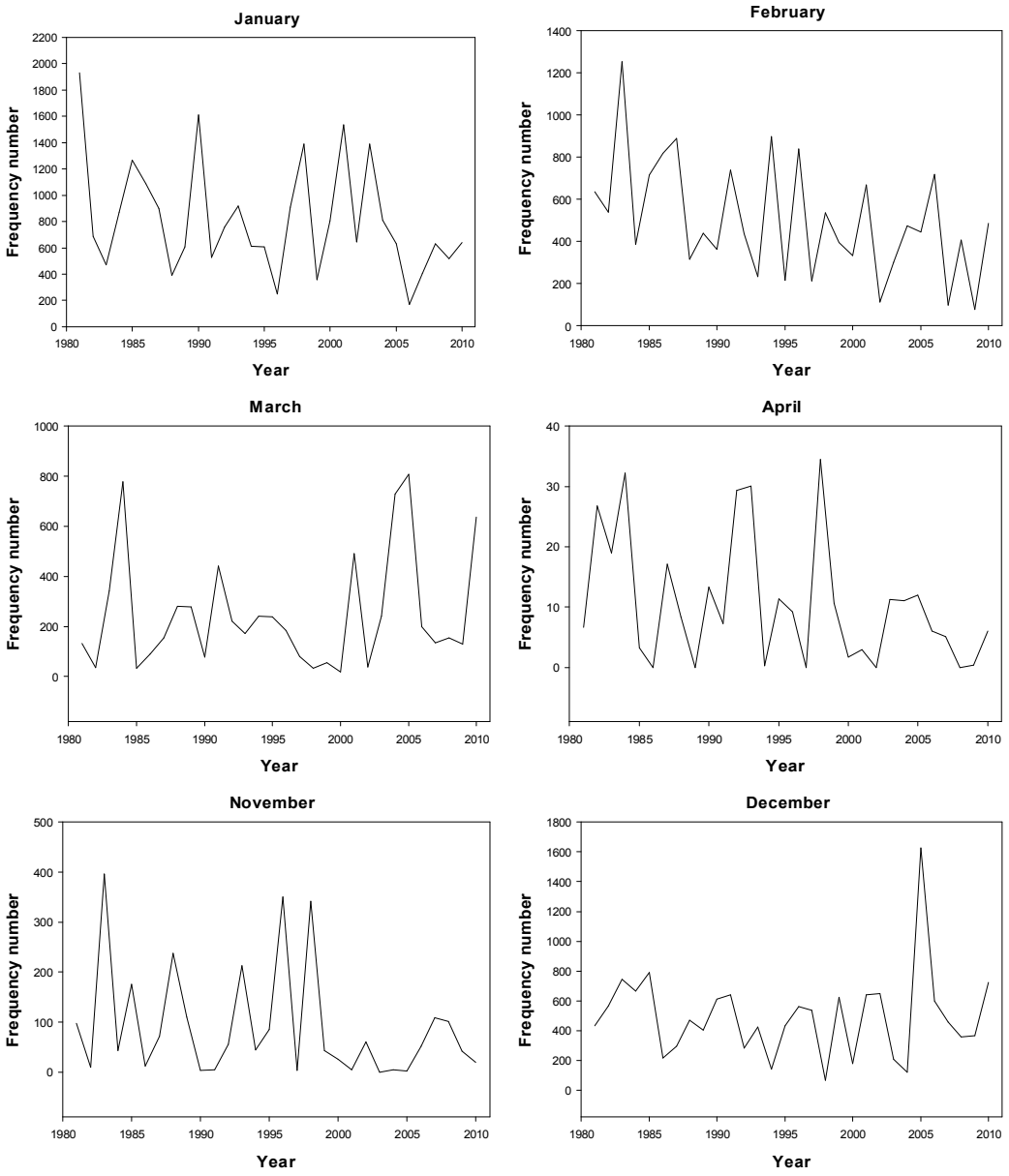

Fig. 1.4. Same as Fig. 1.3 but monthly amount of fresh snowfall.

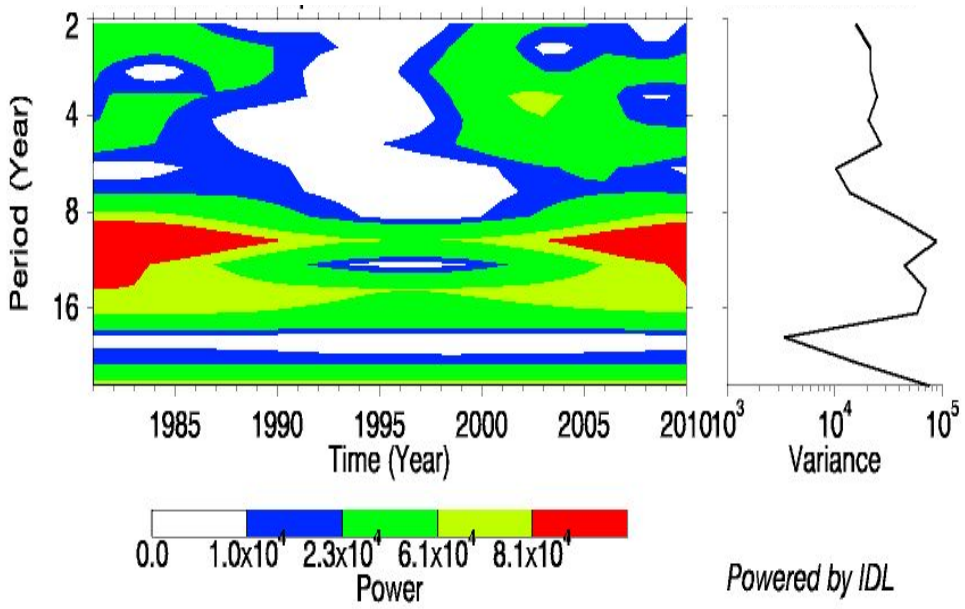

Fig. 1.5. Periodicity of fresh snowfall frequency by using wavelet analysis.

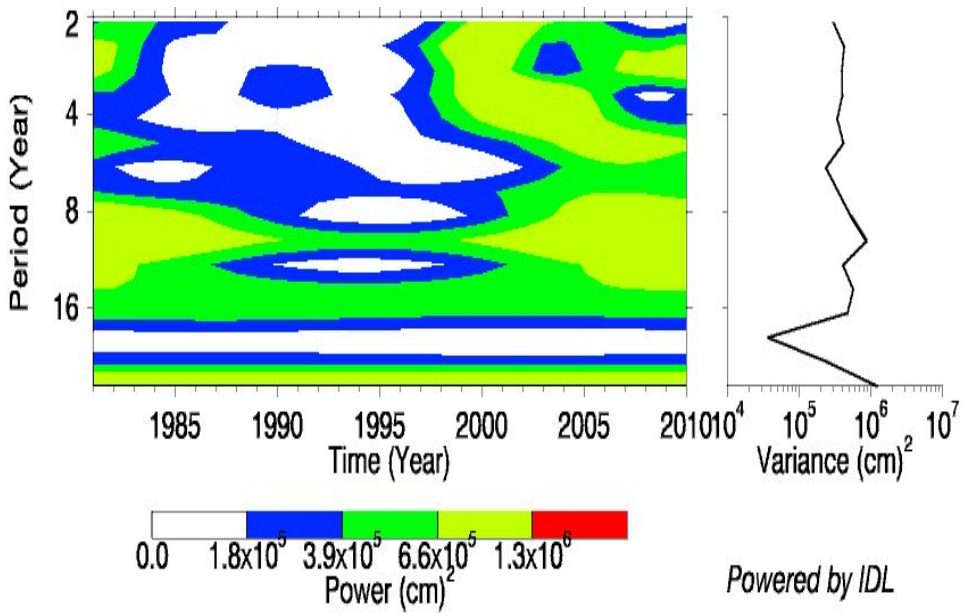

Fig. 1.6. Same as Fig. 1.5 but fresh snowfall amount.

Figs. 1.5 and 1.6 are an analysis of the occurrence cycle of the snowfall through the wavelet analysis about the snowfall day and snowfall amount.

The wavelet analysis is a method which is useful in searching for main change components of irregular time series such as meteorological data (Lee, et al., 2010). The frequency of the snowfall by a unit of 10 years was the most strong in 1980s as 8~12 years. In 2000s also, a cycle of 8~12 years showed to be strong. The dispersion value showed the highest value in the 9 year cycle, and showed a high value in the 12~13 year cycle. The cycle of the snowfall by the unit of 10 years was 8~12 years in 1980s and showed a very weak value in the 1990s. Entering the 2000s, the 8~12 year cycle returned to be very strong again. The dispersion value showed a highest value in the 9 year cycle and showed a high value in 9~10 years cycle. The cycle of the snowfall and the cycle of the snowfall amount showed to be strong around 10 years period or so. The cycle of the snowfall and the snowfall amount increased in 1980s and decreased in 1990s. And then the frequency of the snowfall and the heavy snowfall became frequent entering the 2000s.

Sea is taking an important role in the change of the climate. Sea contains the heat content 1000 times bigger than does the air, And the air that the sea has received purely since 1960s is 20 times bigger than the heat absorption amount by the air (Levitus *et al.,* 2005a). This big amount of heat is generally stored in the upper part of the sea and does a determinative role in the climate change, especially in the change with the 10-year cycle of time size from the seasonal change.

The sea is becoming warm. The temperature of the whole global sea has increased by 0.10℃ for part from the surface to the water level of 700m within the time frame between 1961 and 2003. According to the 3rd assessment report of IPCC, the heat content (0~3,000m) of the whole global sea has increased steadily for the same period of time, and that increasing value corresponds to the energy absorption at an average rate

of 0.21 ± 0.04 W/m2 throughout the whole global surface. Two third of this energy was absorbed in the region of between the sea surface and the water level of 700m. The observation result about the whole sea heat content showed that a several tens of cycles of change is overlapped in a large quantity with the inter annual variability on the long term trend. It was reported that the warming speed was faster during the period of 1993~2003 than the period of 1961~2003, but there was a light cooling since 2003 (IPCC, 2007). Fig. 1.7 predicted the change of the sea surface temperature by way of the RCP 2 scenario, the future climate change scenario. In the fifth IPCC assessment result, the greenhouse gas density was decided by the way of the amount of radiation that the Honam activity affects to the air. In the meaning that the society-economy scenario can be various things about the one representative radioactive forcing, the expression 'Representative' was used. And, in order to emphasize the change according to the time of the greenhouse gas emission scenario, the meaning of 'Pathway' was included.

The RCP scenario has reflected the recent greenhouse gas density change trend and has updated the resolution etc to suit the recent prediction model. As the 4 representative greenhouse gas density, 2.6, 4.5, 6.0 and 8.5 were used in the RCP. The RCP 4.5 corresponds to the case where the greenhouse gas decrease policy is realized to a significant degree and the RCP 8.5 is the case where the greenhouse gas is emitted (BAU scenario) as the current trend (without decrease). When compared with the current climate (1971-2000), the increase of the sea surface temperature was distinct based on the high-altitude of the northern hemisphere excepting the northern pole regions where all the 2 RCP species are covered with ice.

The higher the emission scenario where the greenhouse gas density increases, the sea surface temperature increase depth increased, and the difference of spatial pattern of the sea surface temperature by each scenario is very little. It was predicted that the whole global average sea

surface temperature will increase by 0.9℃, 1.7℃, 1.8℃ and 2.8℃ according to the greenhouse gas scenario at the end of the 21st century(2071-2100).

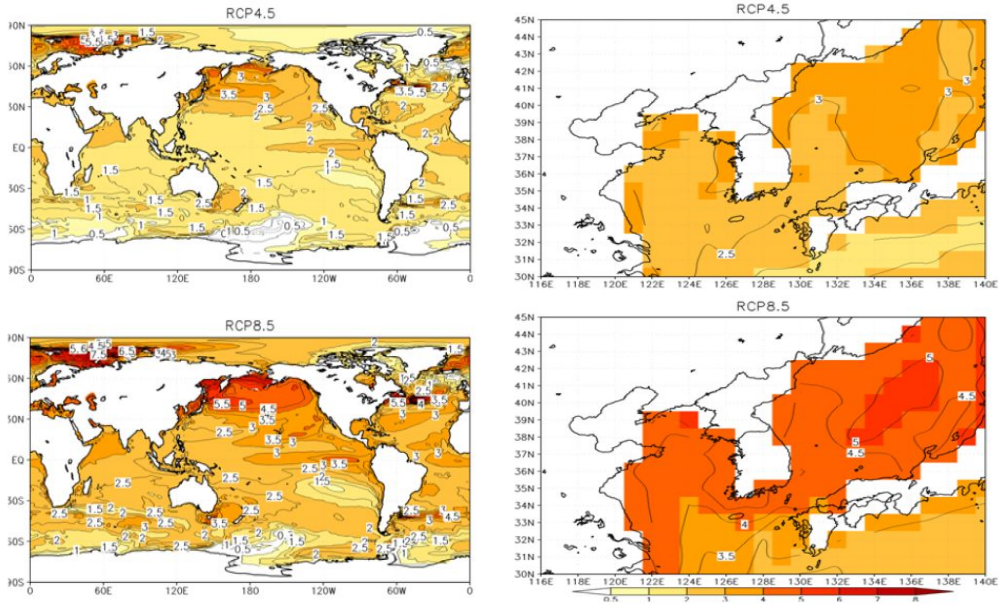

Fig. 1.7. Distribution of global SST by climate change scenarios of RCP 4.5 and RCP 8.5.
(Reference : NIMR, 2012)

In the equator region, the weathermaker similar patterns were shown where the water temperature increase is higher relatively in the east pacific region than in the west pacific region. Our country's adjacent sea regions(120-135° E, 33-45° N) were analyzed to be a region where the sea surface temperature increase is relatively large. It was predicted that the temperature increased by 2.0℃, 3.0℃, 2.9℃, 4.5℃ according to the greenhouse gas emission scenarios and they will all increase by more than 1℃ than the whole global average(National Institute of Meteorological Research, 2012).

On another hand, our country's adjacent average surface water temperature increased by around 0.93℃ for the past 39 years(1968-2006) and increased annually by 0.024℃ in the Fig. 1.8. The east region has increased by 0.8℃, the south region by 1.04℃ and the

west coast region that is related to this research has increased by 0.97℃. It increased by around 0.67℃ for the recent 10 years(1995-2004) and thus the sea temperature is being accelerated.

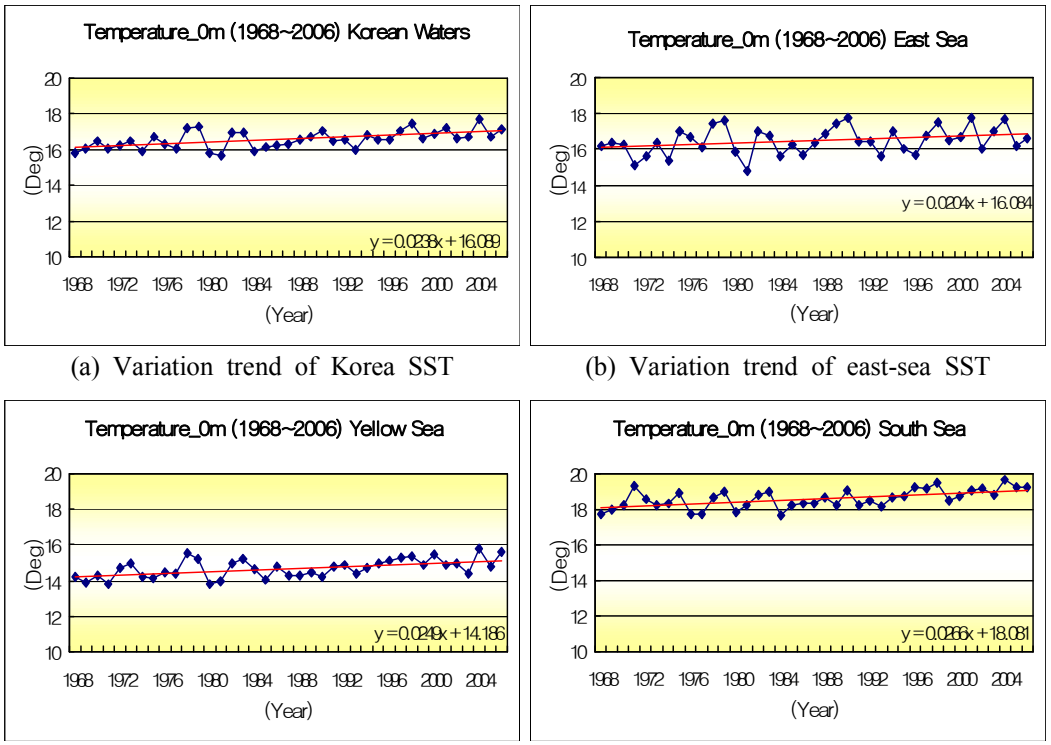

(a) Variation trend of Korea SST (b) Variation trend of east-sea SST

(c) Variation trend of west-sea SST (d) Variation trend of south-sea SST

Fig. 1.8. Changes in sea surface temperature of Korean waters and three seas (East, Yellow, and South Seas) during 39 years (1968~2006). (Reference : KRIHS, 2007)

The Fig. 1.9 shows that the winter time warming is being fortified seasonably and the heavy snowfall phenomenon has distinctly decreased after the end of 1980s. (National Institute of Meteorological Research, 2006 : Choi and Kwon, 2008) The heavy snowfall occurrence days of more than 10 cm in total of the 15 observation sites of our country have decreased by half after the 1990s compared to before 1990s. Choi and Kwon(2008) has revealed that the heavy snowfall days exceeding 5cm snowfall is decreasing mainly in the sea level altitude of under 300m in

the Yeongdong and Yeongseo region, by analyzing the occurrence frequency of the heavy snowfall days during the snowfall seasons(November -April) for our country's 61 regions for the past 35 years(1973-2007).

However, the sea surface temperature is continuously increasing around 1980s as can be seen in the Fig 1.10. Recently and accordingly, the frequency of the snowfall and the amount of the snowfall analyzed above also are increasing.

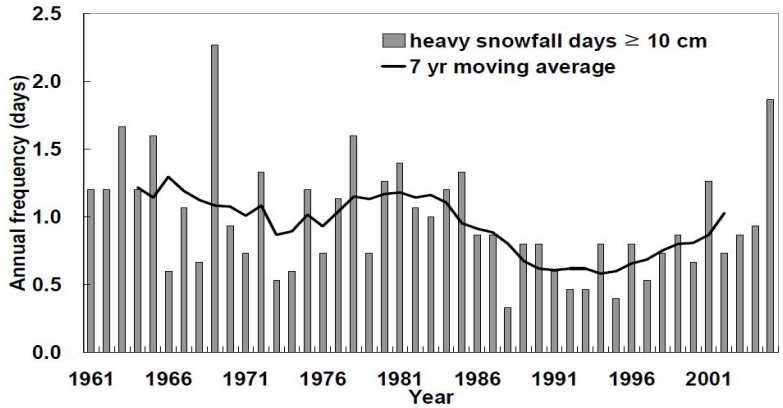

Fig. 1.9. Changes in heavy snowfall (10cm/day) days averaged across 15 stations in Korea during the period of 1961 to 2005. (Reference : NIMR, 2009)

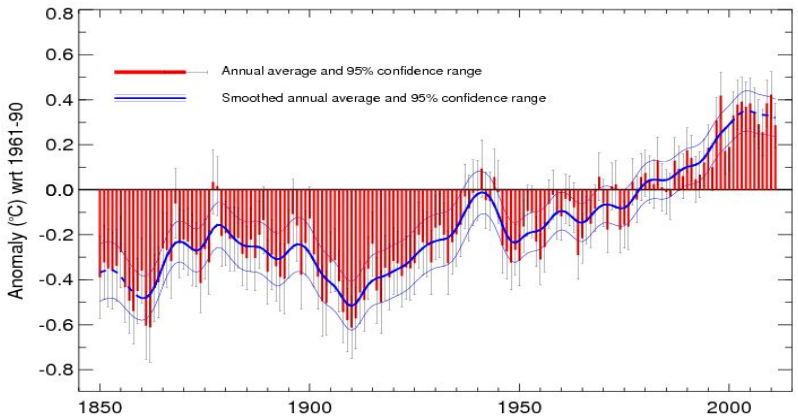

Fig. 1.10. Changes in global averaged sea surface temperature from 1850 to 2011.

(Reference : Mnet office, UK. 2013)

B. Previous Studies

The Cause analysis of heavy snowfall that occurs during magnification of the cP has been much implemented. Kim(1983) proposed several presentation standards in order to enhance the accuracy of heavy rain forecast by studying the objective presentation techniques for the heavy snowfall warning for Honam region. After that, there have been studies by many researchers and forecasters(Jung, 2005; Lee, 2008 *et al.*) about the heavy snowfall in Jeollabukdo (Gwangju Regional Meteorological Administration, 1995) and in Honam region(Song, 1993; Ju, 2001; Park, 2006) based on the Korea Meteorological Administration.

West coast snowfall in the Korean Peninsula mainly occurs from difference in sea temperature and air temperature, when the continental High pressure cold air developed in winter moves above relatively warm sea, and Honam, where the sea is located on the winter wind and frost, has very high occurrence frequency of heavy snowfall (Jung, 1999; Jung, *et al.* 2005). Also, as for the east coast, the screen effect caused by geographic features plays a crucial role because of Taebaek Mountains located from south to north(Lee, 1999; Jung, 2004; Byun *et al.*,2006). But these snowfalls in Korean Peninsula show very strong locality, and it is very difficult to forecast accurately about heavy snowfall region and amount because of the effects of complicated geography (Jun,1994;Lee and Park,1996).

Through heavy snowfall observational data analysis, the drift of cold air in the rear end of Low pressure developed in the sea, and the warm air in the front is the main development apparatus, and Jun, *et al.*(1994) performed dynamic and thermodynamic analysis on cases of heavy snowfall in Korean Peninsula in 1990, and analyzed that heat transport in the sea plays an important role in developing Low pressure, and secondary circulation from these doubles the ascensional power. This study is provided to approximately predict the degree of heavy snowfall in

Honam through synoptic analysis. Also, synoptic scale meteorological phenomena such as heavy snowfall is very much affected by geographical features according to meteorological conditions, and the strength of the effect is influenced by the direction of wind (Ryu and, Lee, 2002; Ryu, *et al.*, 2004). Based on the synoptic data, snowfall mechanism of the east shore and west shore in the Korean Peninsula shows difference, and there is a study result that this difference can't be simply described with the difference in sea air and the occurrence of its Low pressure (Jung, 1999; Jung, *et al.*, 2005; Korea Meteorological Administration, 2006).

According to the heavy snowfall observational data analysis, the drift of cold air in the rear end of Low pressure developed in the sea, and the warm air in the front is the main development apparatus, and Jun, *et al.*(1994) performed dynamic and thermodynamic analysis on cases of heavy snowfall in the Korean Peninsula in 1990, and analyzed that heat transport in the sea plays an important role in developing Low pressure, and secondary circulation from these doubles the ascensional power.

C. Purposes of This Study

This study was implemented to approximately predict the degree of heavy snowfall in Honam region through synoptic analysis. Also, synoptic scale meteorological phenomena such as heavy snowfall is very much affected by geographical features according to meteorological conditions, and the strength of the effect is influenced by the direction of wind (Ryu and Lee, 2002; Ryu, *et al.,* 2004). Based on the synoptic data, snowfall mechanism of the east shore and west shore in the Korean Peninsula shows difference, and there is a study result that this difference can't be simply described with the difference in sea air and the occurrence of its Low pressure (Jung, 1999; Jung, *et al.,* 2005; Korea Meteorological Administration, 2006).

Because of the recent worldwide global warming, extreme weather of

localized heavy rain, heavy snowfall, and drought happens frequently. Weather changes have complicated forms and the cause of extreme weather is diversifying, which requires high-tech analysis technique for the cause analysis and prediction technology development for these extreme weathers. Especially, development of prediction system which concentrates on analyzing meteorological disaster, modeling and quantization is highly required for development of disaster prevention technology and weather prediction technology (Korea Meteorological Administration, 2006).

In this study, we analyzed the heavy snowfall occurrence factor through the case of heavy snowfall in South-west coast of Korean Peninsula, and especially investigated the effects of mid-range weather phenomenon on heavy snowfall. Based on the data of this study and previous studies, this study investigated of how heavy snowfall strength changed due to SST through numerical experiments of two representative cases of heavy snowfall affecting Korea, and helps to improve the accuracy of snowfall prevention through comparison and analysis of SST data.

CHAPTER Ⅱ. DATA AND METHOD

A. Data

1. Meteorological Part

Synoptic meteorological observation data used in Korea Meteorological Administration, aerological data and Forecaster's analysis system data were used in this study to analyze the heavy snowfall cases that occur frequently in Korea. Weather Research and Forecasting, a model used in the numerical mock test as the numerical test for the comparison and analysis of the change of the heavy snowfall according to the Sea surface temperature and 3 types of sea surface temperature data were used to implement the test.

The analysis was implemented by using the synoptic meteorology observation data. The meteorological data through the ground observation implemented for the same time zone in all the observatory offices in order to comprehend the meteorological status for a specific time zone, the aerological observation data such as the radiosonde, wind-profiler etc in order to comprehend the meteorological status of the upper air zone of which the direct observation is difficult, raider and satellite image analysis data and the data through FAS which plays an interface role between the user and the system, display to the user the graphic image data and the model grid data and enables the treatment of such data.

2. Oceanic Part

For the data on the sea surface temperature, 3 sea surface temperature data were used. The used sea surface data are the SST(the average monthly meteorological value data between December 2010 and December 2012 provided by NCEP), the OSTIA(Operational Sea Surface Temperature and Sea Ice Analysis) data(data between 30 December, 2010

and 28 December, 2012) that are produced in the Met-office of England, the data that shows the best credibility in the Korean Peninsular's adjacent seaside, and the RTG SST(Real Time Global Sea Surface Temperature) data(data between 30 December, 2010 and 28 December, 2012) that is being used in the site work model in the NCEP in U.S.A.

The OSTIA is the sea surface temperature data for high resolution developed in the Met-office of England. It was invented as a way of Group for High Resolution Sea Surface Temperature Pilot Project(GHRSST-PP) of the Global Ocean Data Assimilation Experiment(GODAE) in order to apply the mock test of the high resolution space and time size such as the global size numerical meteorological prediction and the site work sea model and to prepare the prediction system of high resolution region size or the regional size for the future. (Stark and others, 2007) This data is being made once a day with the 0.05° of spatial resolution practically real time about the sea surface temperature and sea ice density of the whole earth. In the OSTIA, the bias of the site observatory data that came from the site observatory data of the temperature and salt, microwave of the SSM-I/DMSP, AATSR/EnviSat, AVHRR-LAC/NOAA 17 and 18, AVHRR-GAC/NOAA 18, infrared light reflection channel of SEVIRI/MSGI and the microwave radiator is corrected through the optimal interpolation method(Stark *et al.*, 2007), and the foundation SST and sea ice data are made, the independent sea surface temperature data about work change of the temperature. According to the comparison result with the observation data of the M-AERI radiator that came from the EGEE/AMMA experiment implemented in the tropical atlantic sea, the OSTIA showed a -0.17℃ value of bias and 0.39℃ of RMSE value (Stark *et al.*, 2008) and is showing a much lower bias recently(Stark *et al.*, 2007). The RTG SST is being made everyday since 30 January, 2001 using the 2 dimensional various data assimilation in order to use it in the current numerical meteorological prediction in the NCEP Marine Modeling and Analysis

Branch.(Thibaux *et al.*, 2003) RTG SST produces two data which have the spatial resolution of 0.5° and 0.083° . For the case of the 0.083° , data is not produced in the study object region and thus the data of resolution of 0.5° was used. In the creation of data, the AVHRR sensor data of the current NOAA-17 satellite and the most recent observation data in the buoy are averaged every 24 hours about each grid. (Thibaux *et al.*, 2003) According to the comparison result of the data of resolution of 0.5° with the buoy value, in the scope from south altitude of 30° to north altitude of 30° , RMSE value of 0.4~0.6℃ was detected and in the scope from north altitude of 30° to the north altitude of 90° , an RMSE value of 0.6~1.2℃ was detected. (Thibaux *et al.*, 2003)

B. Method

1. Case Studies

Korean Meteorological Administration defines 5cm of fresh snow in 24 hours from when it started snowing as snowfall warning and 20cm of fresh snow in 24 hours as snowfall watch. Table 2.1 briefly summarizes the patterns of meteorological elements of heavy snowfall type shown through past heavy snowfall case analysis in order for heavy snowfall prediction. Fig. 2.1, in order to investigate past heavy snowfall cases, categorized snowfall patterns that frequently took place in Korea by choosing the cases of snowfalls that are 5 cm or more from 1981 to 2010. Among past cases, three cases were selected (Fig. 2.1) and fresh snow data observed in west coast and Honam region were used, and the on days of snowing: (a) the case of heavy snowfall due to cold, dry cold anticyclone expanding and lower clouds developing on relatively warm sea, (b) case of cold anticyclone corrupted to migratory anticyclone and located in frost are to have west wind inflow, (c) case occurrence from Low pressure or trough of Low pressure developed from the south passing and strong warm, humid air current inflow from the front.

This study reviewed difference between three heavy snowfall types by organizing weather patterns during snowfalls, and adjusted features of each type through past case analysis.

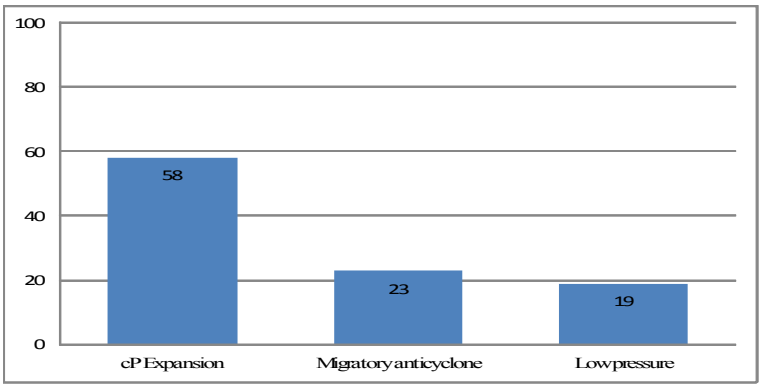

Fig. 2.1. Three synoptic patterns causing heavy snowfall in Korea.

Table 2.1 Summary of statistical characteristics of meteorological elements associated with heavy snowfall by region.

region / Elements	West Coast	Inland	South Coast
Surface H Central pressure	1048hPa	1047hPa	1054.8hPa
Surface H Location	95~115E	100~110E	100~110E
500hPa cold core	-43.5℃	-43.7 ℃	-43.8 ℃
500hPa cold core Location	125~135E, 45~55N	130~140E, 45~50N	130~140E, 40~50N
500hPa Temperature	-27.0 ℃	-27.7 ℃	-28.9 ℃
850hPa Temperature	-12.8 ℃	-11.8 ℃	-13.0 ℃
500hPa Wind speed	73.2kts	72.3kts	100.3kts
850hPa Wind speed	28.5kts	28.7kts	35.5kts
Pressure gradient force (Tiānjin-Gwangju)	0.0028hPa	0.0052hPa	0.0107hPa
Sea air difference (Chilbal-Gwangju)	19.1 ℃	19.9 ℃	20.5 ℃
Sea air difference (Deokjeok-Osan)	20.5 ℃	20.6 ℃	22.6 ℃

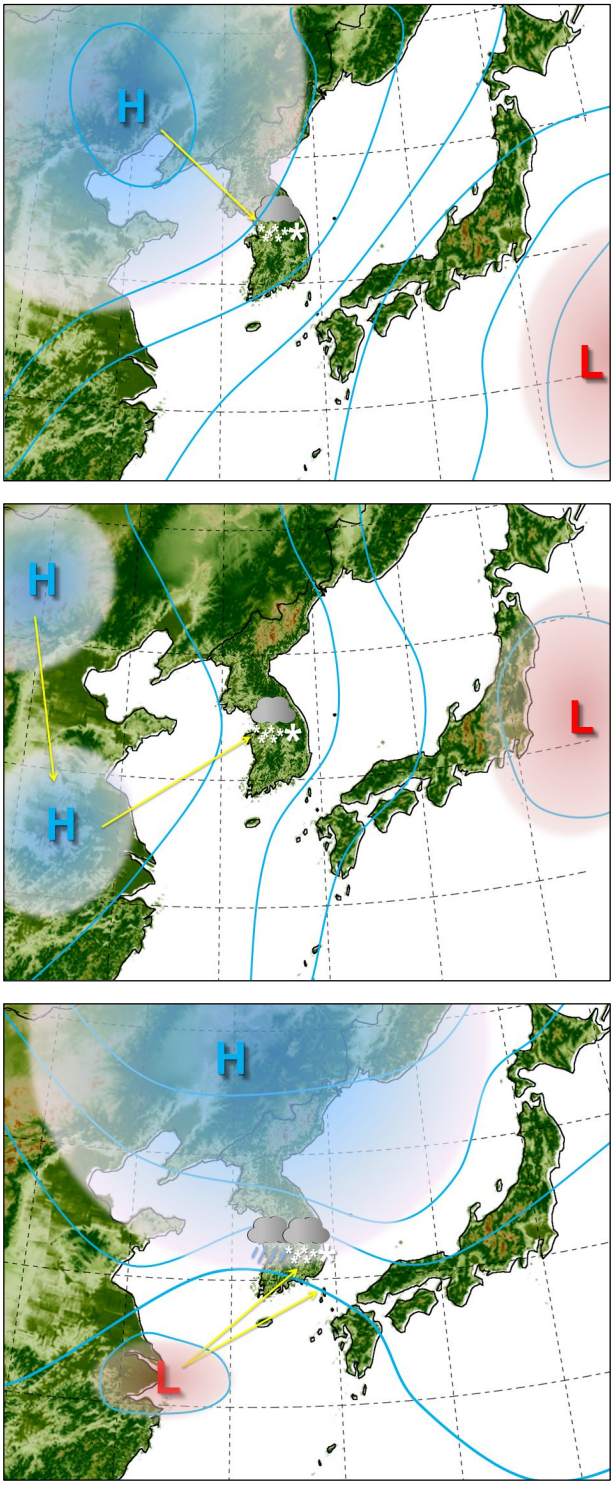

Fig. 2.2. Three schematic maps causing heavy snowfall in Korea.

2. Numerical Simulation

The 5th generation Mesoscale Model (MM5) was mostly used in the past for the work site prediction use, but by complementing the disadvantages of MM5 model of which the development has been ceased with the version of 3.7 as the latest, the WRF is the numerical analysis model that is in operation in various institutes for the air quality prediction and current meteorology prediction. In this research, the numerical experiment was implemented using the WRF 3.4 version and the intensity change of the heavy snowfall according to the sea surface in our country's coast was compared and analyzed.

The numerical experiments were carried out at the center about heavy snowfall case of 30 December, 2010 different heavy snowfall during Honam region recently displayed and (case2010) heavy snowfall case of 28 December, 2012 (case2012). Strong snowfall was revealed around the Honam west coast that was caused by cold Siberian air pressure to extend the Case2010. On the other hand, in Case2012, a lot of snowfall was recorded in the Gyeongsangnamdo southwest region and Honam region south coast and due to traveling cyclone.

CHAPTER Ⅲ. CASE STUDIES OF HEAVY SNOWFALL

A. Continental Anticyclone Expansion

1. Overview

By analyzing the cause of frequent heavy snowfall in 2005, from December 2005, as the barometer in the 500hPa (5km in the sky) upper layer of northern hemisphere became stale through strong blocking phenomenon, three long waves (air parcel) were formed at the center of northern pole, and in the East Asia region, strong cold from the north pole continuously grew over to the middle-latitude to develop strong, cold continental anticyclone(1050~1070hPa) in Siberian region earlier than the average year.

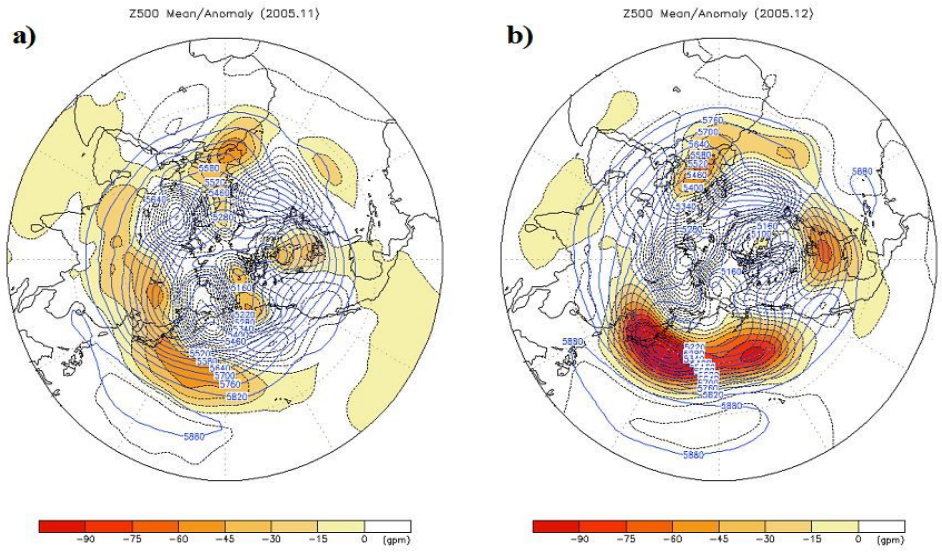

Fig. 3.1. Mean and anomaly of geopotential height at 500hPa on a) November and b) December, 2005. (Reference : METRI, 2006)

'Arctic Oscillation(AO)', a phenomenon of alternative height deviation between high latitude and medium latitude of northern hemisphere, reflected a strong negative state to bring the cold to the south, which caused a dynamic decrease of temperature compared to average years, and this cycle was maintained for more than two weeks.

As cold air remained in sky of Korea for a long time, north-western wind was descended by continental anticyclone, and in the west coast, surface sea temperature was relatively warm as of over 10℃, but the air in the sky 1.5~3km above ground was lower than minus 10~25℃ to form snow clouds caused by the difference between surface sea temperature and atmosphere temperature. As this snow clouds flowed into Gwangju and Jeollanamdo region through strong northwesterly wind to form frequent snow, some regions experiences heavy snowfalls.

This is a case of heavy snowfall concentrating on the west coast of Honam region in 4~5 December, 2006. On this day, cold continental anticyclone developed and expanded to southeast region, the humid air from Low pressure remained in the west coast to form snow clouds, cold air from continental anticyclone passed the west coast, and temperature difference with surface of the sea resulted in developing snow clouds. And the following was strong steering current to arrive in the Honam region by W-NW wind, and a storm and heavy snowfall fell to the inland on December 4~5.

At that time, because of the effect of cold, dry continental anticyclone centered at the northern part of Lake Baikal and expanding south, pressure force in Korea's surroundings was very strong and the northwest monsoon continuously flowed in, and in the 500hPa weather chart, joint Low pressure of center in North Korea region slowly moved eastward through east blocking to strengthen the inflow of northern cold. As the continental anticyclone expanded, over 30cm of heavy snowfall fell from December 4 to 5, and snow in inland region was larger than that in coastal region, where Gwangju recorded the largest amount of snowfall

since observation.

Honam region which ranges from the Jiri Mountain to the south coast has heavy rain in summer and heavy snowfall in winter. Honam inland region which belongs to the northern region from the center of Jiri Mountain indicates distinct difference in the distribution of rain and snowfall with the Noryeong Mountains and Sobaek Mountains as boundaries, and thus it can be inferred that this region is affected by mountain topography.

In this topography, there occurs the perturbation phenomenon in the basic current which inflows into this region and the uprising of the moist air and formation of the Mountains are induced and thus much cloud is formed. The regional convergence and rise that occur by the compulsiveness by the irregular topography affect much on the point and intensity of the snowfall that reaches the ground and the microscopic physical process. (Nickerson *et al.,1*985)

In the occurrence of the topographic snowfall, the speed and direction of the wind, relative humidity and the microscopic physical values etc are important, but the exterior ratios like slope, width and height of the Mountain are also very important. Carruthers and Choularton(1983) have showed that the higher the Mountain is, the bigger change between airs vertically defined is brought and the precipitation structure of the upper layer can be changed. Barros and Kuligowski(1977) showed that more slant the slope of the Mountain is, the more compulsive uprising of the air is fortified and thus deep low layer topographical cloud is developed and the precipitation increases.

It was verified that the occurrence of strong cloud band is strongly related to the stability level of the air, strength of the wind, height of the Mountain and rising congelation altitude etc, and it was proved that in the regions where the wind and frost and low layer convergence exist, the precipitation band is formed. (Smolarkiewicz etal.,1987) In our country, Lim and Lee(1994) have observed that for the case of the strong

conditional unstable air, the cloud that is generated by Mountain topology is developed through the active cumulus air current process and there occurs a lot of precipitation.

Honam region has a high possibility of incurring instability of the air current when cold and dry air passes by the warm west coast in the winter time, and thus low temperature and highly humid air is infused continuously.

Shin(1988) has observed that when the Mountains are adjacent to the sea rather than being far away from it, the thermal gradient with the sea becomes much bigger, and even much stronger circulation is made in this region. This is one of the main causes of generating the snowfall in the west coast and Jeollanamdo and Jeollabukdo inland region in the winter time.

2. Synoptic Weather Analyses

a. Surface and Upper Weather Charts

As the cold continental anticyclone expanded, over 30cm of heavy snowfall took place between December 4~5, 2006, and the amount of snow in the inland region was larger than that in the coastal region, where Gwangju recorded the highest amount of snowfall since its observations began.

A meteorological special report from the Meteorological Administration in the morning on December 4th was a preliminary report of heavy snowfall in the west coast of Jeollanamdo and Jeollabukdo, and in some of the Jeollabukdo inland region, and a preliminary report of strong winds was in effect in the morning on December 4. A preliminary report of wind and waves was in effect in coast at the night of December 3. In total, on 2~3 December, before a Meteorological special report was in effect, five weather information reports were announced.

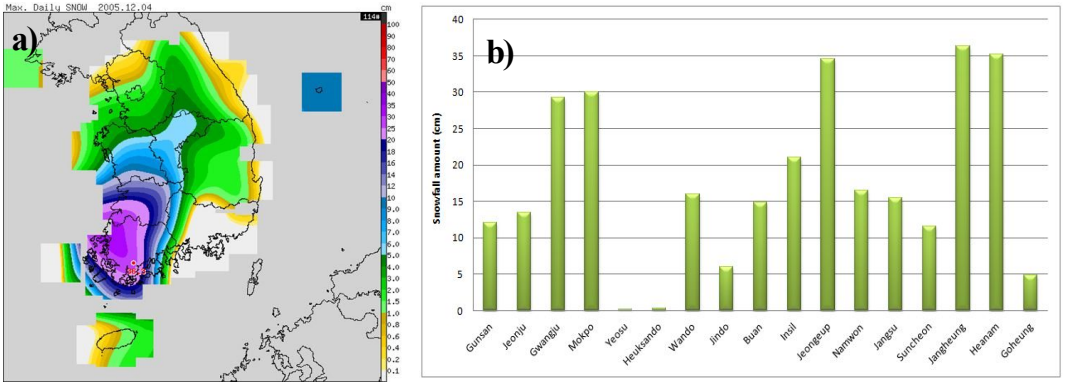

Fig. 3.2. Distribution of a) maximum fresh snowfall amount in Korea and b) snowfall amount by each station in Honam region on 4 December, 2005.

At dawn on 4 December, weak snow and rain were observed in the Jeollanamdo and Jeollabukdo regions, and at two o'clock, some of the Jeollabukdo regions recorded 0.4~1cm of fresh snow cover and a heavy snowfall watch took effect at three o'clock in some of the Jeollabukdo regions. As snow clouds continued to move southeast, the watch was expanded and strengthened to Gwangju, Jeollanamdo and the Jeollabukdo region, which was cleared in the morning on December 5.

Table 3.1. The value of maximum snowfall depth by local provinces (Jeollabukdo and Jeollanamdo) from 4 to 5 December, 2005.

Element / Region	Maximum height of snow (4 to 5 Dec.)			
Jeollabukdo	Jeongeup	46.7	Namwon	18.5
	Buan	23.5	Jangsu	17.2
	Imsil	23.5	Gunsan	17.0
Jeollanamdo	Haenam	38.5	Mokpo	30.4
	Jangheung	37.3	Wando	18.0
	Gwangju	30.0		

Meanwhile, strong wind warnings in Heuksan Island and Hong Island were announced on December 3, and a strong wind warning in the offing of the southern west coast took effect for 23 hours. As the pressure gradient force became stronger and the northwest monsoon continued to flow in, the alert zone expanded and strengthened. The alert was cleared starting from the afternoon on December 5. All special alert was cleared at dawn, on December 6.

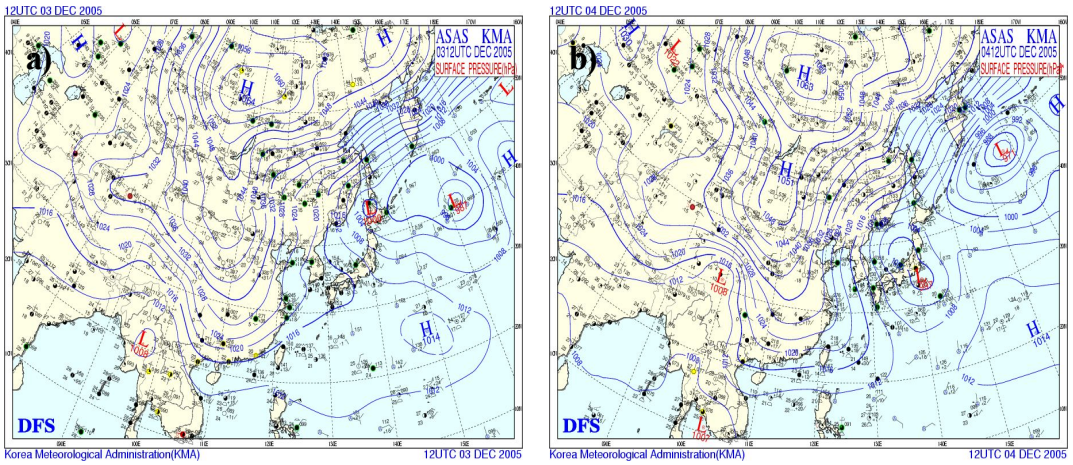

Fig. 3.3. Surface pressure chart at a) 1200UTC 3 December and b) 1200UTC 4 December, 2005.

Fig. 3.3 shows the analysis of surface pressure chart. On December 4, it was under the influence of a continental high after a Low pressure front in the central West Sea at 1200UTC on December 3, which passed rapidly in the Honam region before dawn on December 4, with a continental high as the extension.

A continental high, after passing through the Low pressure, was developed at 1057hPa at Lake Baikal near the extension. The pressure pattern of standing East High and West Low was strengthened, while the isobar standing north and south, pressure hardness of Korea formed nearly the strong form.

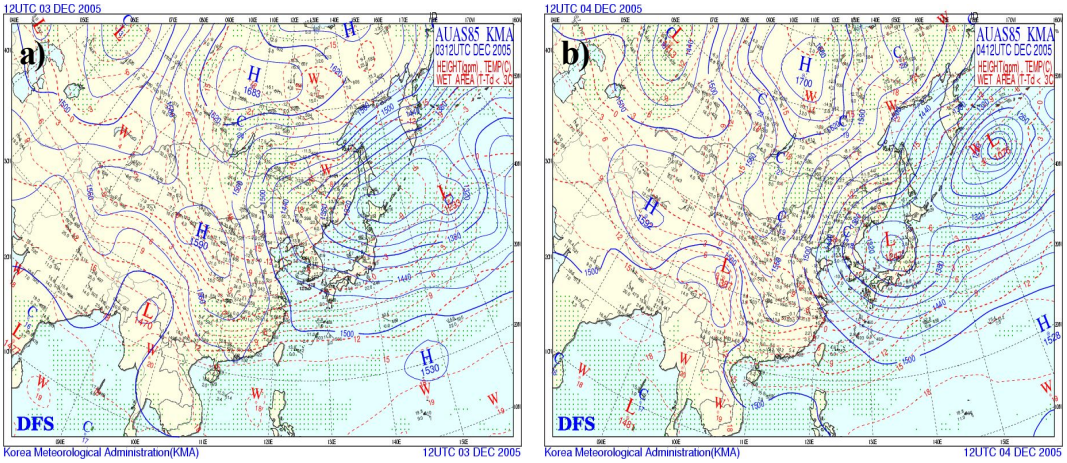

Fig. 3.4. Same as Fig. 3.3 but 850hPa geopotential height and temperature.

Fig. 3.4 shows the analysis of the 850hPa pressure chart. -12 degree line is crossing the central region at 12UTC on December 3, and the strong cold drifted until December 4 at night to gradually ease off on December 5. The temperature change in the Gwangju region was −4℃ (0312) to −9℃(0400), −12℃(0412), and −10℃(0500), which reached a peak point on December 4 at night to be gradually alleviated, and the wind speed appeared to significantly increase from 25kts(0400) to 40kts(0412).

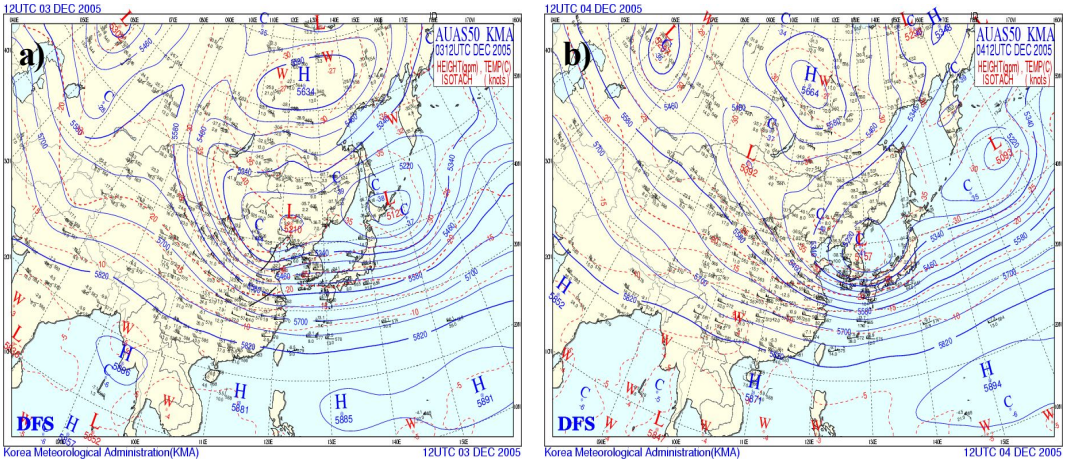

Fig. 3.5. Same as Fig. 3.3 but 500hPa geopotential height, temperature and isotach.

Fig. 3.5 shows the analysis of the 500hPa geo-potential height, temperature and isotach chart where a cold low located near Manchuria rotated to pass Korea and lower the temperature, and the -40 degree line lowered south to northern Gyeonggi at 0000UTC, December 4.

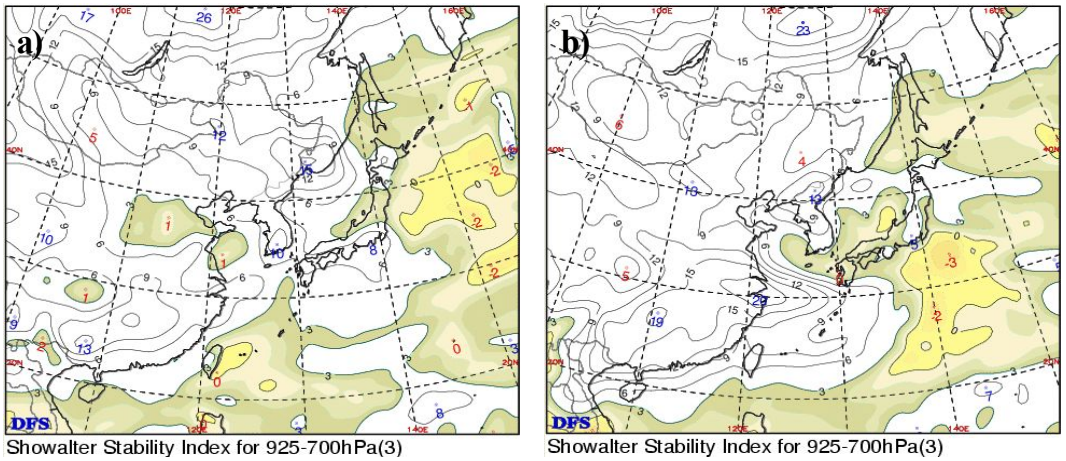

Fig. 3.6. Distribution of Showalter stability index for 925-700hPa at a) 1200UTC 3 December and b) 1200UTC 4 December, 2005.

Fig. 3.6 shows the analysis of Showalter's Stability Index (SSI), which measures the value of elevated altitude of condensation at 850hPa level climbing through the saturation adiabatic to meet the 500hPa level. The meeting point temperature is subtracted from the value of actual temperature on the same side, and when the value is below 4, the possibility of rainfall or snowfall is determined.

At 0000UTC on December 4, instability of SSI 0~3 at the center of west coast and Honam region was strengthened to gradually be weakened from December 5.

Fig. 3.7 shows the 24-hour temperature change analysis at 850hPa, and on December 3, cold air (-13℃~-16℃) located in inner China continent crossed the Korean west coast, resulting in cold air inflow from the morning of December 4 to the night of December 4. The southern

movement of cold air reached a peak point, and was gradually alleviated from December 5.

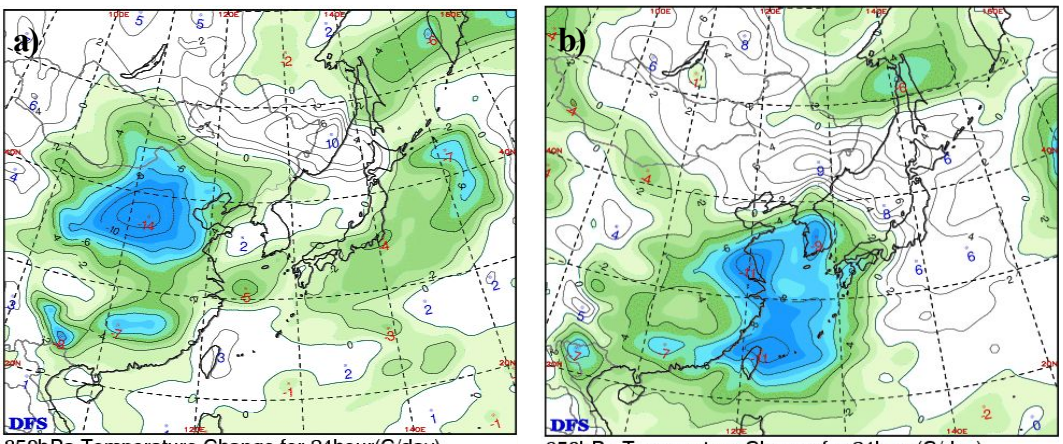

850hPa Temperature Change for 24hour(C/day) 850hPa Temperature Change for 24hour(C/day)

Fig. 3.7. Same as Fig. 3.6 but 850hPa temperature change for 24hour.

Fig 3.8 shows the analysis of a 500hPa vorticity. A joint Low pressure is centered in North Korean regions accompanied by a strong Low pressure vorticity region, which gradually moved south to form in the west coast and Honam region on December 4.

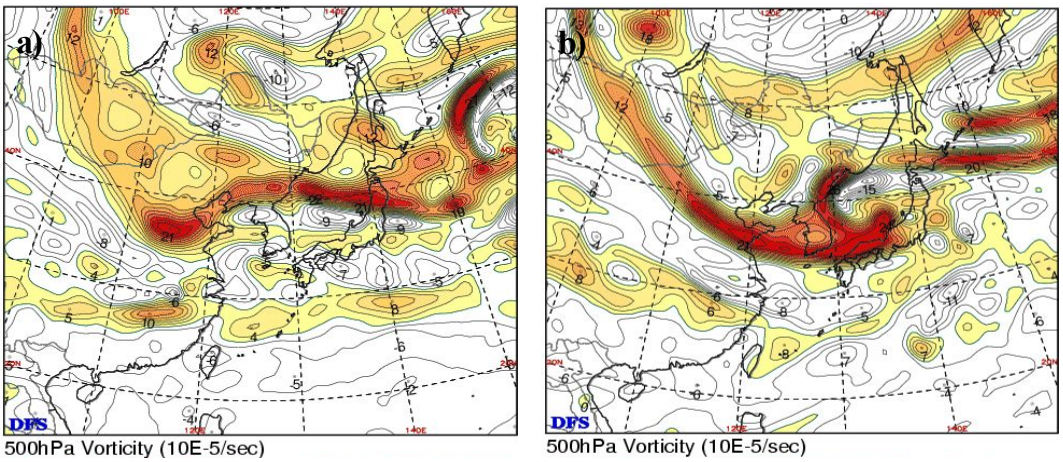

500hPa Vorticity (10E-5/sec) 500hPa Vorticity (10E-5/sec)

Fig. 3.8. Same as Fig. 3.6 but 500hPa vorticity.

b. Radar and Satellite Images

Fig. 3.9 and 3.10 analyzed the radar image and satellite image on the case day, and Echo was formed in the central region on December 3 at night, which gradually moved southeast, and a strong Echo was formed from the Shandong Peninsula to the Honam region in the afternoon of December 4.

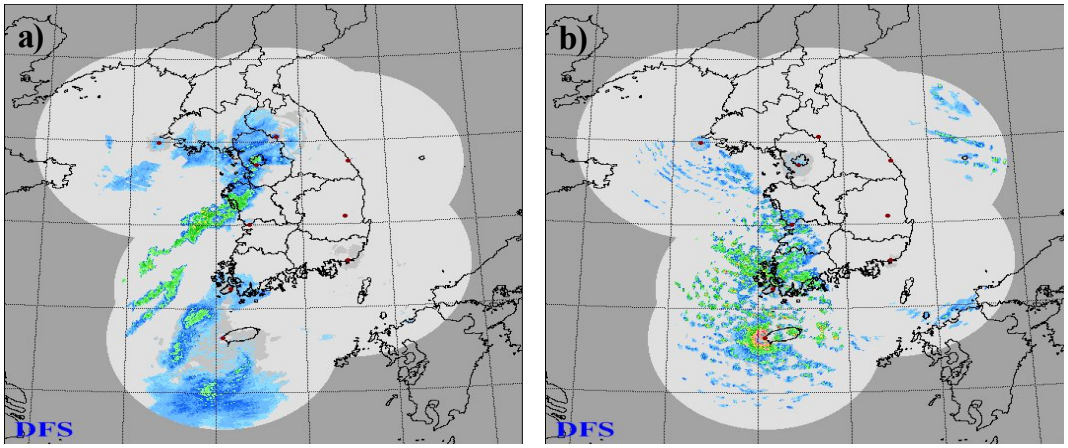

Fig. 3.9. Radar image (echo tops) at a) 1200UTC 3 December and b) 1200UTC 4 December, 2005.

On 4 December, at noon, a strong subtropical convergence from the Shandong Peninsula to the Honam region was formed to develop an updraft; over 3km of cloud was formed to the middle layer of atmosphere.

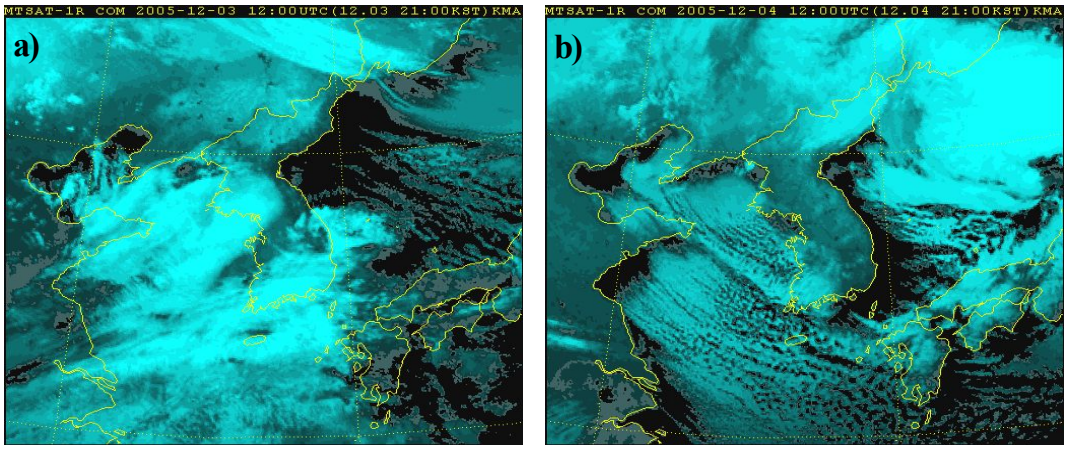

Fig. 3.10. Same as Fig. 3.9 but MTSAT Infrared image.

3. Characteristics of Horizontal and Vertical Structures

Fig. 3.11 shows the analysis of surface temperatures (less than 1℃)+Stream Line[MSAS], at 1200UTC on December 3.

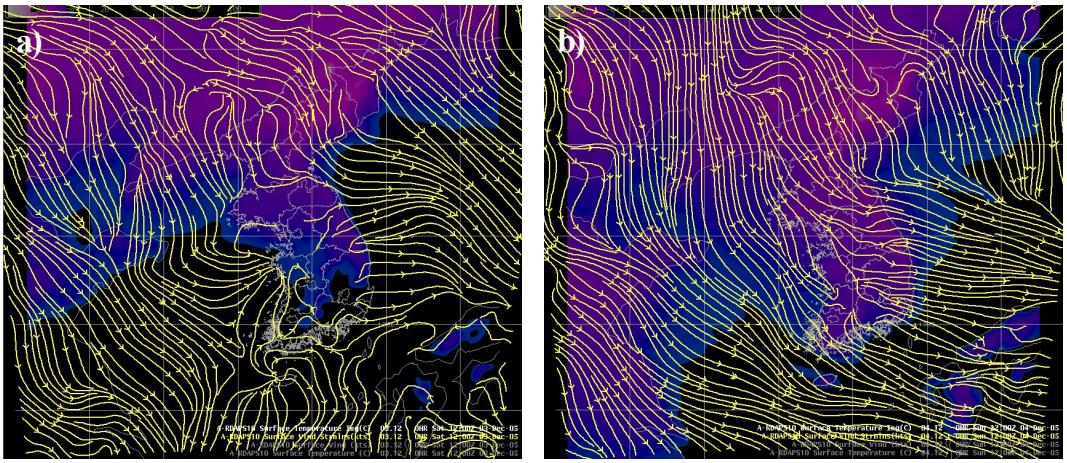

Fig. 3.11. Distribution of surface temperature and streamline at a) 1200UTC 4 December and b) 1200UTC 4 December, 2005.

A Low pressure rotation was shown in the west coast, and in the central region, subtropical convergence was formed according to the inflow of the northwest wind.

On December 4, movement to the south of a cold front strengthened below 1 degree to the southern coast, and a subtropical convergence was shown to be formed in the Jeollanamdo southwest coast according to a strong northwest wind inflow.

Fig. 3.12 shows the analysis of surface temperature advection + moisture advection [MSAS], in which moisture and temperature advection continued in the west coast to cause convective instability; and on December 4, following the steering current, it flowed into the Honam region.

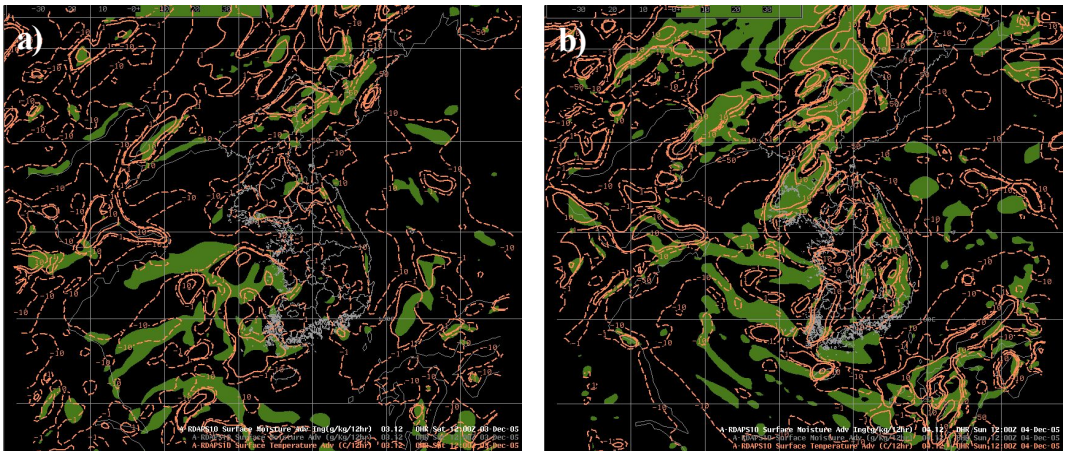

Fig. 3.12. Same as Fig. 3.11 but surface temperature advection and moisture advection.

Fig. 3.13 shows the top and bottom layer temperature and cold nuclear (−40℃), of which on 4 at 1200UTC, the center of the cold air is located on inland of China, and a −9 degree line at 850hPa and −30 degree line at 500hPa descended to the Honam region; and at 1200UTC, a peak point of descending cold air resulted in heavy snowfall.

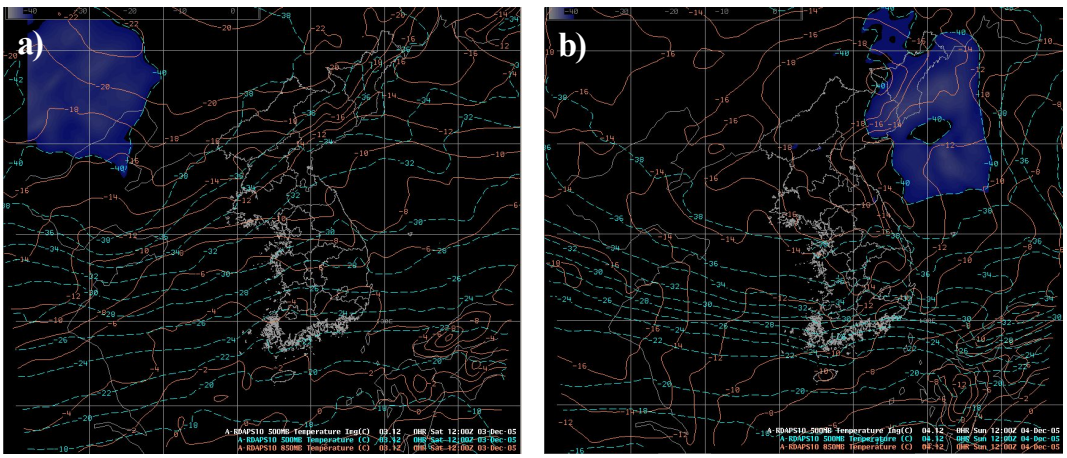

Fig. 3.13. Same as Fig. 3.11 but top and bottom layer temperature and chills nuclear position.

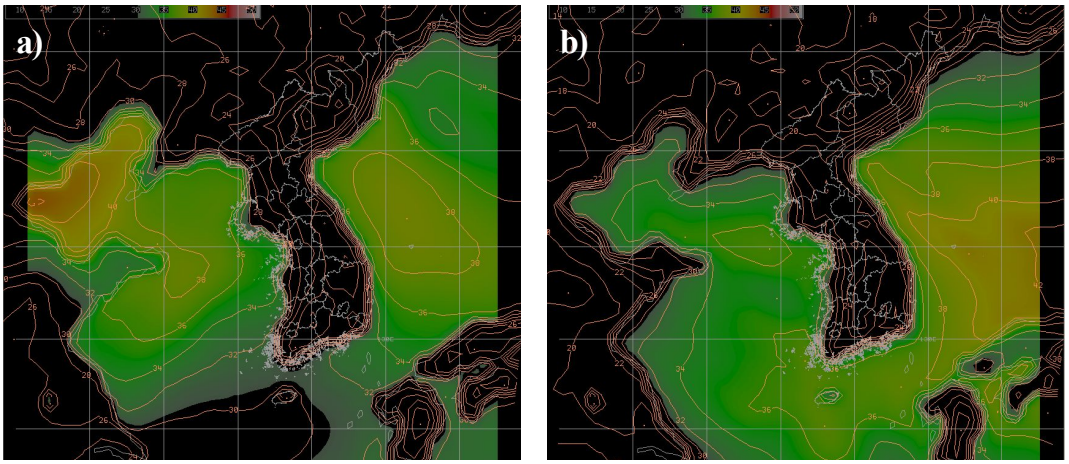

Fig. 3.14. Same as Fig. 3.11 but temperature difference between the top and bottom layer (surface-500hPa).

Fig. 3.14 shows the top and bottom layer temperature difference on the surface at 500hPa. On December 3, temperature difference of over 40 degrees was formed in the west coast to develop a convective cloud from convective instability, and following the strong steering current, it flowed inland to the Honam region.

Fig. 3.15 shows the height and wind speed at 500hPa, and Low pressure with a center in North Korean region rotates and moves east for 5400gpm to descend to the southern coast on 4; it was a strong wind over 100kts until the southwest coast.

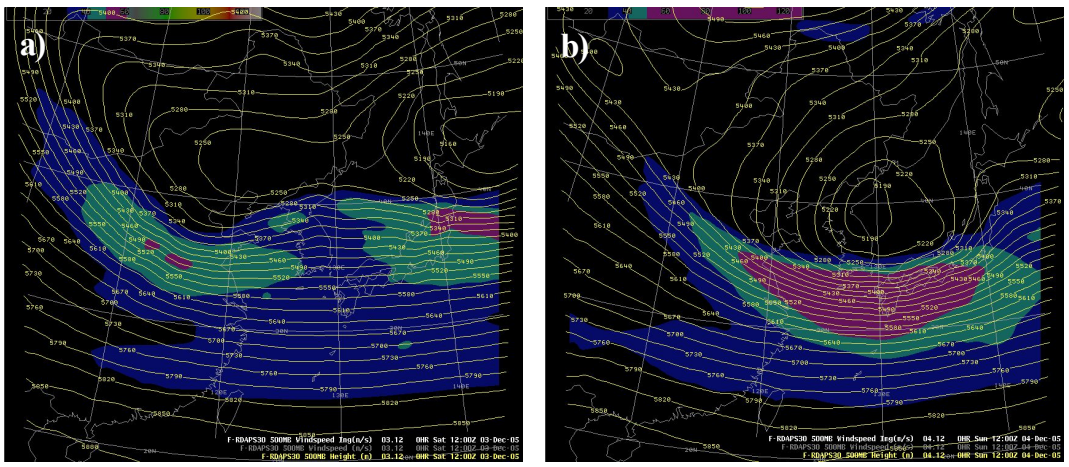

Fig. 3.15. Same as Fig. 3.11 but 500hPa geopotential height and wind speed.

Fig 3.16 shows the analysis of a top and bottom layer jet (850hPa+300hPa), and on 4, the upper and lower jet meet to be located on the west coast and southern coast, and in the morning of 5, it passed the Honam region.

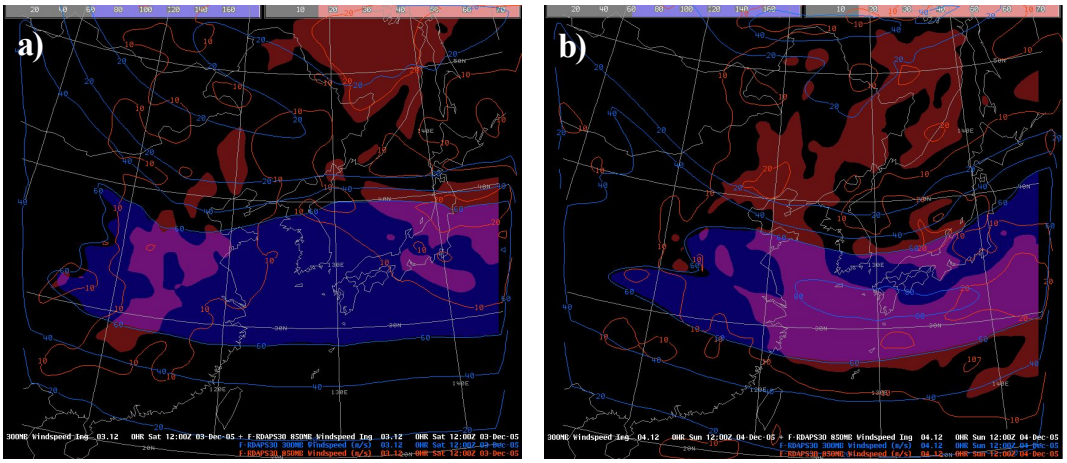

Fig. 3.16. Same as Fig. 3.11 but top and bottom layer jet (850hPa+300hPa).

Fig 3.17 shows the analysis of moisture flux, Q vector convergence and wind with verticality cross section data from Shandong Peninsula to southern coast. At night of 3, a Low pressure circulation was shown in the west coast at the location of Low pressure front.

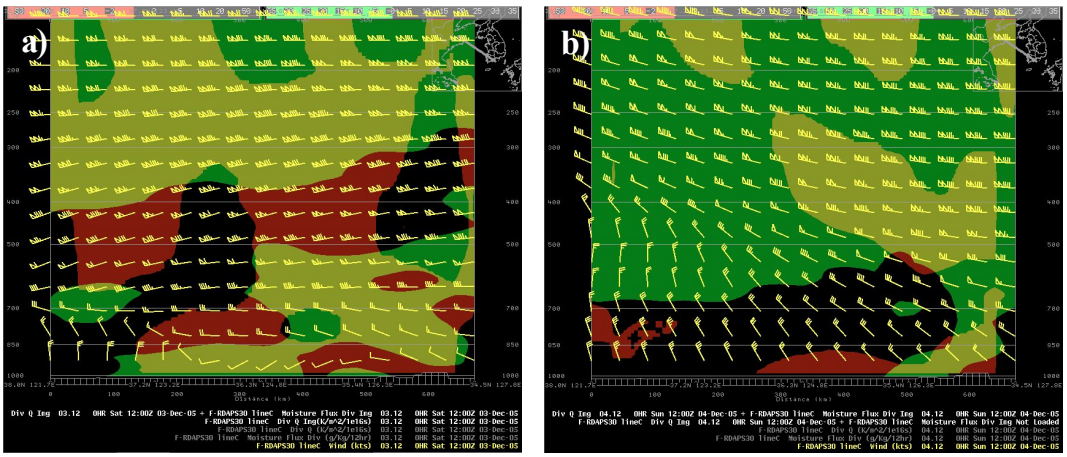

Fig. 3.17. Same as Fig. 3.11 but moisture flux divergence, Q vector convergence, and wind.

Moisture flux divergence and Q vector convergence accompanied by Low pressure are shown in the Honam region, and from the morning of 4, wind direction discontinuity according to a cold drift is shown from the west coast to the inland Honam region.

At noon of 4, a region of convergence is strongly shown from the Shandong Peninsula to the southern coast, and following the steering current, it flowed into the southern coast.

To briefly summarize the characteristics of this case of the continental anticyclone(cP), a cold low located at 500hPa near Manchuria, which is the middle layer of atmosphere, rotated to move the cold air to the south, and the vortex drift of positive strengthened the rising current.

On the ground, a continental anticyclone developed to 1058hPa near Lake Baikal and expanded to move the cold air to the south, (500hPa −40℃ line northern Gyeonggi, Gwangju 850hPa −10~ −12℃) and the sea water temperature of Chilbal Island was 12℃, which is relatively higher than late winter, which created and developed (Chilbal Island sea water temperature − Gwangju 850hPa temperature : 21~23℃) snow clouds from the large sea−air difference. Subtropical convergence was formed from Shandong Peninsula to the Honam region to strengthen the rising current to form strong snow clouds, and these snow clouds flowed into the southern coast by 40~45kts of lower atmosphere layer at 850hPa, and a Low pressure approached from Shandong Peninsula to pass the Honam region in the dawn of 4 to inflow vapor. This is a case when after passing the Low pressure and as the continental anticyclone expanded, this vapor collided with cold air to develop snow clouds.

B. Migratory Anticyclone Transition

1. Overview

As in the case of December 31, 2004, it is a system of cold continental air mass from the north expanded south to Honam region, and on the southeastern coast of Kyushu, developing Low pressure could not move north and moved northeast across southern coast of the Japan to form west high east low type distribution of atmospheric pressure. This is the case of west coast in Honam region blowing strong wind due to cold continental anticyclone, and expansion from Jeonllanamdo west coast to Chungcheongbukdo west coast from temperature difference of northwest cold air and west coast surface of the sea.

Heavy snowfall was expected, and heavy snowfall watch announcement started from southwest coast of Honam region and expanded to northern west coast, recording heavy snowfall in Jeonllanamdo west coast region.

On the day of this case, most regions of Honam region west coast recorded heavy snowfall, and especially, it is the case of strong heavy snowfall shown in regions affected by geographical features.

The heavy snowfall in this case started from the southern west coast of Honam and expanded to northern west coast, which was maintained for about a day, and 5~10cm of heavy snowfall fell on Jeonllanamdo west coast region and some inland region. From 1600UTC, 31 December, starting from Heuksan Island and Hong Island, heavy snowfall watch was announced in west coast of Honam region and as time passed, heavy snowfall region expanded north from the southern Honam region to Jeollabukdo west coast region. Most regions of Honam region had heavy snowfall, but Jeongeup, Jindo, and Mokpo, which were affected by geographical features, showed distinct amount of snowfall. In Jeju Island, by the effect of Low pressure passing through southern Jeju, rain fell from the night of the 30, but in Heuksan Island region which is located on the east of low pressure, started to snow from early evening and changed

to snow on 20 o'clock to record the most extreme snowdrifts.

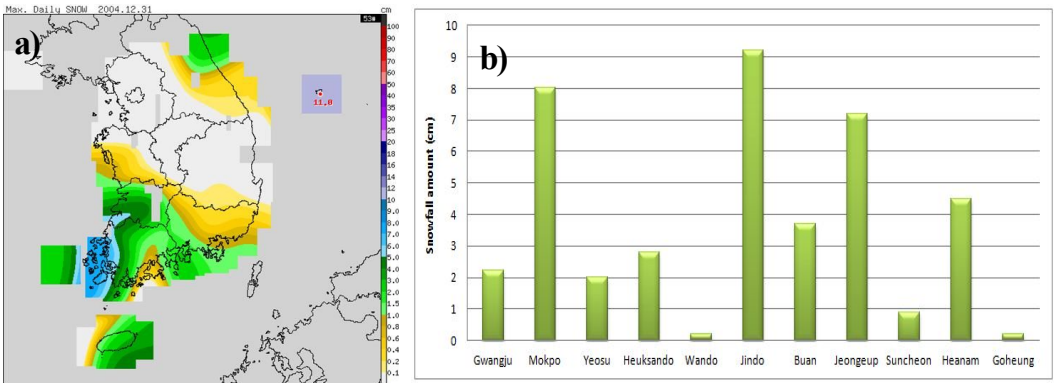

Fig. 3.18. Distribution of a) maximum fresh snowfall amount in Korea and b) snowfall amount by each station in Honam region on 31 December, 2004.

Fig. 3.18 is the maximum fresh snow depth and distribution amount of snowfall on December 31, 2005. In the inland regions including Chungcheongnamdo west coast and Jeollabukdo west coast, heavy snowfall fell, and especially in the Jeonllanamdo southern west coast, heavy snowfall appeared. As Low pressure located below South Korea gradually moved east, and a west high east low type distribution of atmospheric pressure caused it to start snowing in the southern west coast from the morning of December 31.

2. Synoptic Weather Analyses

a. Surface and Upper Weather Charts

Looking through surface pressure analysis distribution in Fig. 3.19, the Low pressure located southwest of Kyushu at 1200UTC, 30 December moved to Kyushu at 1800UTC and caused rain in the southern region of South Korea including Jeju Island. Meanwhile, along with the movement of the low pressure, the High pressure located on the inland of China started to descend slowly south.

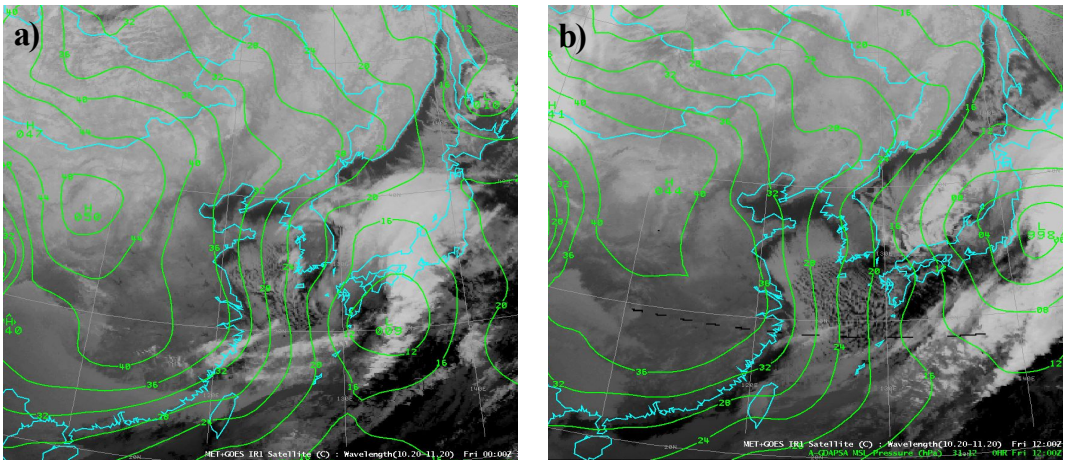

Fig. 3.19. Surface pressure chart with satellite image at a) 0000UTC and b) 1200UTC 31 December, 2004.

From 0000UTC, December 31 the Low pressure located in Kyushu started moving slowly to the southeast coast of Japan, and at the same time, the High pressure located on the inland of China gradually expanded to 1044hPa to approach the west coast to show a west high and east low-type distribution of atmospheric pressure.

As the isobaric line stretched long from south to north, a pressure gradient was strongly formed near South Korea. From 31, cumuliform clouds developed in the west coast and snow started to fall on the entire southern west coast, including the inland Honam region.

Looking at the surface pressure chart in Fig. 3.20, the center of the Low pressure developed on the coast of east China and approaching, it passing through the southern coast of Jeju and developed as it moved near Japan.

From the effect of the low pressure, rain fell in the southern region, and on 31 because of the effect of the High pressure expanding in the Central China region, strong wind was blown. As a temperature trough approached, cumuliform cloud was formed to cause heavy snowfall in the west coast of the Honam region.

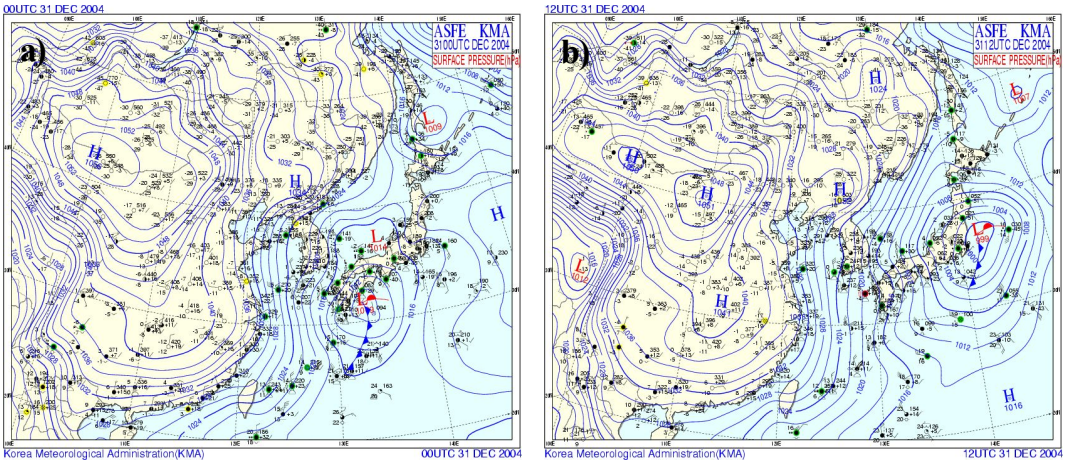

Fig. 3.20. Surface pressure chart at a) 0000UTC and b) 1200UTC 31 December, 2004.

According to the meteorological weather map in Fig 3.21, the center of the low pressure which was developed in the east Chinese sea and was approaching passed by south Jeju and approached Japanese area and developed. There fell rain in the southern region by the effect of the low pressure, and on the 31th a strong wind occurred due to the high pressure which was expanding in the central China. As the temperature trough approached, a cumuliform cloud was formed and a heavy snow fell in the west cost of Honam area.

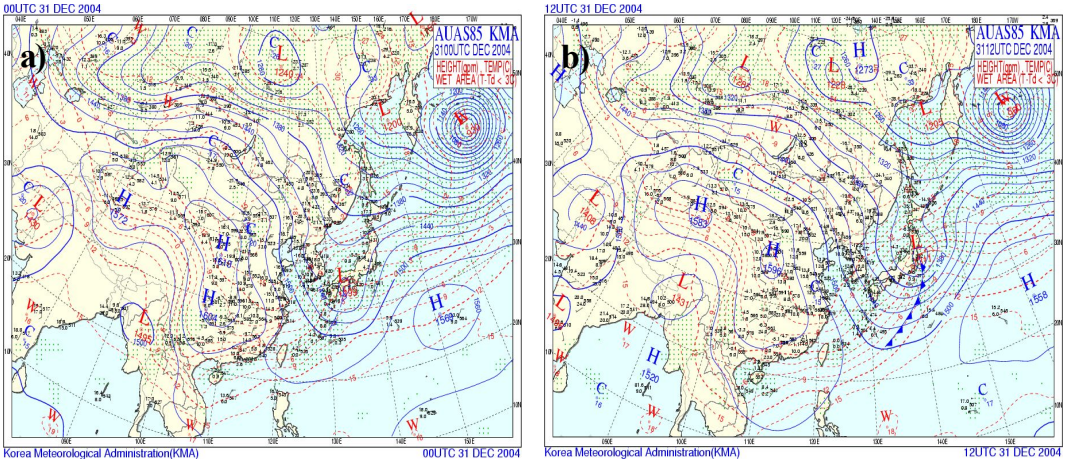

Fig. 3.21. Same as Fig. 3.20 but 850hPa geopotential height and temperature.

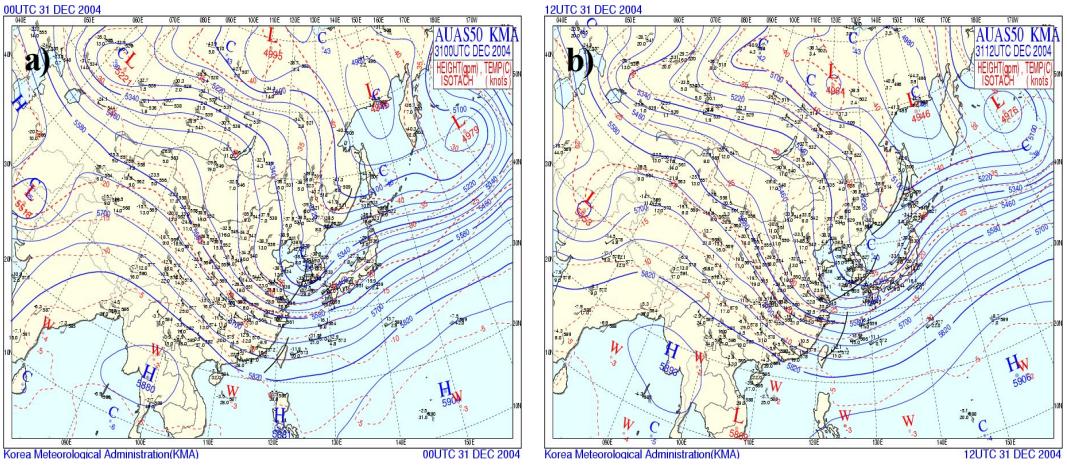

Fig. 3.22. Same as Fig. 3.20 but 500hPa geopotential height, temperature and isotach.

In the Fig 3.22, it could be seen that the pressure trough which was accompanied by strong vorticity was fortified in the northwest area of Shandong peninsula of China. When the center axis was passing by the east coast including Honam region at 0000UTC on the 31th, the baroclinic zone was moving toward the south of our country but moved northeast as time passed by.

As for the temperature, the cold air center which was close to -40℃ showed a tendency of being weakened little by little in Shandong peninsula on the 30th, and it induced warm air until the dawn of the 31st, and induced cold air in Honam region starting from the morning of the 31st.

And, when it reached the pressure ridge of the pressure starting from the afternoon of the 31st, the inflow of the northwest wind weakened. Due to this, the heavysnow stopped in Honam inland, and only snowfall showed in west coast region and the southwest coast region.

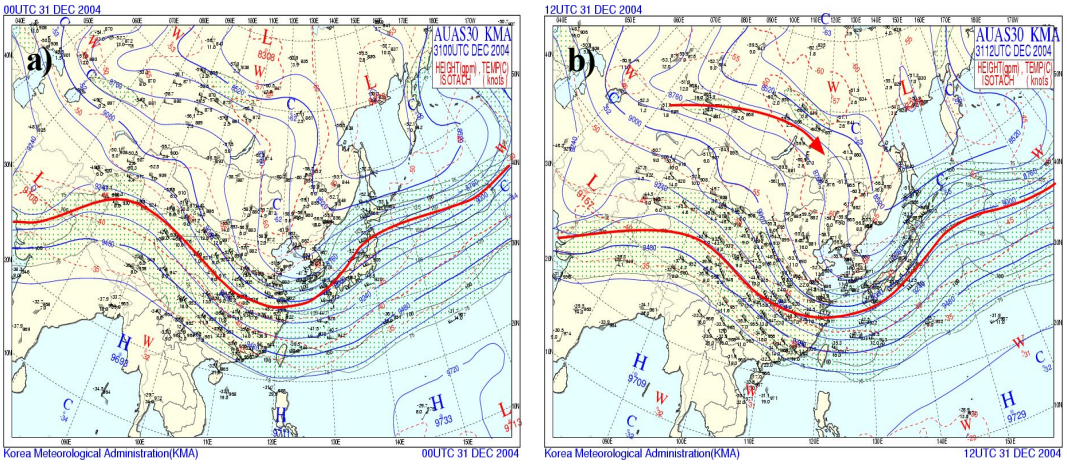

Fig. 3.23. Same as Fig. 3.20 but 300hPa geopotential height, temperature and jet.

In the weather map at 300hPa in the Fig, 3.23, it can be seen that the z axis was widely formed in the south coast of our country, forming a big trough in the southeast of China, and being fortified in the south region of Taiwan area and thus it can be inferred that it was inducing the axis of strong cold air from southwest current toward south.

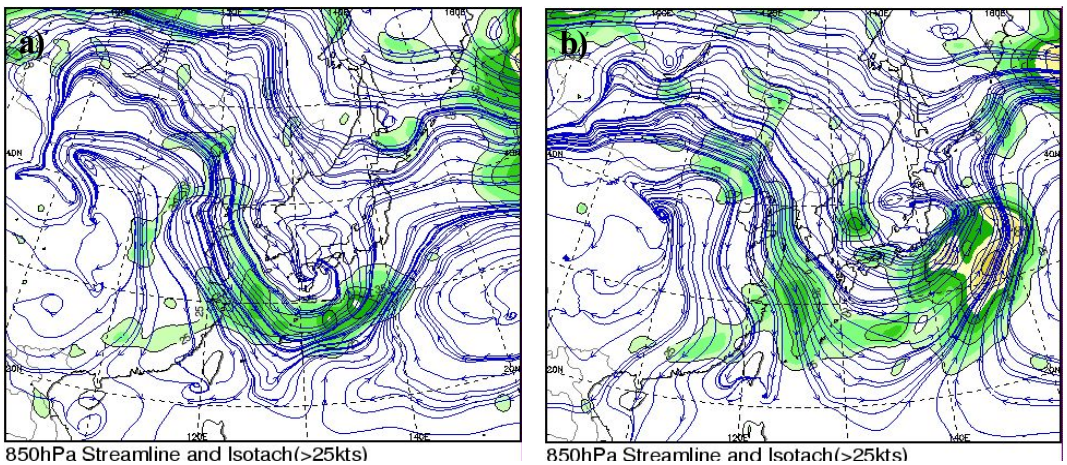

Fig. 3.24. Distribution of 850hPa streamline and isotach at a) 0000UTC and b) 1200UTC 31 December, 2004.

In the 850hPa streamline and Isotach in the figure 3.24, a low pressurized and convergent weather front is rotating to the southern region of South Korea and strong wind current is also seen expanding from the west coast to south coast following the strong steering current.

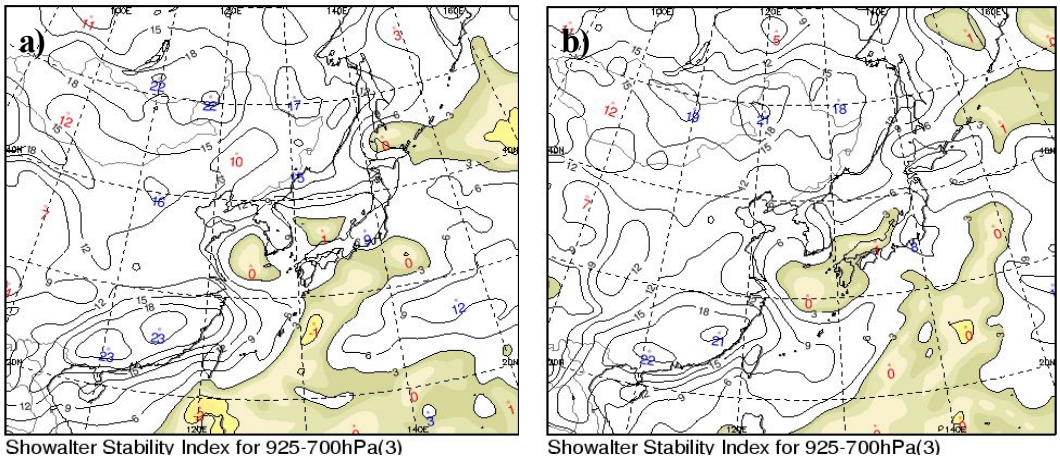

Fig. 3.25. Same as Fig. 3.24 but Showalter stability index for 925-700hPa.

According to the instability index in the figure 3.25, the instability of SSI 0~3 has been fortified starting from 0000UTC on December 31 and then weakened slowly in the west coast and south region of our country.

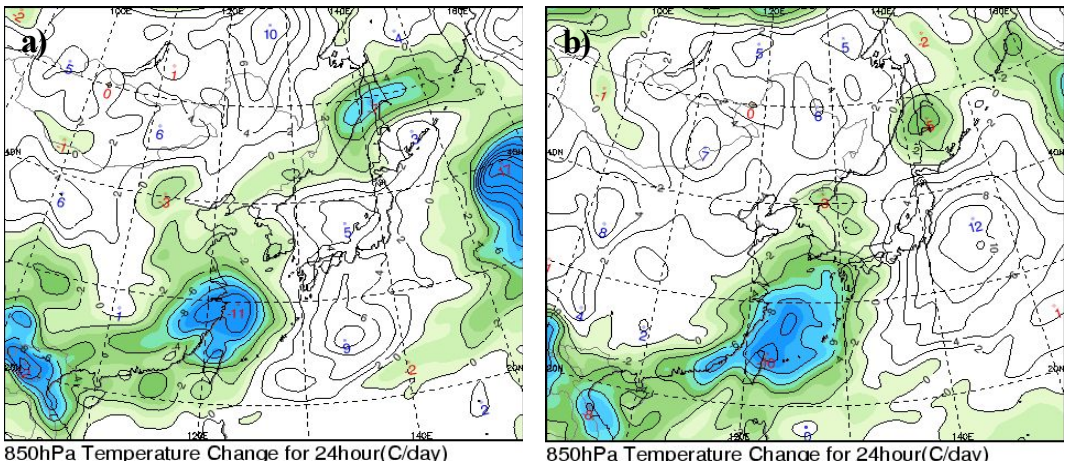

Fig. 3.26. Same as Fig. 3.24 but 850hPa temperature change for 24hour.

According to the 24-hour temperature change analysis at 850hPa in Fig. 3.26, the main change axis for the tendency of temperature change of 850hPa which brings snowfall in the west coast region in the winter time was moving southeast from the east of Shandong peninsula of China and passing by our country closely to the south region of our country.

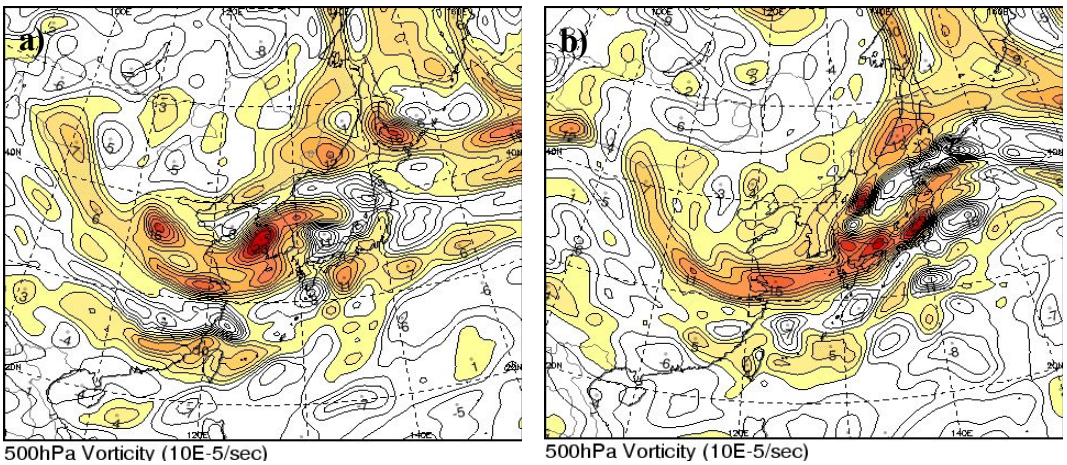

Fig. 3.27. Same as Fig. 3.24 but 500hPa vorticity.

According to the meteorological radar analysis image in figure 3.28, there showed a regionally strong echo at 0000UTC which passes the pressure trough, and in the afternoon when the trough has passed a relatively regular long stripe type of echo zone was maintained in the west coast region of Honam area and this echo has weakened as time passed by and an echo was formed in the south coast region.

b. Radar and Satellite Images

According to the satellite data from figure 3.29, as the low pressure passes through the south region of our country, a large cloud band was formed and rain fell in Jeju region and south coast region and when the low pressure moved northeast and passed by, cold air was infused from the northwest and cumuliform cloud was formed and the cloud was largely

distributed in the west coast region of Honam including west coast.

According to the satellite data from figure 3.29, as the low pressure passes through the south region of our country, a large cloud band was formed and rain fell in Jeju region and south coast region and when the low pressure moved northeast and passed by, cold air was infused from the northwest and cumuliform cloud was formed and the cloud was largely distributed in the west coast region of Honam including west coast.

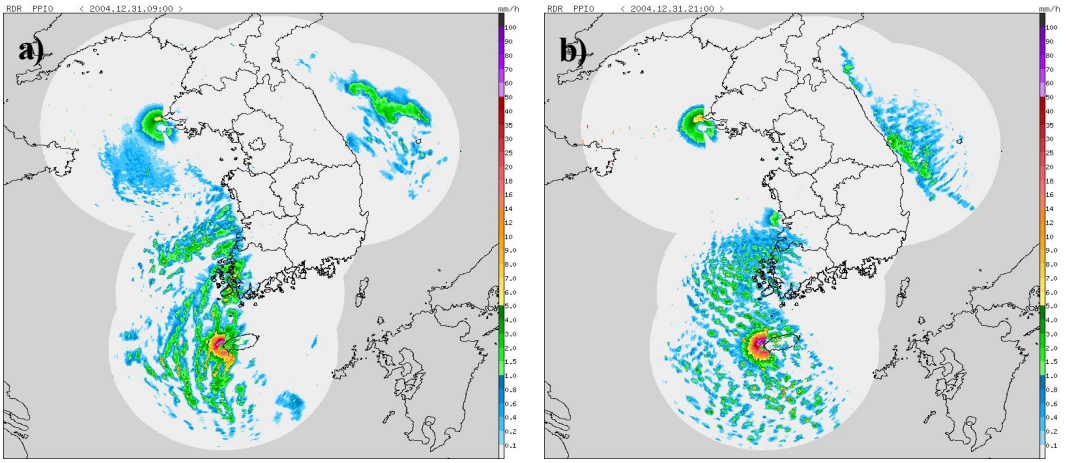

Fig. 3.28. Radar image (echo tops) at a) 0000UTC and b) 1200UTC 31 December, 2004.

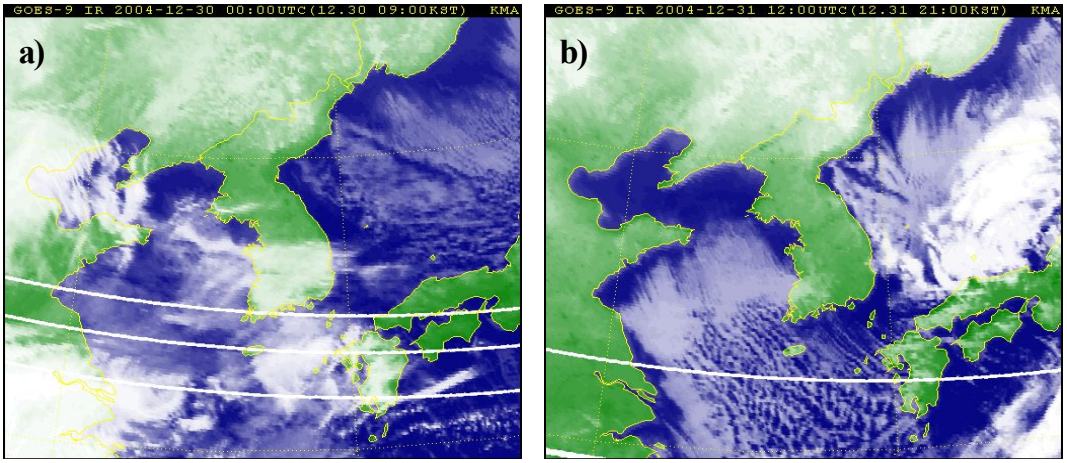

Fig. 3.29. Same as Fig. 3.28 but GOES-9 image.

3. Characteristics of Horizontal and Vertical Structures

Figure 3.30 is the analysis of the ground temperature (under 1 degree) +Stream Line[MSAS]. At 1200 UTC on the 3th, a convergence zone was formed due to the expansion of the pressure located in the east which occurred as the northwest current was infused in most of our country, the low pressure located in the south of our country moved slowly to the east of Japan and cold air is affecting our country gradually.

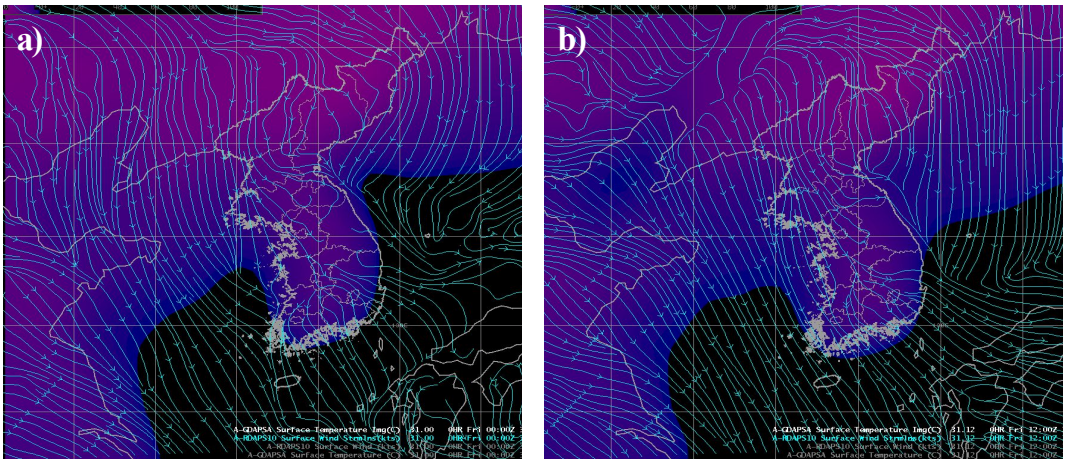

Fig. 3.30. Distribution of surface temperature and streamline at a) 0000UTC and b) 1200UTC 31 December, 2004.

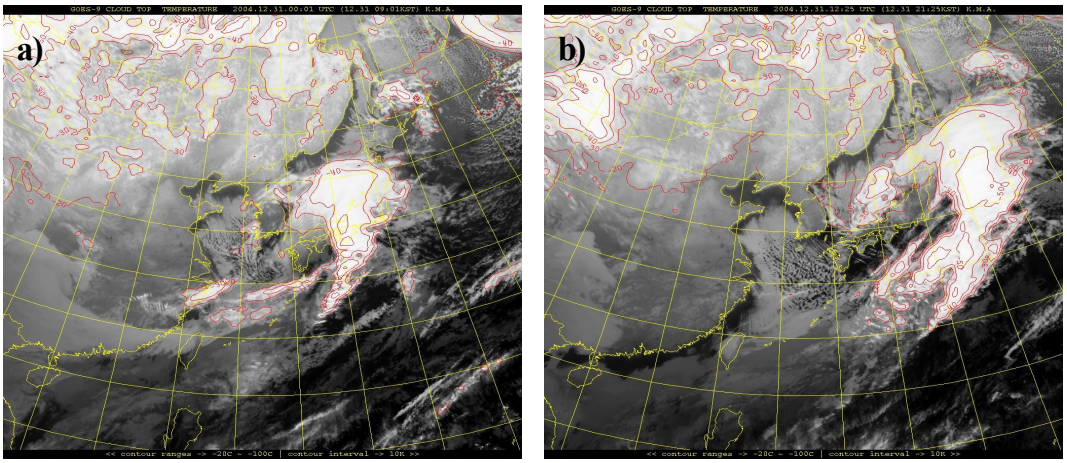

Fig. 3.31. Distribution of Cloud top temperature at a) 0000UTC and b) 1200UTC 31 December, 2004.

According to the cloud top temperature and cloud top altitude in figure 3.31 and figure 3.32, a convergence zone was formed in the west coast in the morning of the 31st and a lot of snowfell in west coast of Jeonlanamdo and Honam inland area.

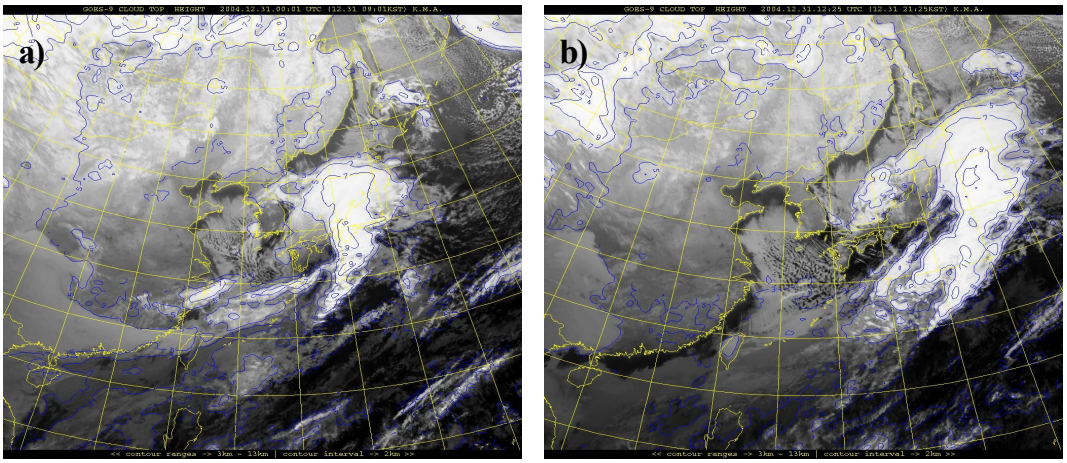

Fig. 3.32. Same as Fig. 3.31 but Cloud top height.

Here, the cloud top altitude was 3km and the cloud top temperature was recorded to be -30℃, but the cloud top altitude was 1~2km and the cloud top temperature was -20℃ in the afternoon when the snowfall only occurred in the west coast region. This is a difference from the characteristic of snowfall by way of pressure trough which affects inland also. The average sea surface temperature for the 7 days was 10~15℃ in the west coast.

When we look at the condition which occurs during heavy snow through our case, it could be seen that according to the overall temperature analysis at 850hPa, the normal snowfall was much at under -7℃ and heavy snowfall was much at -12℃.

As for the sea air difference, there was a big difference between the normal snowfall and the heavy snowfall. When looking at the deviation for the 850hPa and temperature of-SST, we can see that the snowfall fell at over 13℃ and the heavy snowfall fell at over 22℃ and in the ground

temperature-SST, the temperature was over 4℃ during normal snowfall and over 9℃ during heavy snowfall. The summary of the temperature, humidity, wind strength and deviation is as follows. The pattern and strength of the snowfall change depending on the steering current.

In other words, when the NW current blows hard, the possibility of heavy snowfall was big in the west coast region and especially when NW current of over 20m/s was infused strongly at around 850hPa, snowfall showed even in the inland. Also, when the NW current changes into a north current, the temperature deviation between the upper and low layers increase but the snowfall either weakens or terminates.

According to the comparison result of the temperature deviation between the low and upper layers, the higher the temperature deviation for the 850 to ground is rather than the deviation between 500-850hPa, the possibility of snowfall was big. The time zone when the heavy snowfall falls was mostly in the dawn when the cooling of the upper atmosphere is intensified. Heavy snowfall fell up to the inland of Honam region when the upper layer' s trough passed during expansion of cP and when a convergence zone was formed in the west coast region during expansion of cP, a regional heavy snowfall occurs. The dew point depression change in the lower and upper layers can be utilized as a reference data to judge the possibility of snowfall, start and termination of it and the intensity of it.

C. Extratropical Cyclone Effect

1. Overview

The migratory anticyclone centered in the west and south coast affected and weak pressure trough was following it from behind from central China region and southern China region. A weak low pressure occurred in the north of gulf of Pohai also and there was developed low pressure behind it. And the Korean peninsula showed a status of weak wind and low waves of sea because the pressure gradient force was small. A weak pressure trough which has moved toward the east from the Central China as the strength of migratory anticyclone weakened advanced toward the south coast and passed between the January 22 and 23.

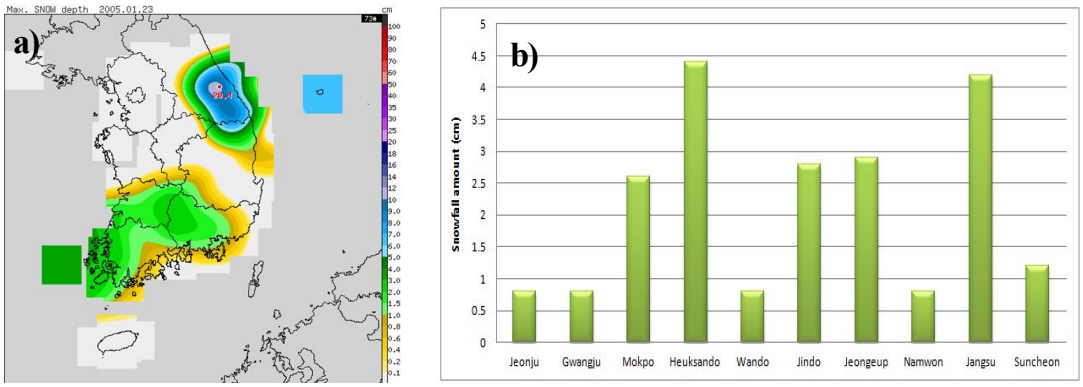

Fig. 3.33. Distribution of a) maximum fresh snowfall amount in Korea and b) snowfall amount by each station in Homan region on 23 January, 2005.

It was expected that the pressure trough which was moving east and southward from East of Mongolia would pass Manchuria and Maritime province, advance toward the northern coast of East Sea around dawn on 23nd and develop and move eastward. And, the pressure gradient force in the surroundings of our country showed a lying type and thus the wind was weak. There were areas where snow or rain fell in the southern region on the January 23 due to the pressure trough which was moving eastward from the south coast area of Jeju island.

As the pressure trough which was formed from southern Mongolia to the south region passed Manchuria on the January 23 and the migratory anticyclone was divided between the east and the west, a pressure trough was formed in the east coast. And the moist which flowed into the southern region on the January 22, affected the pressure trough in the south region until the afternoon. On the January 24, the pressure trough developed in the north coast of east sea and moved eastward and the continental high pressure entered into the phase of expansion. As the cold and dry continental high pressure which develops in Siberia goes into the phase of expansion, the pressure distribution of north high and south low type was formed and Yeongdong are a of Gangwondo and east coast area of Yeongnam were affected by northward current. A gradually slanted temperature ridge was reached and the temperature was in the rising trend, and the moist flowed from west coast of south sea passed southern region during the morning of January 22 and flowed into the southern region from the east Chinese sea around the end of the second day from January 22 and snow fell.

2. Synoptic Weather Analyses

a. Surface and Upper Weather Charts

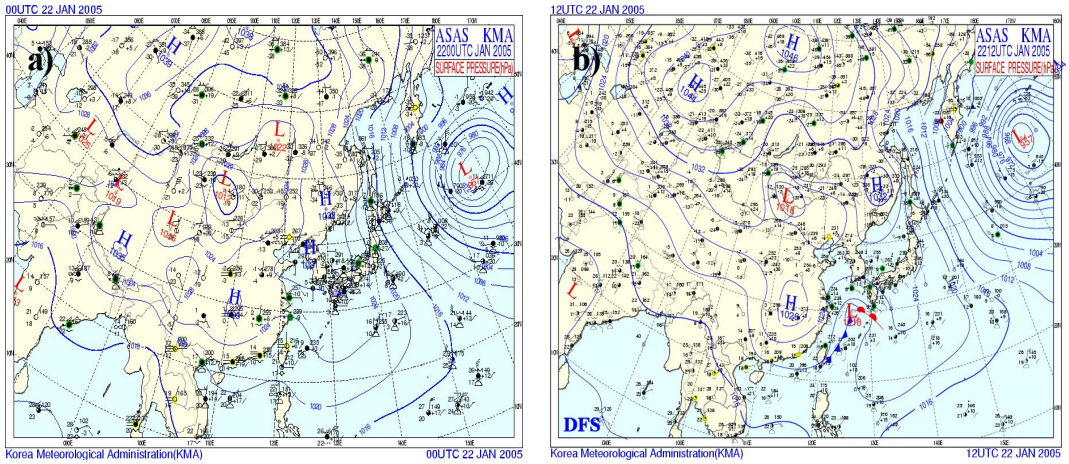

Fig. 3.34. Surface pressure chart at a) 0000UTC and b) 1200UTC 22 January, 2005.

The figure 3.34 is a meteorological weather chart. Our country was affected by cold high pressure in most of its regions on the January 22.

A cold high pressure was located in the north of our country and snow fell in the south and west coast of our country due to the low pressure located in the southwest of Kyushu. Figure 3.35 is a weather analysis of 850hPa. The pressure trough and the temperature trough were very deep in the west and south coast of our country in the morning of the January 22, and they affected the southwest coast and west coast.

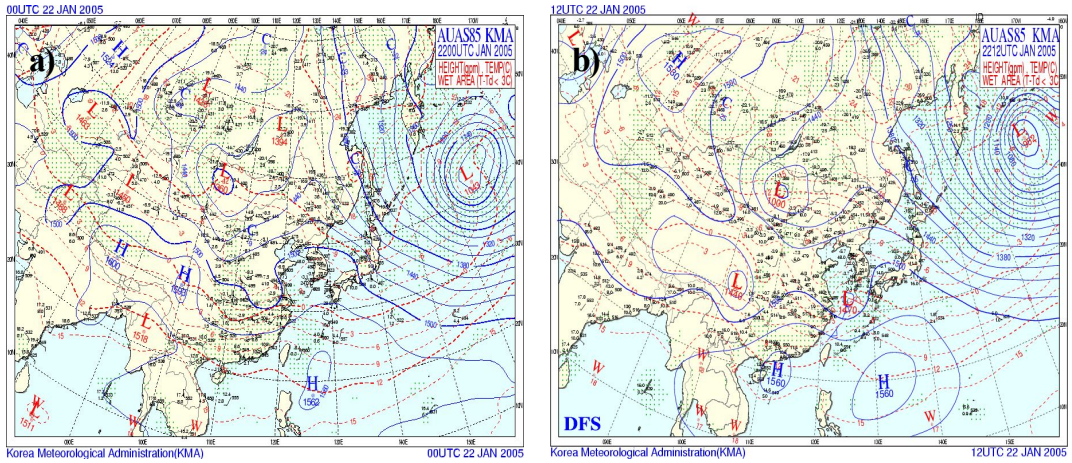

Fig. 3.35. Same as Fig. 3.34 but 850hPa geopotential height and temperature.

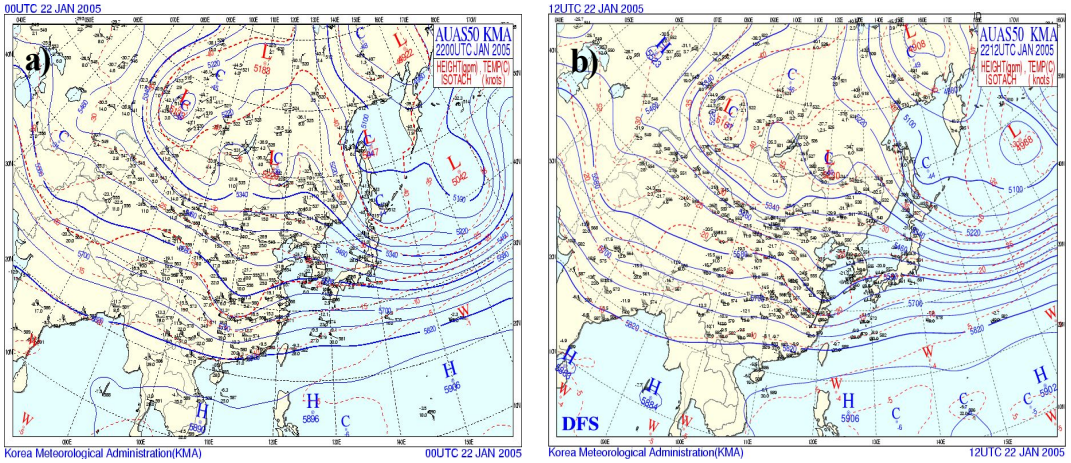

Fig. 3.36. Same as Fig. 3.34 but 500hPa geopotential height, temperature and isotach.

According to the weather analysis for 850hPa as in figure 3.35, the pressure trough located in Shandong area of China started to be fortified in the northeast area. The Baroclinic zone passed the east coast centering In Fig. 3.36, we can see that at 500hPa, the pressure trough associated with both strong northwest of the Shandong Peninsula in China began to be strengthened. At 1200UTC on 22, a Baroclinic zone was seen moving to the southwest of South Korea while passing the west coast, including the Honam central axis.

b. Radar and Satellite Images

According to the meteorological analysis radar image in Fig. 3.37, an Echo occurred in the southwest coast at around 0900UTC at 9 o' clock when the pressure trough passed by, and the round and long type of the echo band was maintained in the west coast region of Honam area, and an Echo was formed in the south coast region.

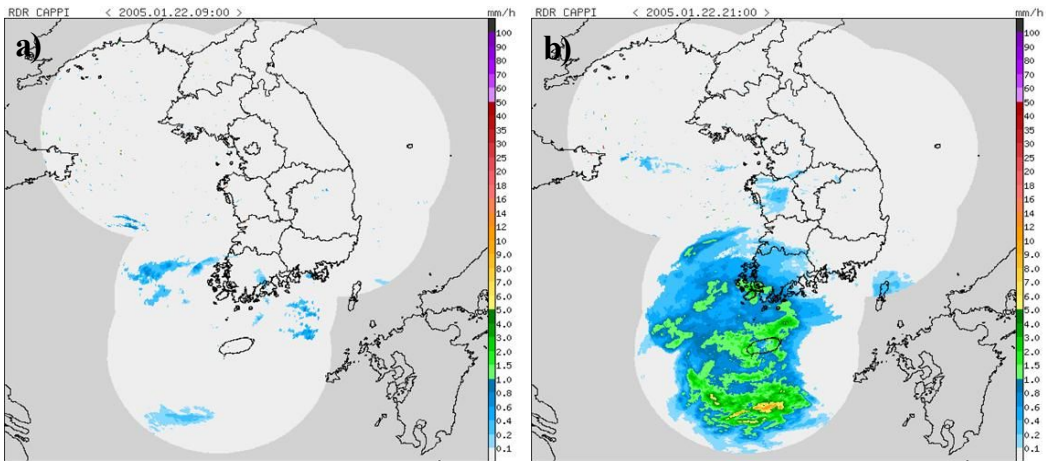

Fig. 3.37. Radar image (echo tops) a) 0000UTC and b) 1200UTC 22 January, 2005.

According to the satellite data in the figure 3.38, as low pressure passed by southwest region of our country, a large cloud band was formed and snow fell in Jeju region including south coast region. As cloud

formed when low pressure moved northeast by the effect of the high pressure in the north, a large distribution of cloud was seen in Honam west coast region including west coast.

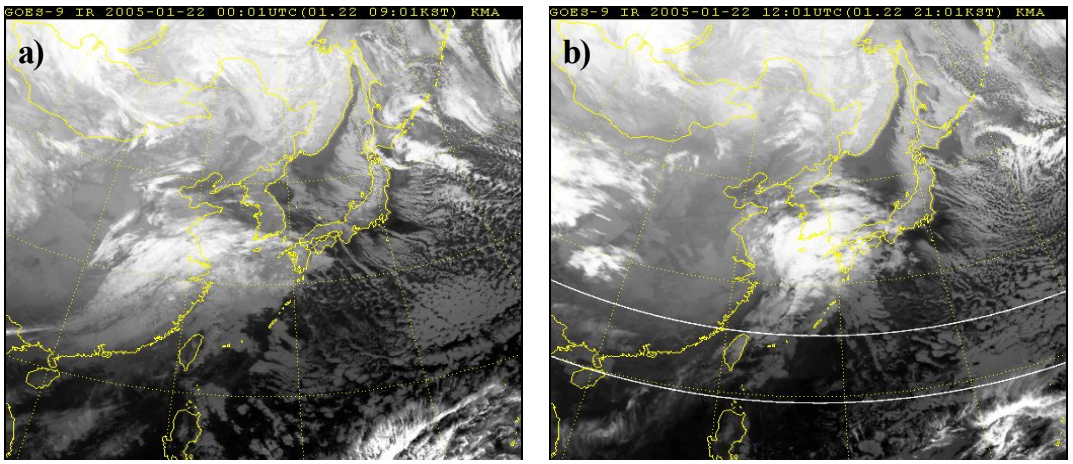

Fig. 3.38. Same as Fig. 3.37 but GOES-9 Infrared image.

3. Characteristics of Horizontal and Vertical Structures

According to the figure 3.39, it can be seen that a convergence region is strongly shown at 700hPa in the center of Mopko in the cross-section from north to south at 1200UTC.

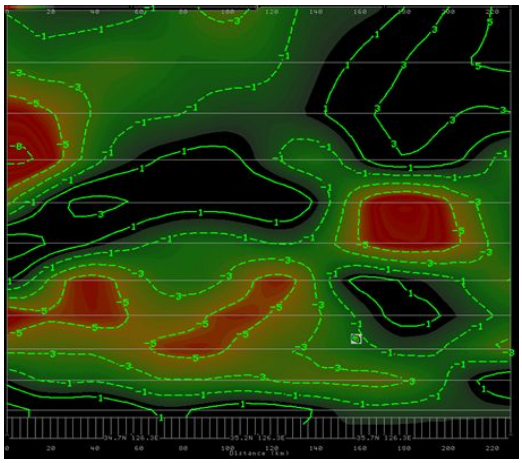

Fig. 3.39. Vertical cross-section of moisture flux advection along west coast at 1200UTC 22 January, 2005.

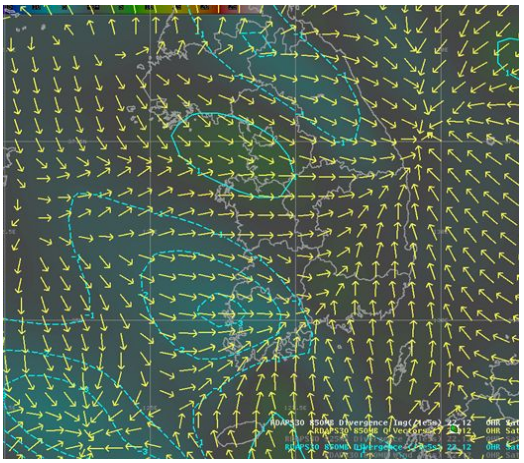

Fig. 3.40. Distribution of 850hPa convergence at 1200UTC 22 January, 2005.

Fig. 3.40 is the analysis of the convergence region at 850Pa, and a Q vector convergence is formed in the center of Jin Island, and a frontal surface is distinctly shown. Especially, a convergence region at 850hPa is formed in the center of the west coast and Heuksan Island and a surface of discontinuity was formed.

Fig. 3.41 is the analysis of the Vertical cross-section of Omega value, and at 09UTC, the overall omega value is not high, but after three hours at 12UTC, the omega value started to increase slowly near the upper layer between Heuksan Island and Jin Island. It could be seen that the omega value increased rapidly on Jin Island at 18UTC.

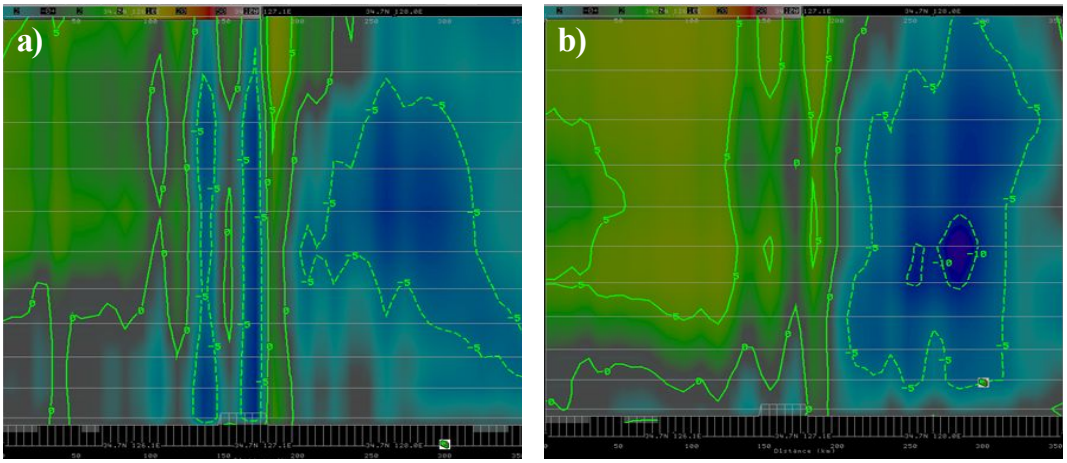

Fig. 3.41. Vertical cross-section of Omega along the area from west sea to Busan at a) 0900UTC and b) 1200UTC 22 January, 2005.

Fig. 3.42 is the Skew T - Log P diagram chart at 0900UTC and 12UTC, and at 12UTC, helicity became stronger to be up to 116, and when analyzing the vertical wind shear of the upper and lower layer, wind shear showed strongly on the lower and upper layer to be approximately 180° . Fig. 3.43 displays the Vertical cross-section of moisture flux advection in the west coast. In the center of Jin Island and Mokpo, the value over five showed strongly at up to 700hPa, and at 15UTC, it showed distinctively on the lower layer.

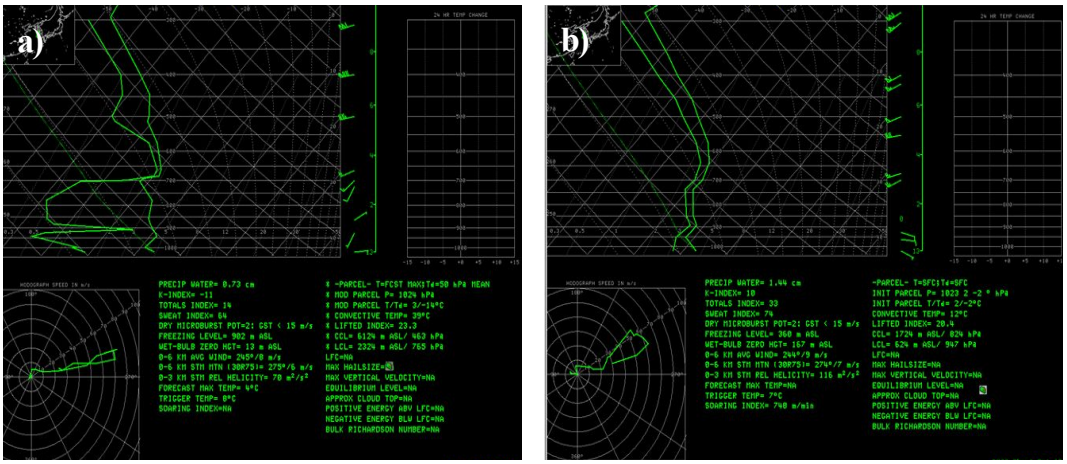

Fig. 3.42. Skew T – Log P diagram at a) 0600UTC and b) 1200UTC 22 January, 2004.

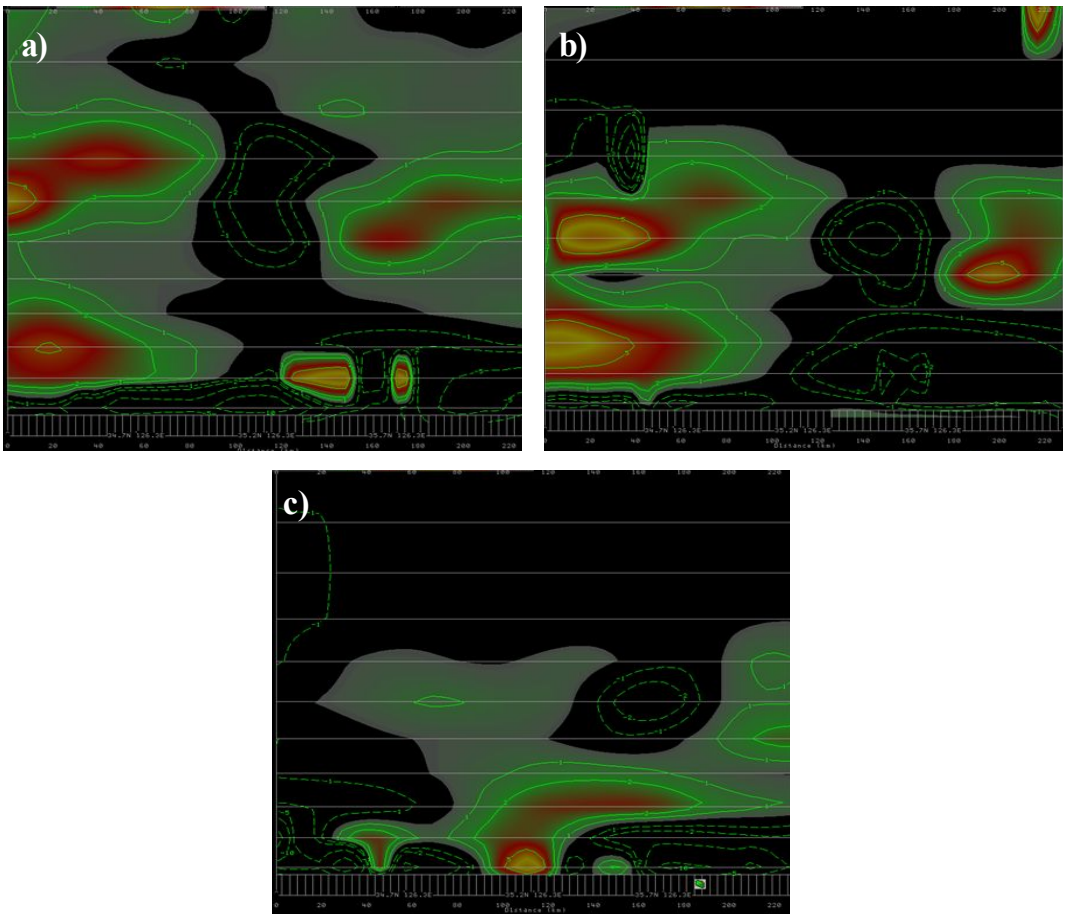

Fig. 3.43. Vertical cross-section of moisture flux advection along west coast at a) 0900UTC, b) 1200UTC, and c)1500UTC 22 January, 2005.

Fig. 3.44 shows the direction of wind shear rapidly changing to form a surface of discontinuity in Jin Island at 12UTC. And on the lower layer, hot and humid mild drift (vertical direction: clockwise) is strengthened and cold drift appeared after 1200UTC. Also on the upper layer, cold air from the northwest part could be seen moving south. Similar to Jin Island, Heuksan Island experienced a very strong direction of wind shear at 1200UTC and showed a surface of discontinuity, and a front formed near 850hPa.

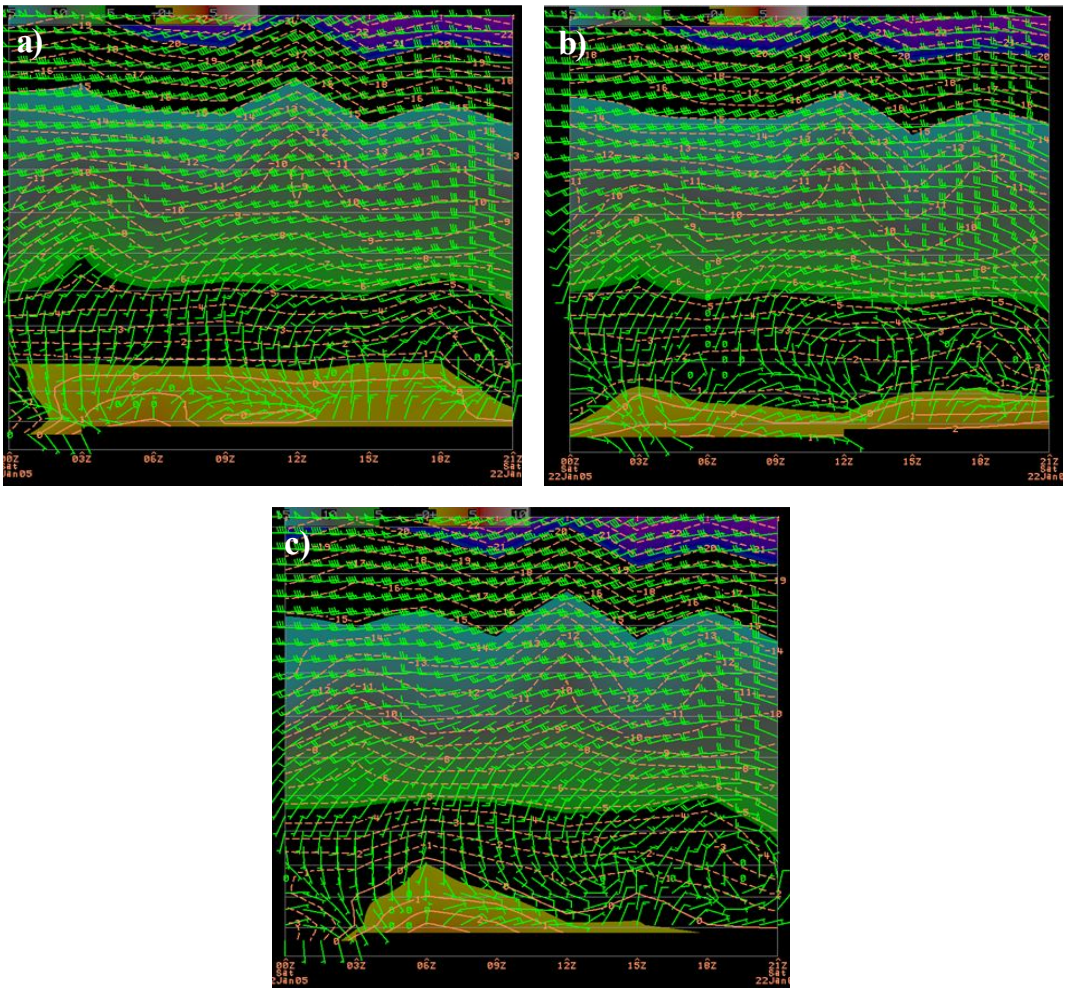

Fig. 3.44. Time-height distribution of temperature and wind at a) Jin-do, b) Heuksan Island, and c) Gwang-ju from 0000UTC to 2100UTC 22 January, 2005.

Also on the upper layer, cold air from the northwest part can be seen moving south. Similar to Jin Island, Heuksan Island experienced a very strong direction of wind shear at 1200UTC and shows a surface of discontinuity, and front form near 850hPa. Before 1200UTC (peak), the mild drift is strengthened, and afterwards the cold drift becomes strong. As the wind system at 700hPa changes from the southwest to northwest, it can be seen that rainfall gradually weakens. In the center at 18UTC, a snowdrift started and at this time near 850hPa, a surface of discontinuity is formed. Before this starting point, a mild drift is followed by a cold drift, not as strong as in Heuksan Island and Jin Island.

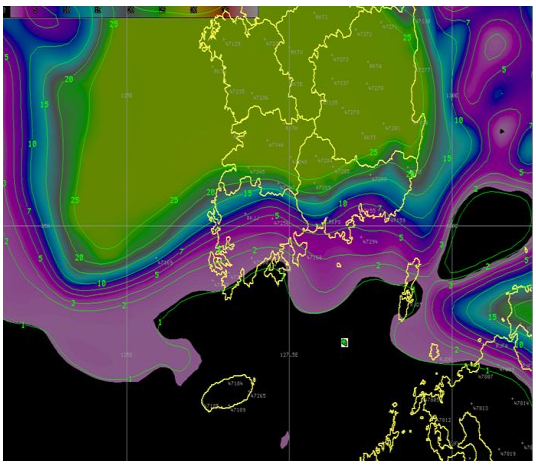

Fig. 3.45. Same as Fig. 3.40 but 850hPa dew point depression.

Fig. 3.45 is the form of a carriage line below the 2 degrees line located on the southern coast. A cold dry part was formed in the northwest part in the boundary of Heuksan Island, and a warm and very humid part was formed in the southeast.

Looking at the conditions of heavy snowfall in this case, during the observation period, the center of Low pressure is located on the south side, and the area seems affected by the trough of low pressure. In

addition, deviation by region showed greatly in regions with heavy snowfall.

As for the wind system of the ground, the main wind specie was NE~ENE sort of wind in southwest coast of Jeonnam including Heuksan island and Jin island and the N wind and N~NNW sort of wind in inland area of Jeonbuk including Jangsu and Imshil.

A 500hPa temperature line of -22℃ showed in a long shape in the south to north direction on South Korea' s west coast, and an 850hPa temperature line of -3℃ showed across the southern coast from the east to west direction. Here, the cold air from the north met with warm air on the south and a surface of discontinuity, such as temperature and direction of wind shear was formed and as a warm front was formed, heavy snowfall fell in Jin Island.

For analysis of the role of the low layer, analysis of wind and the equivalent potential temperature at 850hPa, 925hPa is important; it is important to analyze a convergence field and the equivalent potential temperature-density region.

For geographical features, a topographic effect analysis in the center of the Sobaek Mountain range and the difference in the equivalent potential temperature between the east and west were analyzed to find where convective instability is strengthened, and the analysis of the downwind side by way of the vertical side is important.

For time series data analysis, the direction of wind shear analysis is important along with temperature analysis, and it is very useful in rainfall strength analysis. The difference in the equivalent potential temperature of the upper and lower layer and wind data analysis are important factors in determining the degree of convective instability.

Analyzing the date of this case, in the case of heavy snowfall due to a Low pressure effect, it is considered that the role of the lower layer, vertical side analysis, geographical feature effect, and time series data are important.

CHAPTER Ⅳ. SST SENSITIVITY EXPERIMENTS TO HEAVY SNOWFALL

A. Numerical Experiments

1. Model Design and Initial Condition

This experiment was to comprehend the effect of the 2 dimensional distribution of the sea surface temperature of various types on the heavy snow and the numerical experiment was performed around regions which include West coast of Jeollabukdo and West of Gyeongsangnamdo.

Generally, the Sea Surface Temperature data used in the numerical experiment is the climate value or the sea surface temperature data composed by overlapping the satellite data for around 15 days to obtain the data from which the cloud is removed. However, the west sea is very shallow in depth, and the effect of tide is very big compared to other regions and thus the trend of the sea surface temperature has a strong trend of changing rapidly. (Korea Meteorological Administration, 2006).

As the sea surface temperature data used in this experiment, the climate value explained in the introduction and the sea surface temperature data of RTG SST and OSTIA where the daily sea surface temperature was reflected were used. The initial data used in the numerical mock test is the FNL (Final operational global analysis data) data provided by NCEP and each domain is lattice spacing of 27km, 9km and 3km. The physics option used in this study is showed in Table 4.1.

The RTG SST which has the spacial resolution of 0.5° × 0.5° is being used in the work-site model in NCEP of U.S.A and the OSTIA SST from England which has a higher spacial resolution than this, 0.25° × 0.25° were interpolated and compared in order to investigate the effect of the heavy snowfall condition which develops through the interaction between the atmosphere and the sea depending on the SST change.

The numerical experiment was performed based on the heavy snowfall case of 30 December, 2010 (case 2010) and the heavy snowfall case of 28 December, 2012 (case 2012) of which the snow occurrence mechanism of Honam region are different. The case 2010 occurred by way of the cold Siberian air pressure which expands as we have analyzed in the previous chapter, and strong snowfall appeared based on west coast of Honam region.

On the other hand, the case 2012 was by way of the migratory cyclone and heavy snowfall was recorded in the south sea of Honam region and west region of Gyeongsangnamdo.

Table 4.1 The configuration of numerical model WRF.

	Domain 1	Domain 2	Domain 3
Horizontal grid	50 x 50	61 x 61	85 x 121 (2010) 112 x 112 (2012)
Resolution	27km	9km	3km
Vertical layers	28 Layers		
Physical process	WRF Single-Moment 6-class scheme		
	RRTM scheme		
	Dudhia scheme		
	MM5 similarity		
	Noah Land Surface Model		
	YSU scheme		
	Kain-Fritsch scheme		
Initial data	NCEP FNL Operational Global Analysis data		
Time period	2010.12.29.0000UTC ~ 2010.12.31.0000UTC 2012.12.27.0000UTC ~ 2012.12.29.0000UTC		

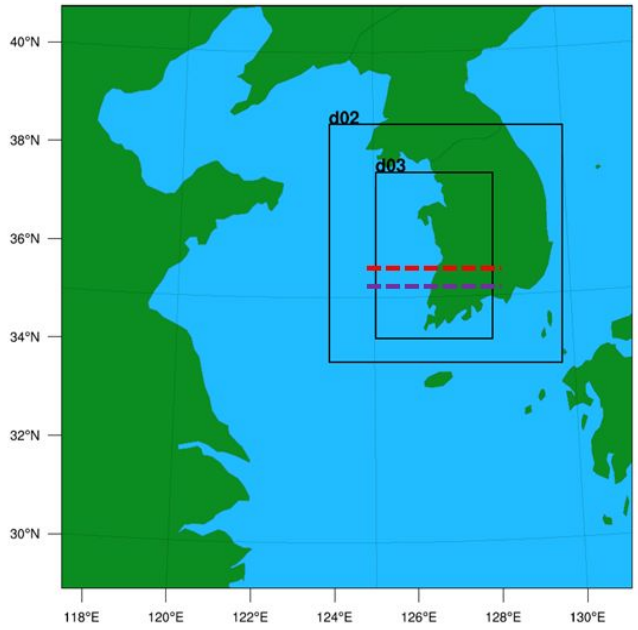

Fig. 4.1. Model domain with intervals of 27㎞ (domain 1), 9㎞(domain 2), and 3㎞(domain 3).

Accordingly, the domains of this simulation were configured to be different from one another. The nested grid of numerical models of each case is showed in Fig. 4.1. Firstly, the number 1 nested grid comprises East Asian region which includes West Sea and East Chinese Sea and the lattice spacing is 27km. The 2nd nested grid has 9km of horizontal lattice spacing, comprising the west and east regions and the whole south regions of Korean peninsula. The nested grid 1 and 2 were applied to the same extent in the two experiments.

The last nested grid has different heavy snowfall occurrence regions and thus was configured to be different. Case 2010 was composed based on the west coast of Honam and the case 2012 was configured based on the southwest coast of Korean peninsula. The lattice spacing is the same to be 3km.

2. Case Selection

a. Continental Anticyclone Expansion(30 December, 2010)

In 29~30 December, 2010 these two days are the case starting from west coast, and on the 29 December, by the effect of Low pressure from northwest part, cold continental anticyclone expanded, resulting in cloudy weather nationwide, and central region (Gangwon Youngdong excluded) including Seoul and Jeollanamdo and Jeollabukdo with snow.

On 30 December, the Low pressure in the east coast of Japan developed and slowly moved east; the Low pressure near Gulf of Pohai slowly moved southeast.

Continental anticyclone near Lake Baikal was slowly moving southeast, the whole country had snow due to effect of the low pressure and then the cold continental anticyclone which was expanding in the northwest. By blocking High pressure located east of Siberia, barometer flow on high latitude slowed down, but as joint Low pressure accompanied by cold air from central Manchuria backlashes to let pass the short wave trough, and trough of Low pressure passed from the continent, etc. The medium latitude was regularly influenced by the trough of Low pressure.

Trough of Low pressure near Gulf of Pohai developed with the support of cold air (−44℃), and moved southeast, and as it keeps moving southeast to promote development of surface Low pressure, it affected South Korea until morning in 30 December. Meanwhile, joint Low pressure near Manchuria accompanied by short wave trough are each located in central Manchuria and Maritime Province, and as the short wave trough backlashed to pass trough of Manchuria on dawn of 31st and the trough of maritime province passed through southern region on the 31st, making the cold air drift and induced strong snow cloud in the west coast.

From dawn on the 30 December, with a lot of wind, a strong wind warning and heavy snowfall watch were announced in part of southern west coast in Honam and when afternoon of the 30 December approached,

due to the effect of trough of Low pressure, most regions of inland Honam were expected to have strong wind warning, heavy snowfall watch, and thus heavy snowfall fell. A lot of snow fell in the central region and there were regions in east coast of Gangwondo where snow fell in the midst of the night due to the infuse of the eastward current.

On 30th December, heavy snowfall fell in inland Honam region and west coast region, and from late afternoon, with the cold continental anticyclone influence, all parts of the country became relatively clear and as blocking high located in Siberia gradually weakened and move southeast, joint Low pressure which was developed and located in Manchuria slowly weakened and moved east. As joint Low pressure developed and located in Manchuria almost stagnated and short wave trough regularly moved south, cold air was continuously lowered to show cases of severe cold for the time being.

Fig. 4.2. displays the distribution of maximum fresh snow depth in South Korea on 30 December. A lot of snow fell in the Honam region, and most regions had snow excluding some regions of Gyeongsang.

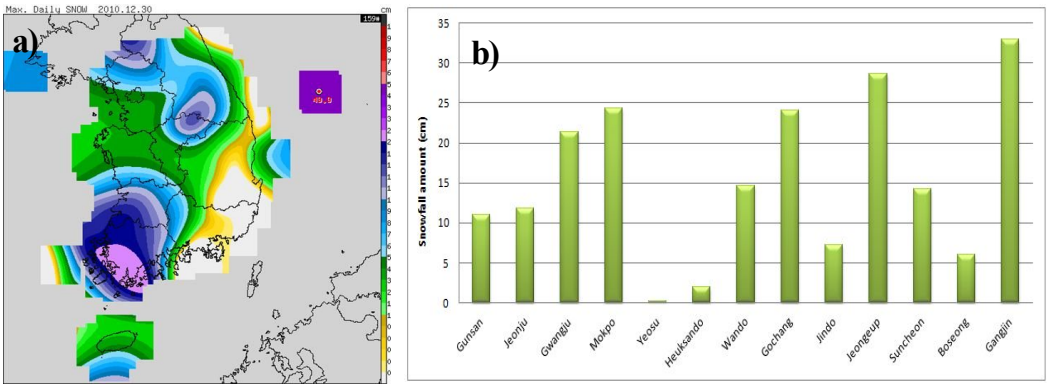

Fig. 4.2. Distribution of a) maximum fresh snowfall amount in Korea and b) snowfall amount by each station in Homan region at 30 December, 2010.

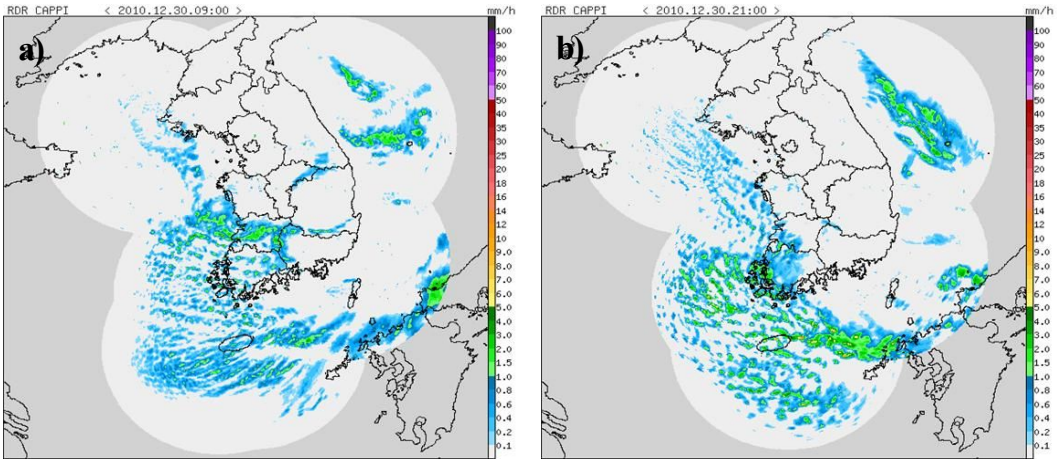

Fig. 4.3. Radar image (echo tops) at a) 0000UTC and b) 1200UTC 30 December, 2010.

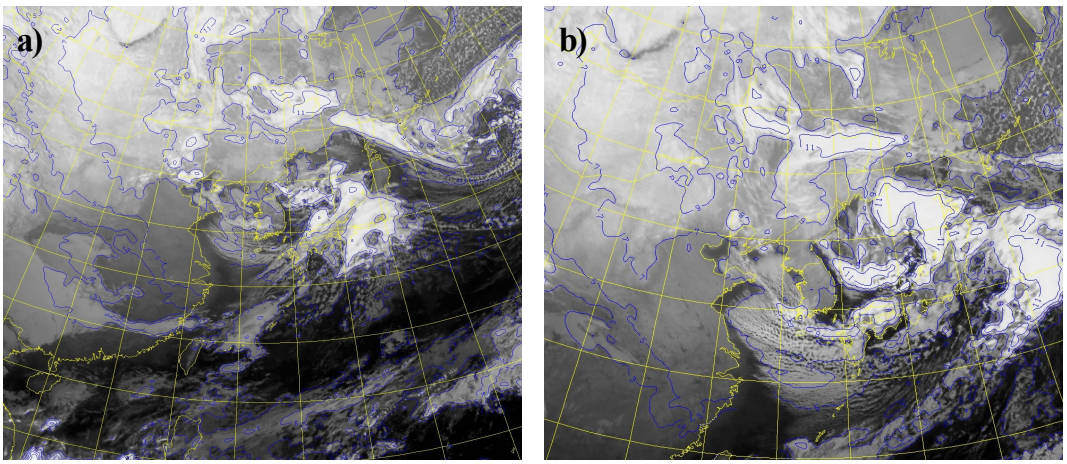

Fig. 4.4. Distribution of cloud top temperature superposed on satellite image at a) 0000UTC and b) 1200UTC 30 December, 2010.

Fig. 4.3 is the radar image of 30 December, and at dawn, Echo was formed in front of the west coast, and as it slowly moved southeast, snow cloud was formed on the west coast at dawn on 30 December. Afterwards, the snow clouds formed in the front of west coast gradually weakened. In Fig. 4.4 at noon of the 29th, cP expanded from the Shandong Peninsula to the Honam region and a strong convergence was formed and a rising current developed and cloud was formed up to more than 9km up to the middle atmospheric layer.

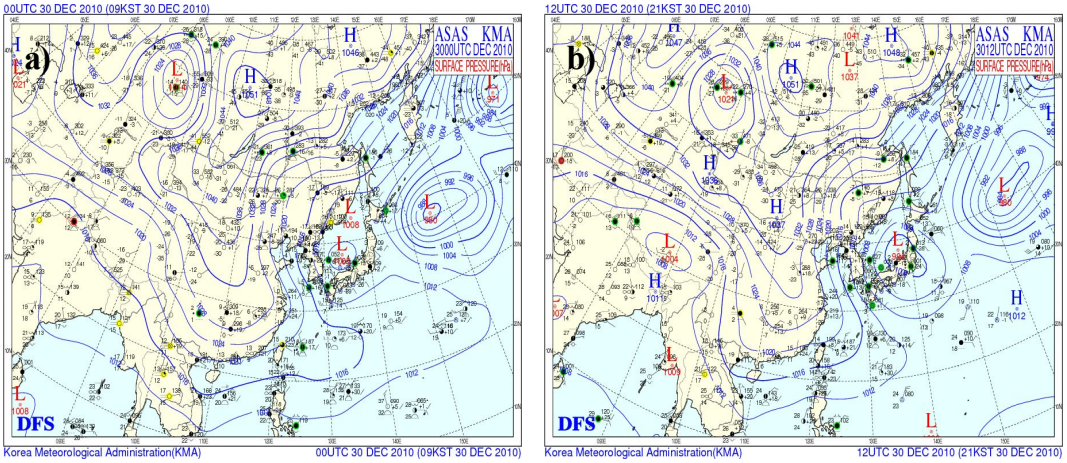

Fig. 4.5. Surface pressure chart at a) 0000UTC 30 and b) 1200UTC 30 December, 2010.

Fig. 4.5 is the surface pressure chart of the case day. A Low pressure from the eastern coast of Japan developed and was moving east, and the Low pressure near the Gulf of Pohai slowly moved southeast. A continental anticyclone near Lake Baikal was slowly moving southeast, and in the morning of 31 December, a cold continental anticyclone will take effect, but the Chungcheongnamdo west coast and Jeonllanamdo and Jeollabukdo, Jeju Island, Ulleungdo · and Dokdo regions were affected by snow cloud generated by the sea-air difference.

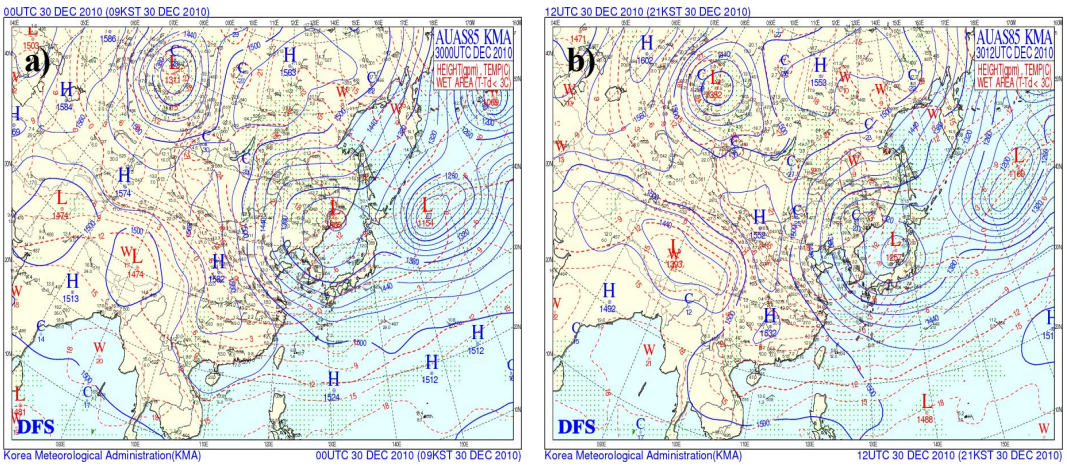

Fig. 4.6. Same as Fig. 4.5 but 850hPa geopotential height and temperature.

Fig. 4.6 is the 850hPa pressure chart of the case day. In front of the trough formed in the Gulf of Pohai, a lot of vapor was flowing in from the west~southwest current, creating snow on the western region of South Korea. As it moved southeast and expanded slowly nationwide, most of the snow stopped in the morning. Afterwards, in the eastern part of China, a temperature trough and baroclinic zone is formed, which slowly moved southeast and thus the temperature dropped with a strong wind.

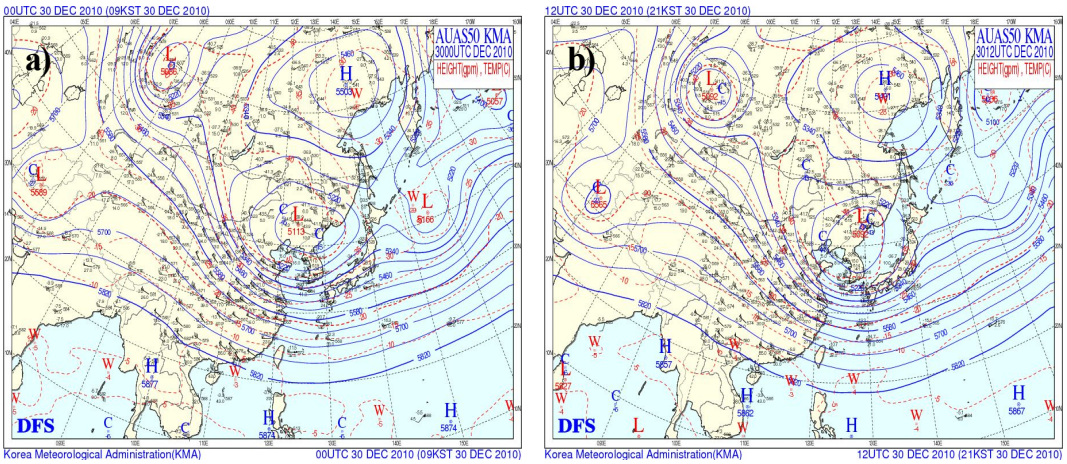

Fig. 4.7. Same as Fig. 4.5 but 500hPa geopotential height and temperature.

Fig. 4.7 is the 500hPa pressure chart of the case day. By the blocking of High pressure located east of Siberia, the barometer flow at a high latitude slowed down, and as a joint Low pressure accompanied by cold air in central Manchuria backlashed, a short wave trough passed, and just as a trough of Low pressure passed from the continent, the medium latitude was regularly influenced by the trough of low pressure. The trough of Low pressure near the Gulf of Pohai developed with the support of cold air (−44℃) to move southeast, and as it promoted the development of surface low pressure, it affected South Korea until morning. Short wave troughs near Manchuria were located in central Manchuria and the Maritime Province and backlashed to pass the southern region and the cold air drifted and strong snow clouds developed on the west coast.

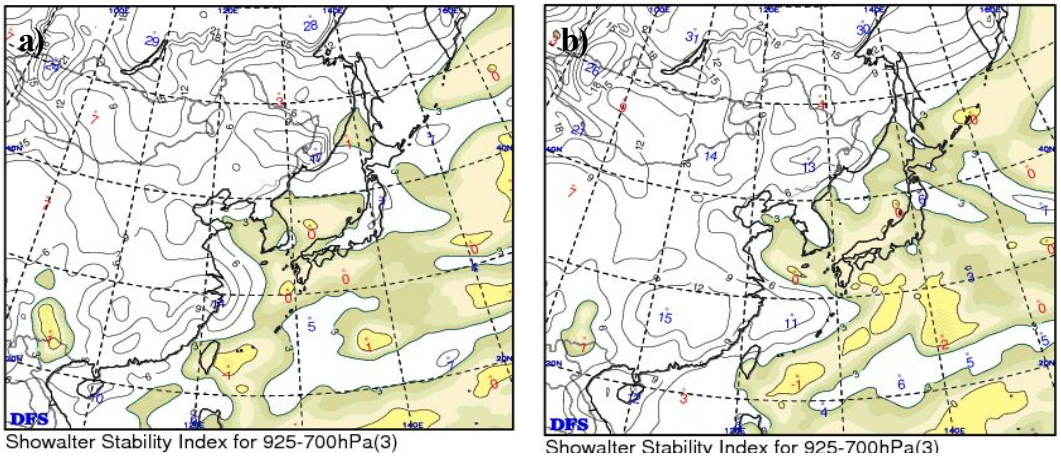

Fig. 4.8. Distribution of Showalter stability index for 925-700hPa at a) 0000UTC and b) 1200UTC 30 December, 2010.

Fig. 4.8 is the analysis of the Showalter Stability Index (SSI). SSI is the value of the elevated altitude of condensation at the 850hPa level climbing through the saturation adiabatic and meeting the 500hPa level. The meeting point temperature is subtracted from the value of the actual temperature on the same side, and when that value is below 4, the possibility of rainfall or snowfall is judged to be positive. From 1200UTC, 29 December after the SSI instability of 0~3 strengthened in all parts of South Korea, it gradually weakened from the afternoon of 30 December.

Fig. 4.9 shows the 24-hour temperature change analysis at 850hPa, and on 29 December, cold air (-11℃~-15℃) located in the inner China continent crossed the Korean west coast and cold air inflowed from dawn on 31 December; and on the morning of 31 December, the southern movement of cold air reached a peak point, and gradually eased off from the afternoon of 30 December.

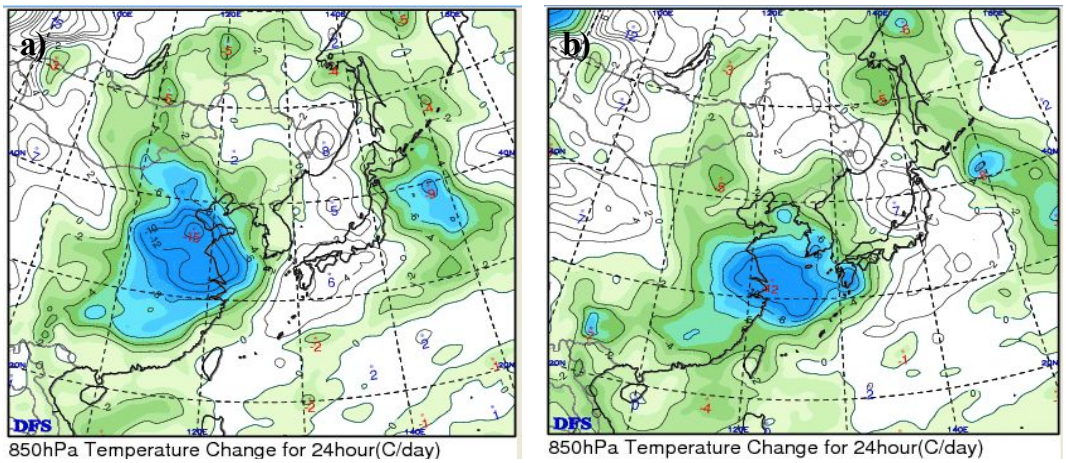

Fig. 4.9. Same as Fig. 4.8 but 850hPa temperature change for 24hour.

Fig. 4.10 shows the analysis at 500hPa vorticity. A joint Low pressure centered in the North Korea region from inland China was accompanied by a strong Low pressure positive(+) vorticity region and gradually moved south to form in the west coast and Honam region from dawn to morning on 30 December.

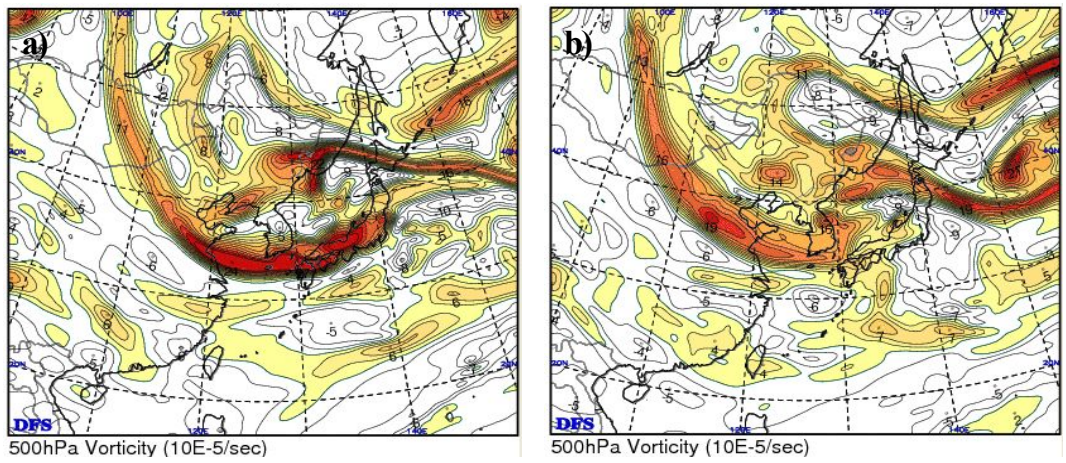

Fig. 4.10. Same as Fig. 4.8 but 500hPa vorticity.

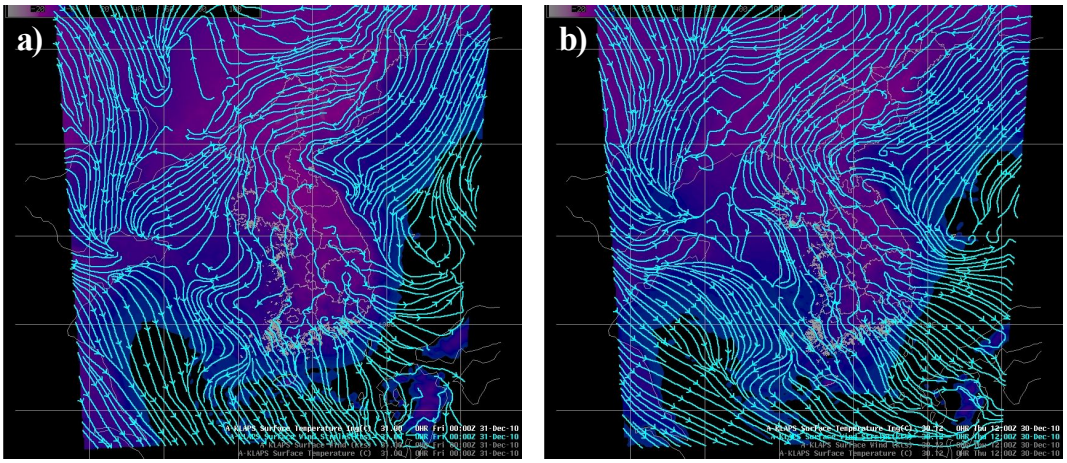

Fig. 4.11. Distribution of surface temperature and streamline at a) 0000UTC and b) 1200UTC 30 December, 2010.

Fig. 4.11 is the analysis of surface temperature (less than 1 degree) and Stream Line[KLAPS], and the inflow of the northwest current near Shandong Peninsula in China made a convergence zone, and the cold air moved south. On 30 December, all parts of the west coast were less than 1 degree and cold air moved to strengthen; and from the afternoon on 30 December, a constant effect of a cold High pressure was received.

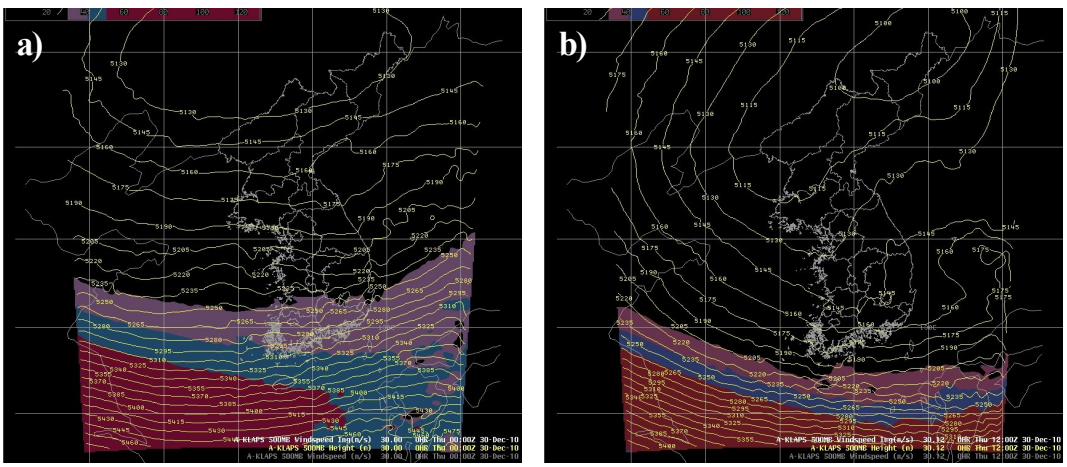

Fig. 4.12. Same as Fig. 4.11 but 500hPa geopotential height and wind speed.

Fig. 4.12 shows the 500hPa geopotential height and wind speed, and a joint Low pressure with the center in the North Korean region rotates and moves east for 5400gpm to descend to Jeollanamdo and Jeollabukdo and the coastal water of the west coast on 30 December, and strong winds over 100kts to the southwest coast was experienced. As the influence of the cold High pressure expanded, the strong wind moved south to create an inflow of strong cold air.

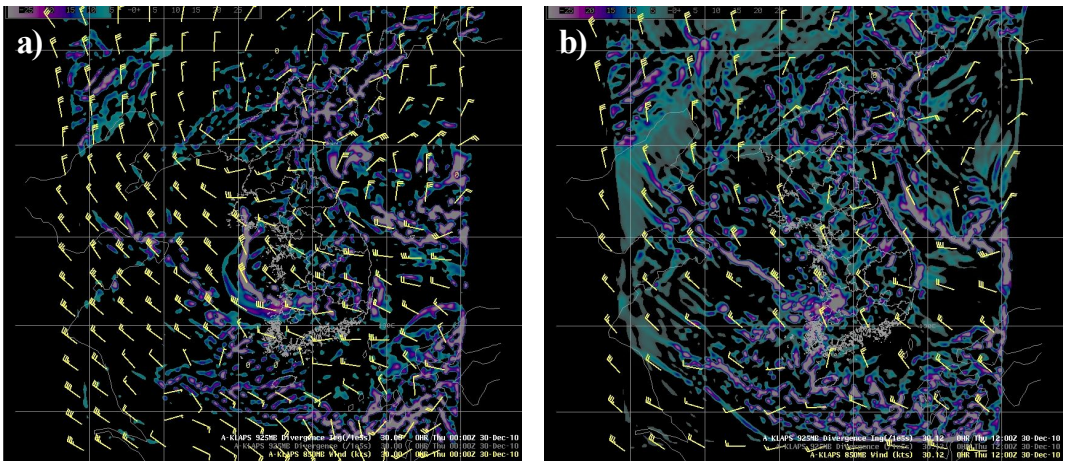

Fig. 4.13. Same as Fig. 4.11 but lower convergence, 925hPa divergence, and 850hPa wind.

Fig. 4.13 is the analysis of the lower convergence, 925hPa divergence, and 850hPa wind, and the overlap data at the 925hPa divergence field and 850hPa wind vector. On the night of the 29th, a strong convergence of the negative(−) field was formed in the central seas of the west coast, and at dawn of 30 December, after a Low pressure passed, a strong convergence showed in the west coast of the Honam region. Also in the 850 wind field, the northwest wind type changed to the west wind type from dawn to morning on 30 December, and strongly entered northern inland of Jeonllanamdo including Gwangju. Convergence region was also widely distributed, and it snowed a lot.

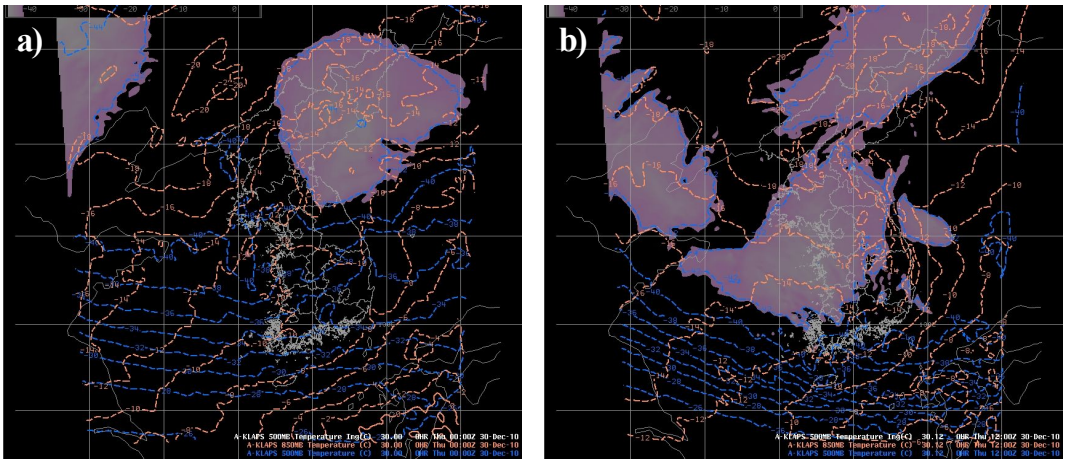

Fig. 4.14. Same as Fig. 4.11 but temperatures at top and bottom layer and chills nuclear(-40 Degrees) position.

Fig. 4.14 shows the temperature of the top and bottom layer and the location of the cold air center (−40℃), which at 0000UTC on 30 December is located in the inland China and North Korea region, and two cold air centers met and moved south through the west coast and inland of South Korea. A −10 degree line at 850hPa and −30 degree line at 500hPa descended onto the Honam region, and at 12UTC, a peak point of cold air moving south was recorded.

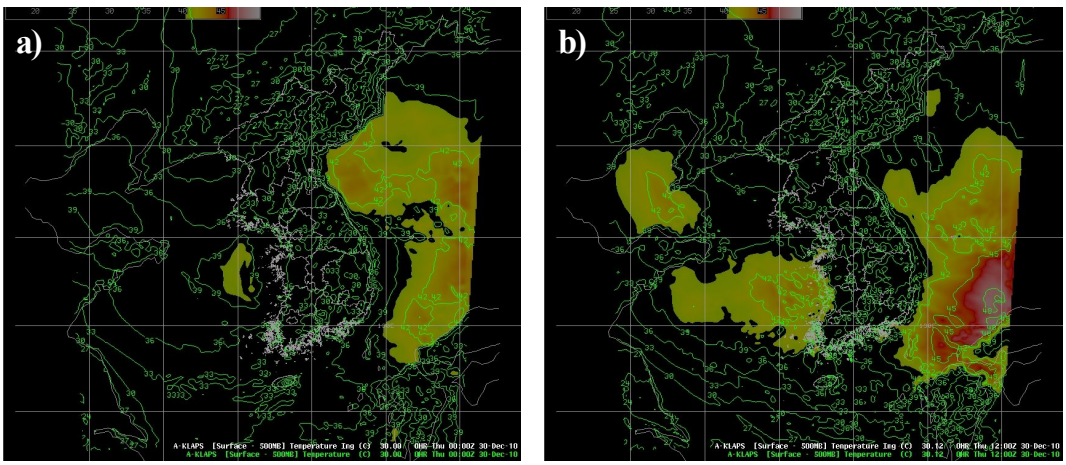

Fig. 4.15. Same as Fig. 4.11 but temperature difference between the top and bottom layer (surface-500hPa).

Fig. 4.15 is the analysis of the temperature difference between the top and bottom layer (surface−500hPa). On 30 December, as the temperature difference between the upper layer and lower layer reached over 40 degrees, it passed through all parts of the west coast to affect the southern west coast and inland of Jeollanamdo.

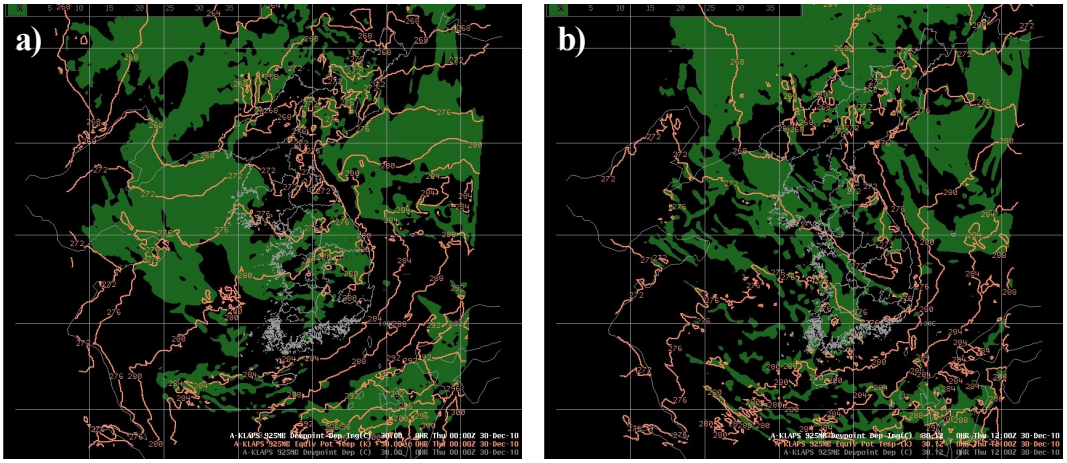

Fig. 4.16. Same as Fig. 4.11 but dew point temperature and equivalent potential temperature at 925hPa.

Fig. 4.16 is the analysis of dew point temperature difference at a 925hPa (less than 1℃) and equivalent potential temperature. At dawn on 30 December, moist troughs and equivalent potential temperature density troughs showed in the inland of the Honam region, and from the afternoon of 30 December, a heavy snowfall fell in the cold Honam region and cold air moved south. Fig. 4.17 shows the analysis of the top and bottom layer jet at 850hPa and 300hPa, and on 30 December, the top and bottom jet met to be located on the central coastal waters of the west coast; and on the morning of 30 December, a 300hPa strong wind trough became stronger and joined the trough and moved south to affect the Honam region; and after 06UTC, the joined trough moved south to Jeju Island and snow came to a lull.

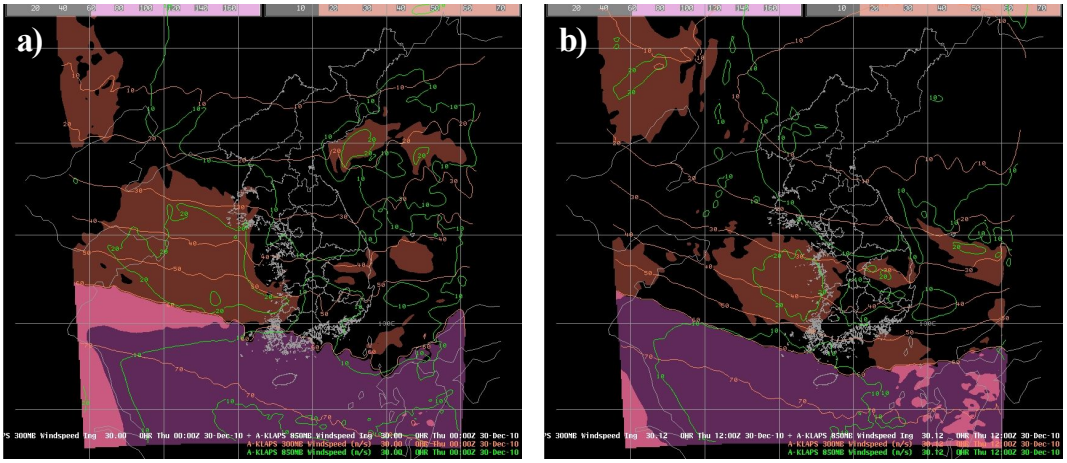

Fig. 4.17. Same as Fig. 4.11 but top and bottom layer jet at 850hPa and 300hPa.

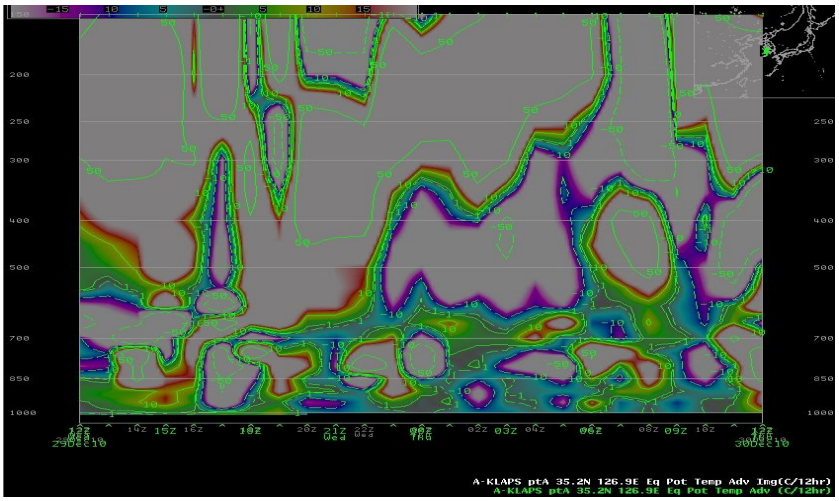

Fig. 4.18. Time-height distribution of equivalent potential temperature from 1200UTC 29 to 1200UTC 30 December, 2010.

Fig. 4.18 is an image of the Time-height distribution of equivalent potential temperature. On 29 December, the upper layer temperature dropped rapidly to cause convective instability and from 1300UTC, it started to be a high equivalent potential temperature trough. At 1500UTC, a strong cold air drift started from the surface to cause snowfall. At 2000UTC, an upper layer cold air drift continued; hot air current flowed

into the middle layer, causing convective instability, and with the a strong cold air current effect from the surface, the strength of the snowfall intensified. At 0000UTC, 30 December, a cold air drift in the upper layer continued whereby hot air current expanded to the middle layer and caused convective instability, and a strong cold air current developed on the surface, strengthening the intensity of the snowfall.

2. Extratropical Cyclone Effect(28 December, 2012)

The case day of 28 December, 2012 is the case when the Low pressure passed the south coast and recorded much deeper snow in the center of south region and which has recorded heavy snowfall in Chungcheongbukdo and south region.

In this case day, much precipitation was expected in the Low pressure regions when the thick humid layer was formed in the high and low layers. According to the forecast of the meteorological office on the case day, the Low pressure center location was expected to form to the south on 28 December(15cm of deep snow case in the south inland region), and the amount of precipitation was expected to be much greater because the thickness of cloud was thick. While the precipitation falls during the time between dawn and morning, the temperature falls to minus degrees in most regions except Jeju Island and the snow falls and in many regions, there were piles of snows and the snow fell as a wet moist type for a short period of time and much snow was piled up.

The south coast was also 925hPa and the temperature was around 0 degree and had many places where snow fell and the south region was expected to be 3~10cm (15cm maximum in certain regions) Being affected by the Low pressure that passes south coast, the east coast of Gangwon region was affected by the topography and the east wind infuse until evening as this Low pressure goes away toward the east side, and with the effect of the Low pressure that passes the south of Jeju on 28

December, our country had snow in most of the regions except the north Gyeonggi region starting dawn. In Chungcheongbukdo region, snow started falling since dawn with the south and middle region as the center and relatively large snow fell up to 7cm in Chupungnyeong, 3cm in Chungju etc. Fig. 4.19 is the analysis of the meteorological radar image of the case day.

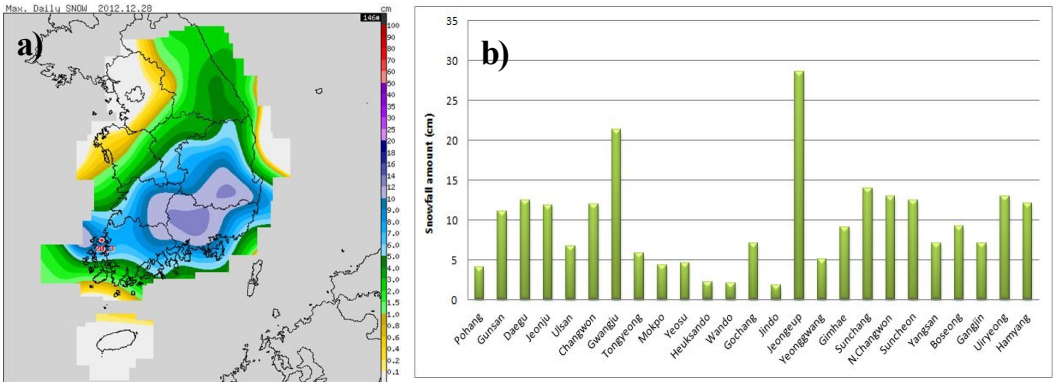

Fig. 4.19. Distribution of a) maximum fresh snowfall amount in Korea and b) snowfall amount by each station in Southern region at 28 December, 2012.

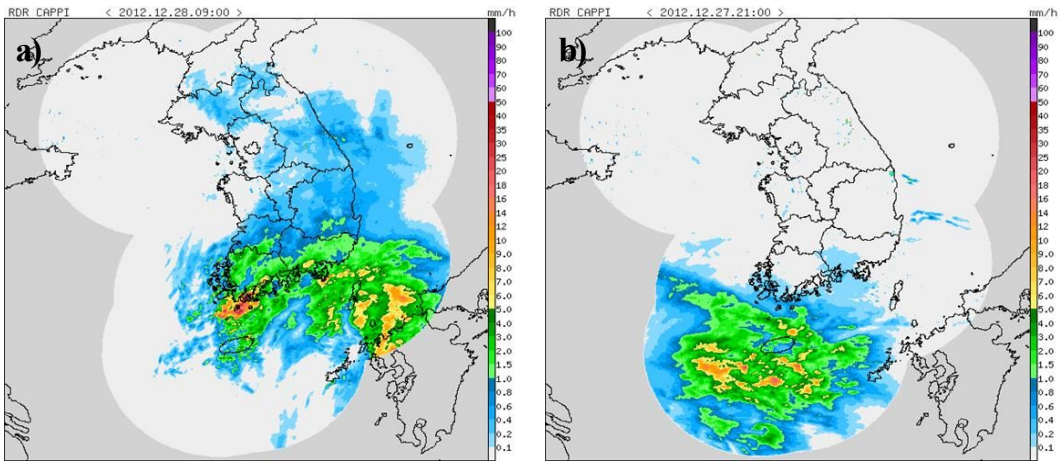

Fig. 4.20. Radar image (echo tops) at a) 1200UTC 27 December and b) 0000UTC 28 December, 2012.

Fig. 4.20 is an Echo detected in the afternoon of 27 December, in the front coast of the east and south region of our country. An Echo with a lot of snow was detected along the south coast of our country starting from dawn until morning. On this case day especially, the Echo was strongly detected in the Honam region of Chungcheongnamdo and Gyeongsangnamdo region. This time the Echo was firstly detected in the west south coast and moved, centering on the south coast during the observation day, and moved toward the east in the afternoon of 28 December, and passed by Korea.

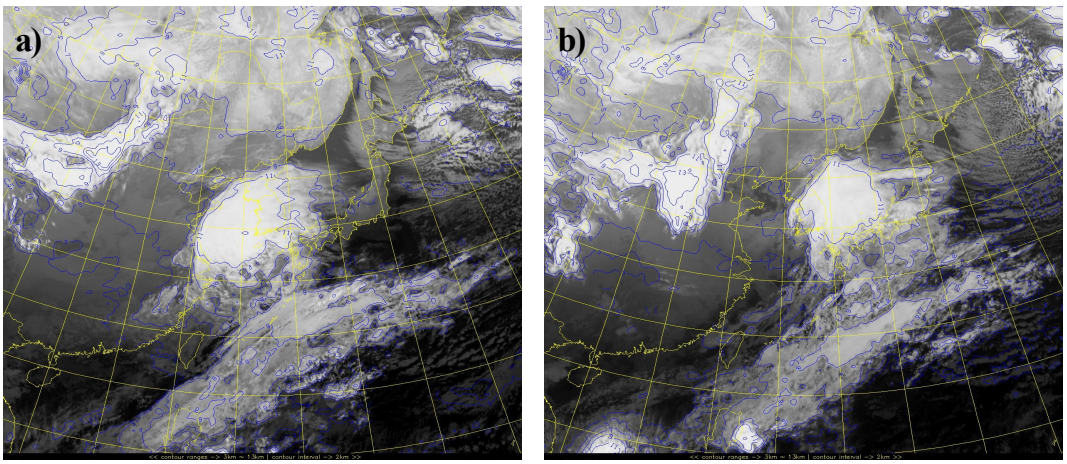

Fig. 4.21. Distribution of cloud top temperature superposed on satellite image at a) 1200UTC 27 December and b) 0000UTC 28 December, 2012.

The case in Fig. 4.21 is the analysis of the cloud top temperature superposed on satellite image. During the observation day, the cloud with snow was making a long band shape and was moving in long lines horizontally. Fig. 4.22 is the analysis of the surface pressure chart for the case day. There expected a lot of precipitation in the Low pressure region because a humid layer formed thickly in the upper and lower layers, and the Low pressure center location was expected to form toward the south but since the cloud is thick, the precipitation was expected to be much

larger. A lot of snow fell in most regions except Jeju with the temperature being minus degree during the time between dawn and morning when the precipitation was falling.

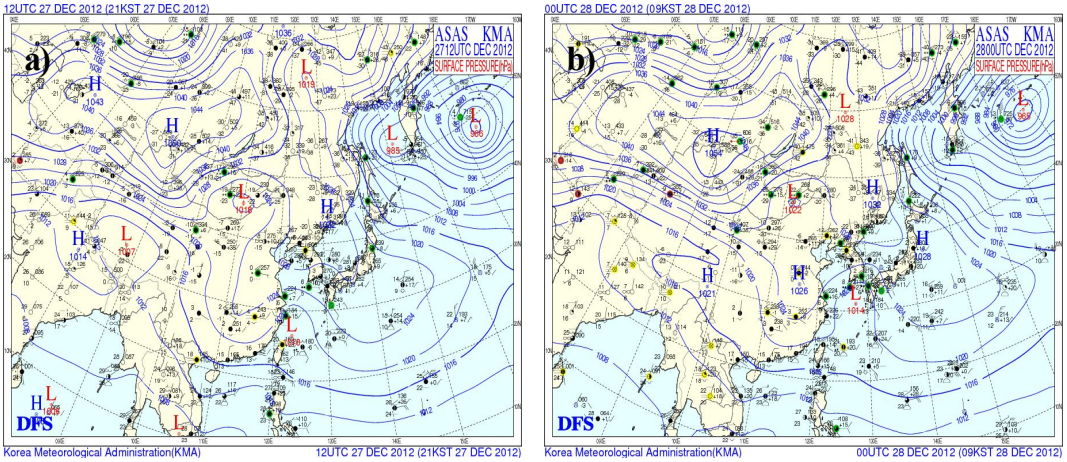

Fig. 4.22. Surface pressure chart at a) 1200UTC 27 December and b) 0000UTC 28 December, 2012.

Fig. 4.23 is the analysis data of the 850hPa pressure chart. As the cold air came down along the Chinese south inland, the temperature line was shown to be dense, and in the High pressure margins centered on the Japanese south coast, the warm moist advection was active in the route of the south current.

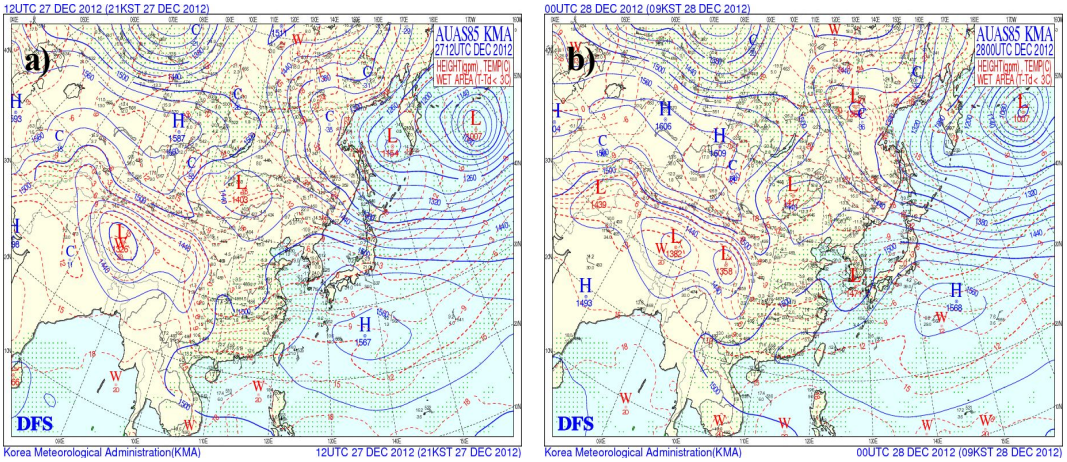

Fig. 4.23. Same as Fig. 4.22 but 850hPa geopotential height and temperature.

The Low pressure was expected to be gradually active in the region adjacent to Shanghai as the High pressure recedes toward the east, and because the precipitation region is fortified as it passes by the Jeju south coast, a large precipitation was expected in the south region and Jeju Island. As the isothermal line of 0 degrees remains in the south coast and this Low pressure recedes toward the east, most of the regions came out of the effect of the Low pressure in the afternoon of 28 December.

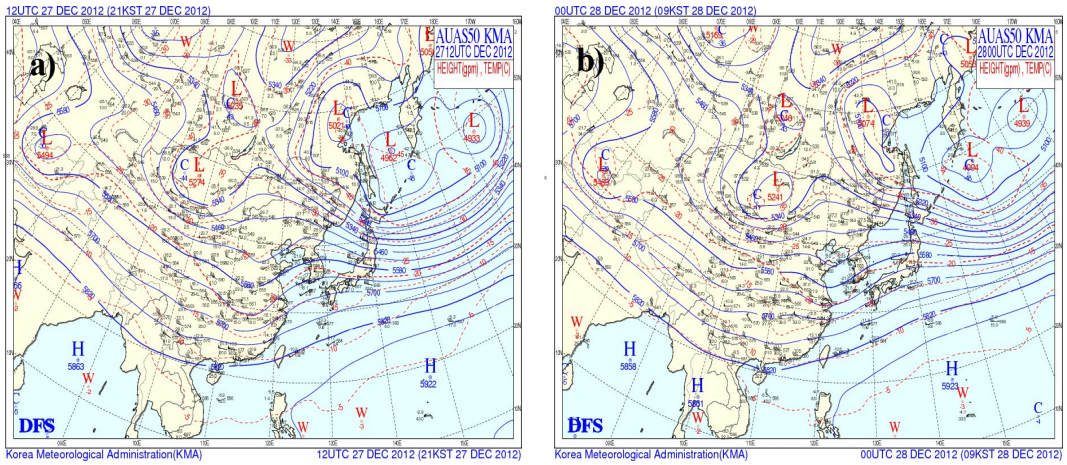

Fig. 4.24. Same as Fig. 4.22 but 500hPa geopotential height, temperature and isotach.

Fig. 4.24 is the analysis data of 500hPa pressure chart. As −20 degree−isothermal line moved southward to the southern Chinese inland, the pressure trough was developed; and as the strong wind appeared in the front of the pressure trough, a divergence field was formed and thus a ground Low pressure gradually grew in the Shanghai regions, and because the pressure band is generally zonal, the center of the Low pressure could not move toward the north but advanced eastward and passed he south Jeju coast. Furthermore, a week pressure trough appeared in middle Chinese inland.

As the Low pressure moved to the east due to the southern pressure trough, snow started falling in Jeju Island and was enlarged to encompass

Chungcheongnamdo the next dawn. Although the Low pressure could not advance to the north as far, as the upper trough continues from south to north in a substantial length, the precipitation in the Gyeonggi bay regions occurred in Seoul, Gyoenggi and the Kangwon Yeongseo region by the sear accompanied with a northern pressure trough.

The precipitation stopped on 27 December, and at the end of 27 December, snow started to fall in the middle and north region, and the snow precipitation area expanded to cover the whole country overnight. Because the vapor source is weak, the precipitation was not much; numerous regions were covered with a lot of snow precipitation. Even though the current pressure band is stagnated in the middle and high altitude region because the pressure ridge is situated in the middle of Siberia, blocking high in the Arctic Ocean and in the pressure ridge in the East Pacific and North America' s east coast, there seems to be an active current in Korean regions. As the short-wave trough situated in the south and middle region of China passes Korea from dawn to afternoon, the effect on the middle and south regions and a very large altitude falling limb have emerged nationwide starting from 29 December. While the blocking high is situated in the east Siberia region, centering on the high latitude regions of over 40N, the pressure band currently stagnated. The regions under that region have a relatively smooth status of the pressure band current. And in the Sandong Bay and Shanghai regions, due to the short-wave trough that moves to the east, the development of a ground Low pressure that passes the south coast was being supported, but the effect gradually decreased in late afternoon.

From Fig. 4.25, in 850hPa streamline and isotach, the Low pressure is converged in Sandoong Bay while making rotations. And according to the movement of strong low pressure, the Low pressure subtropical convergence emerged in the Kyusyu region of Japan centering on the Southern far-away sea.

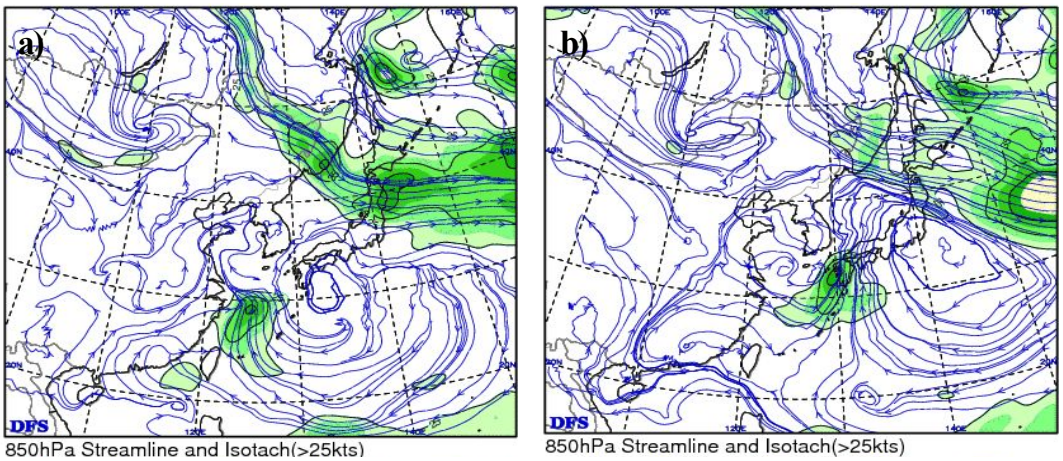

Fig. 4.25. Distribution of 850hPa streamline and isotach at a) 1200UTC 27 December and b) 0000UTC 28 December, 2012.

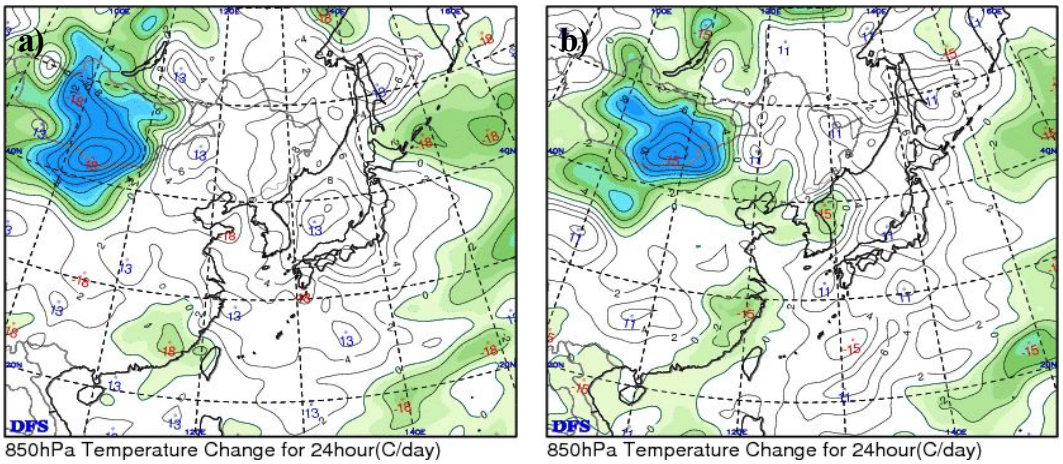

Fig. 4.26. Same as Fig. 4.25 but 850hPa temperature change for 24hour.

Fig. 4.26 is the temperature change analysis for 24 hours at 850hPa, and according to this analysis, the cold air that has moved from the north is stagnating in the north region, and as the Low pressure moves toward the Gyusyu region of Japan from the far-away sea from the south coast, it affects our country and this effect becomes weak starting in the afternoon of the 28th.

Fig. 4.27 is the analysis of the Showalter Stability Index (SSI), and according to it, in most of Korean regions, the SSI index value did not show any sign of precipitation or snowfall. However, for the whole south region located in the front of the low pressure, the possibility of precipitation or snowfall was strong and fortified starting from 27 December, and then gradually became weak again afterward.

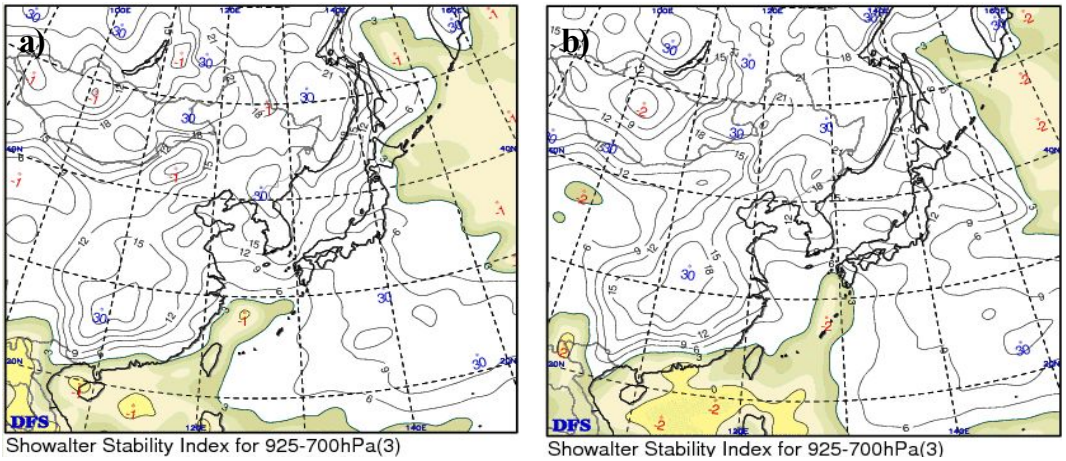

Fig. 4.27. Same as Fig. 4.25 but Showalter stability index.

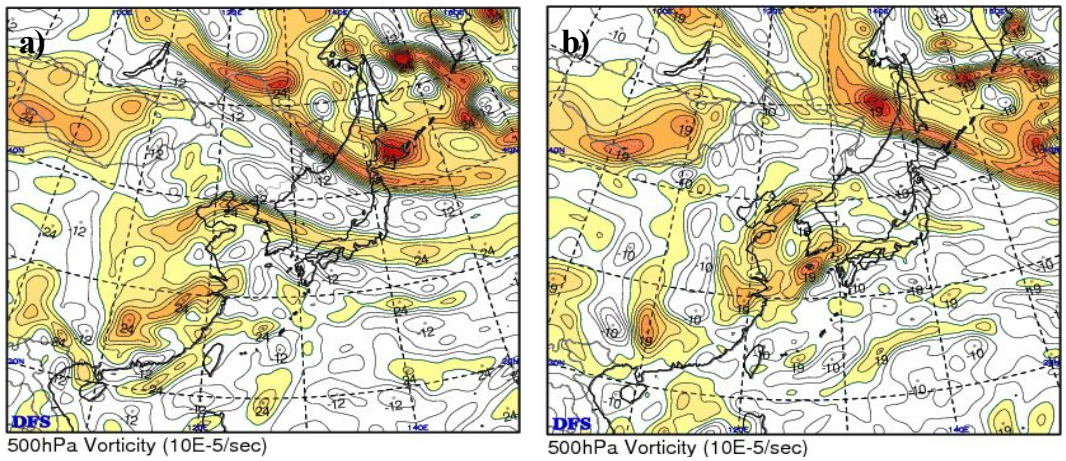

Fig. 4.28. Same as Fig. 4.25 but 500hPa vorticity.

Fig. 4.28 is the analysis of the vorticity at 500hPa. The vorticity region of plus value of the Low pressure type, which is accompanied by a strong Low pressure centered on the inland of China formed strongly starting from the night of 27 December till the morning in the south coast and inland region of Gyeongsangbukdo.

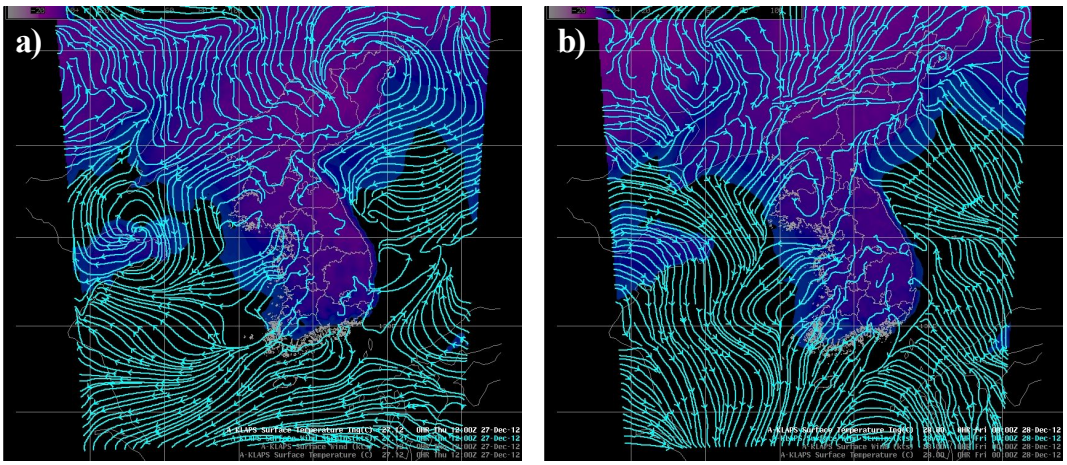

Fig. 4.29. Distribution of surface temperature and streamline at a) 1200UTC 27 December and b) 0000UTC 28 December, 2012.

Fig. 4.29 is the surface temperature and streamline. Since the center of the Low pressure is located in the south region of Jeju Island, the Stream Line of ground is converging in the south of Jeju, and there was a difficulty in discerning rain from snow. But since the borderline of under 1 degree is located in the south coast, it can be inferred that the main element that changes rain into snow was the temperature of lower layer of atmosphere.

Fig. 4.30 is the Changes in surface air temperature from KLAPS by regions (a: Jeju, b: Wando, c: Geochang). During the case day in Jeju, the ground temperature was around 5~7 degrees, a very high temperature distribution, and the precipitation form was rain, in Wando. The rain fell when the temperature was positive, and as the temperature fell below

zero in the dawn of 28 December, the precipitation changed into sleet and fell in the morning of 28 December. As the temperature fell under zero, the sleet changed into snow and fell in the morning of 28 December. The temperature was around zero and the sleet type of precipitation fell but there was not much snowfall. Geochang, which had a lot of snowfall, maintained a temperature at around −1~−2 Celsius degrees.

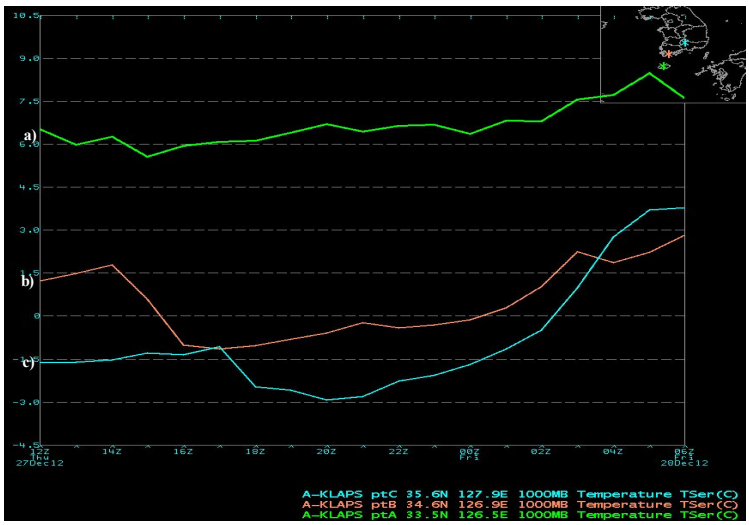

Fig. 4.30. Changes in surface air temperature from KLAPS from 1200UTC 27 December to 0600UTC 28 December, 2012(a: Jeju, b: Wando, c: Geochang).

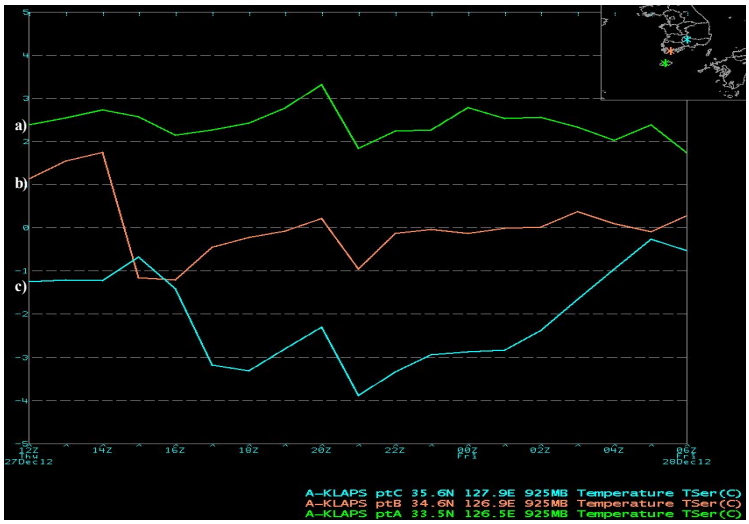

Fig. 4.31. Same as Fig. 4.30 but 925hPa temperature.

Fig. 4.31 is the Changes in 925hPa air temperature from KLAPS by each region (a: Jeju, b: Wando, c: Geochang).

Jeju where the precipitation fell as rain during the case period showed a plus temperature distribution of around 2~3 degrees of ground temperature starting from the beginning till end. Wando showed 0~1 degrees when it rained, and 0~−1 degrees when it was sleet. Geochang, which is located inland, showed −1~−4 degrees and the amount of snow was the largest, which may indicate that the temperature of the ground and the 925hPa is an important element for the decision of distinguishing between snow and rain.

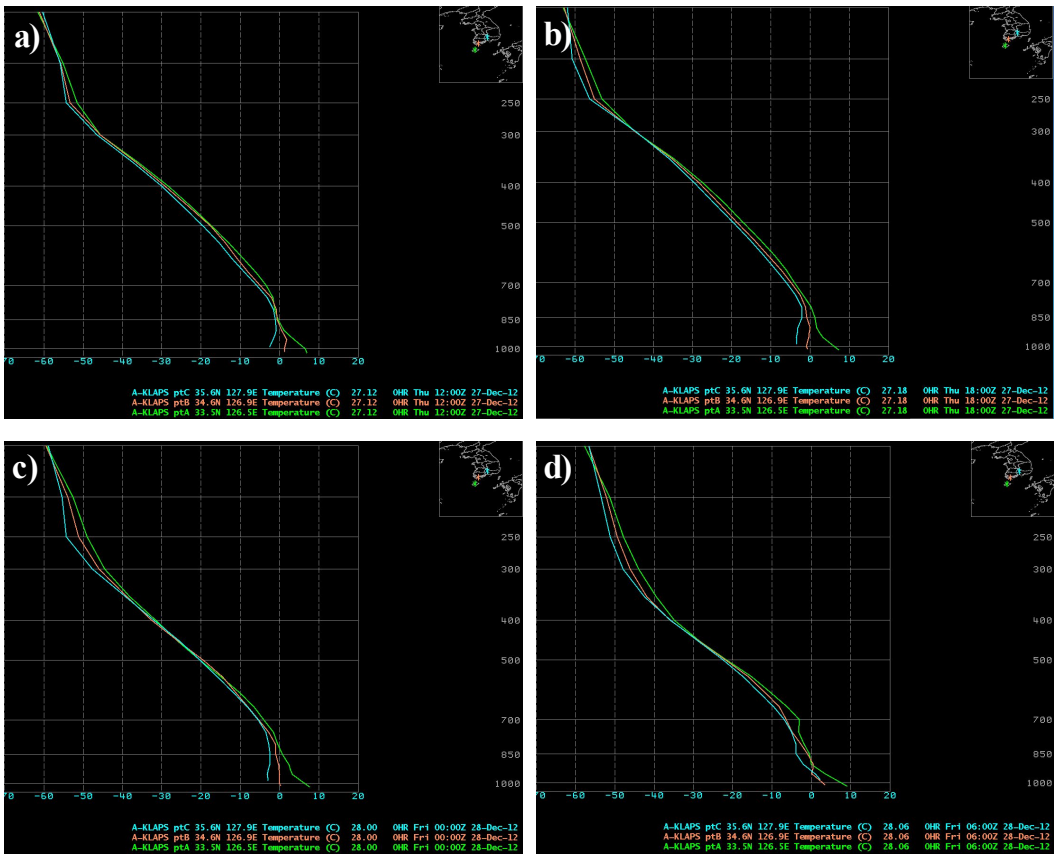

Fig. 4.32. 6-hourly vertical profile of temperature at three stations of Jeju, Wando, and Geochangne from 1200UTC 27 December to 0600UTC 28 December, 2012.

Fig. 4.32 is the 6-hourly vertical profile of temperature by each region (Upper: Jeju, Middle: Wando, Lower: Geochang) depending on the altitude. All the regions showed a minus degree temperature in the altitude of over 850hPa, but at an altitude of under that value, the temperature varied depending on the region.

As for the peak of the snowfall, looking at the dawn of 28, the ground temperature in Jeju decreased slowly from the +8 degrees to the congelation altitude, but those of Geochang and Jeju where snow and sleet fell uniformly from the ground to the 850hPa altitude exhibited a different pattern.

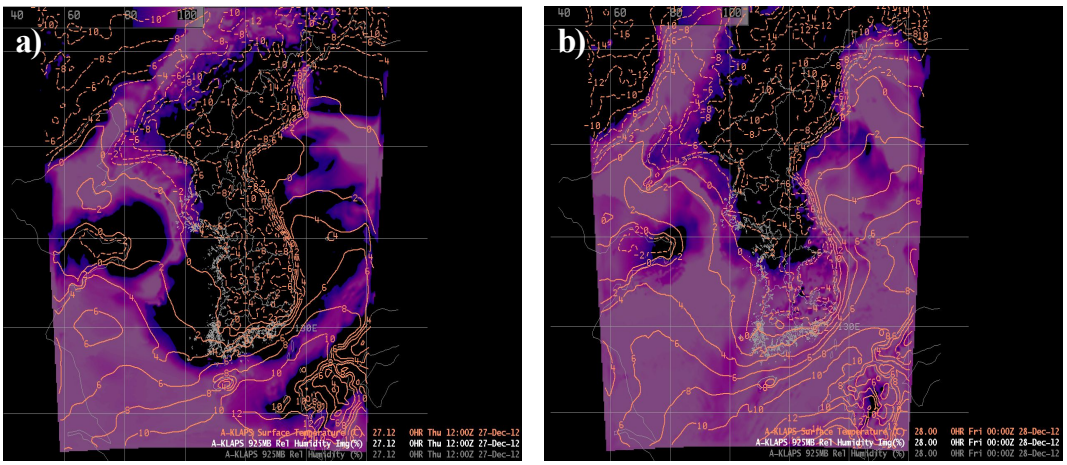

Fig. 4.33. Same as Fig. 4.29 but 925hPa relative humidity.

Fig. 4.33 is a Same as Fig. 4.29 but 925hPa relative humidity. According to records at 1200UTC on 28 December, the south Jeonllanamdo inland and south coast region shows a plus degree temperature, and in only Jeju where the relative humidity was high it rained. At 925hPa, the relative humidity scope started in the inland of Jeonllanamdo and enlarged into Gyeongsangdo at dawn on 28 December; in a region in which the ground temperature is over 2 degrees, it rained. In the regions in which the ground temperature was under 1 degree, it

snowed; and in the regions where the temperature was around 0, a sleet-type of precipitation fell. Especially, in Geochang, where the ground temperature started to be a minus value on 27 December and fell to -4 degrees in the dawn of 28 December and had much snow, and as the Low pressure went out of the region starting from the afternoon of the 28, the ground temperature regained the plus value and the snow stopped.

Fig. 4.34 is the Same as Fig. 4.29 but 925hPa temperature and specific humidity. In the regions where the specific humidity is over 3g/kg and the 925hPa temperature is around 0℃ or above, rain formed; and in the region with the same specific humidity condition and a ground temperature of around 1 degree, snow formed. When the specific humidity is over 3g/kg, the 925hPa temperature seems to be a very important element, and for a quantitative limit value, statistical analysis on more cases will be necessary.

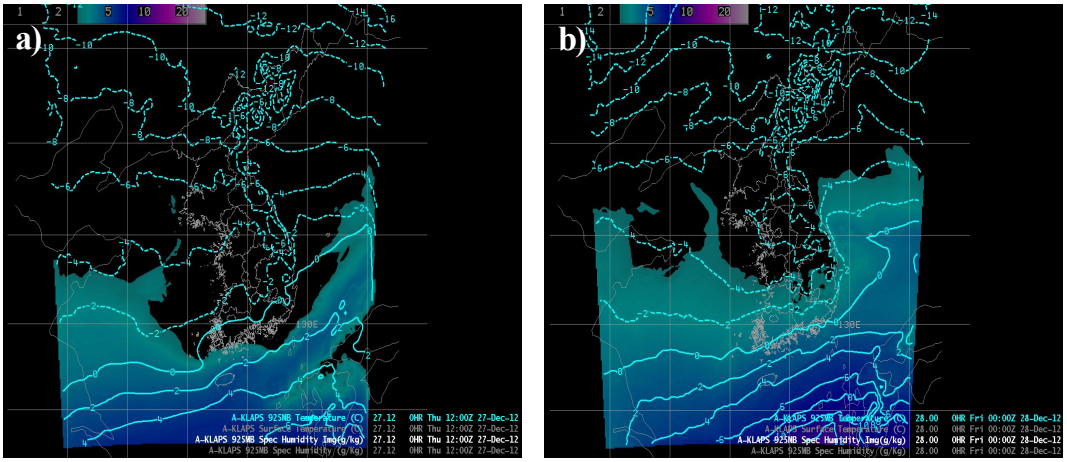

Fig. 4.34. Same as Fig. 4.29 but 925hPa temperature and specific humidity.

Fig. 4.35 and 4.36 are the Skew T - Log P diagram of Geochang and Jeju. It is the sounding structure that is seen when the typical precipitation appears when all the layers are saturated with precipitation due to Low pressure from 27 December. Especially, the freezing level is 1~2km in height, and rain transforming into snow is very difficult.

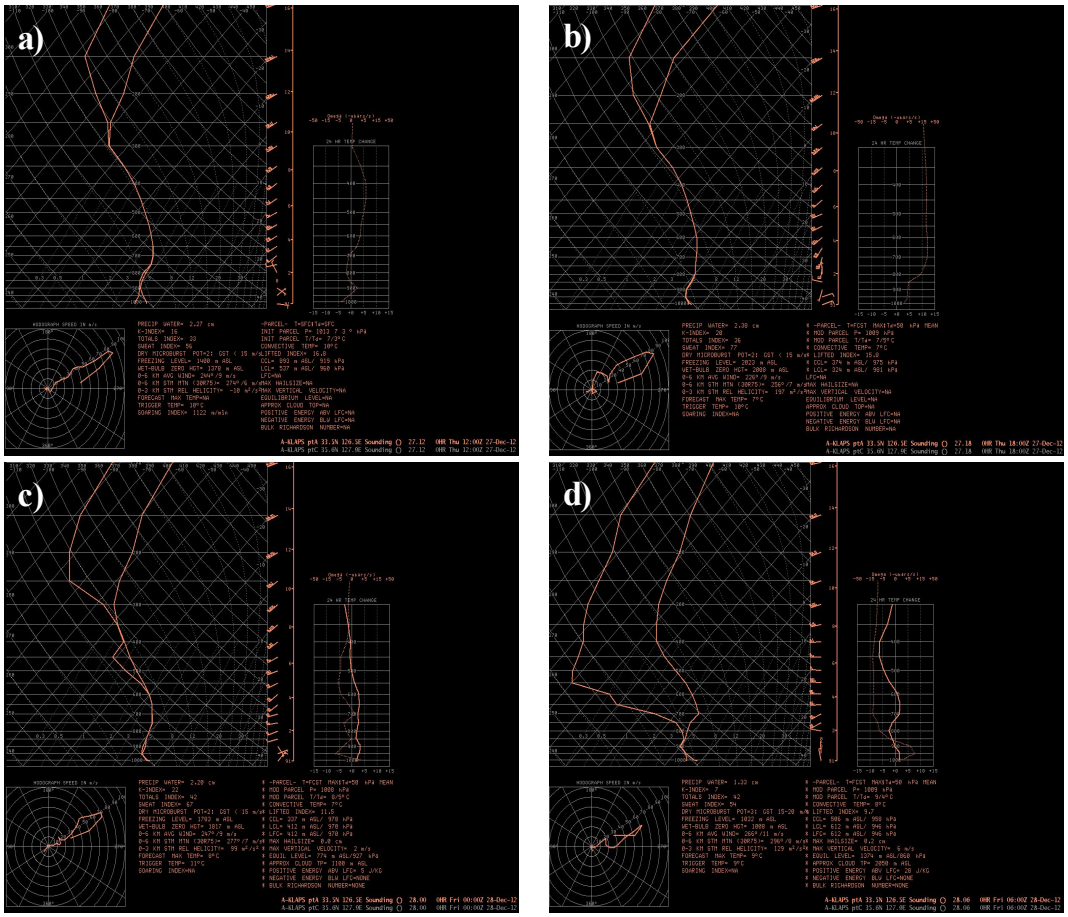

Fig. 4.35. Skew T – Log P diagram at Jeju from a) 1200UTC and b) 1800UTC 27 December and c) 0000UTC and d) 0600UTC 28 December, 2012.

On the other hand, for the case of Geochang in Fig. 4.36, the middle layer of the atmosphere is only saturated during the night, and the lower layers are not saturated, but the freezing level was 0m. As all the layers became saturated in the dawn of 28 December, the precipitation started to fall in the form of snow immediately without the sleet stage. The snow form continued until the morning of 28 December, and starting from the day time of 18th; as the region moved out of the effect zone of the low pressure, the snow terminated.

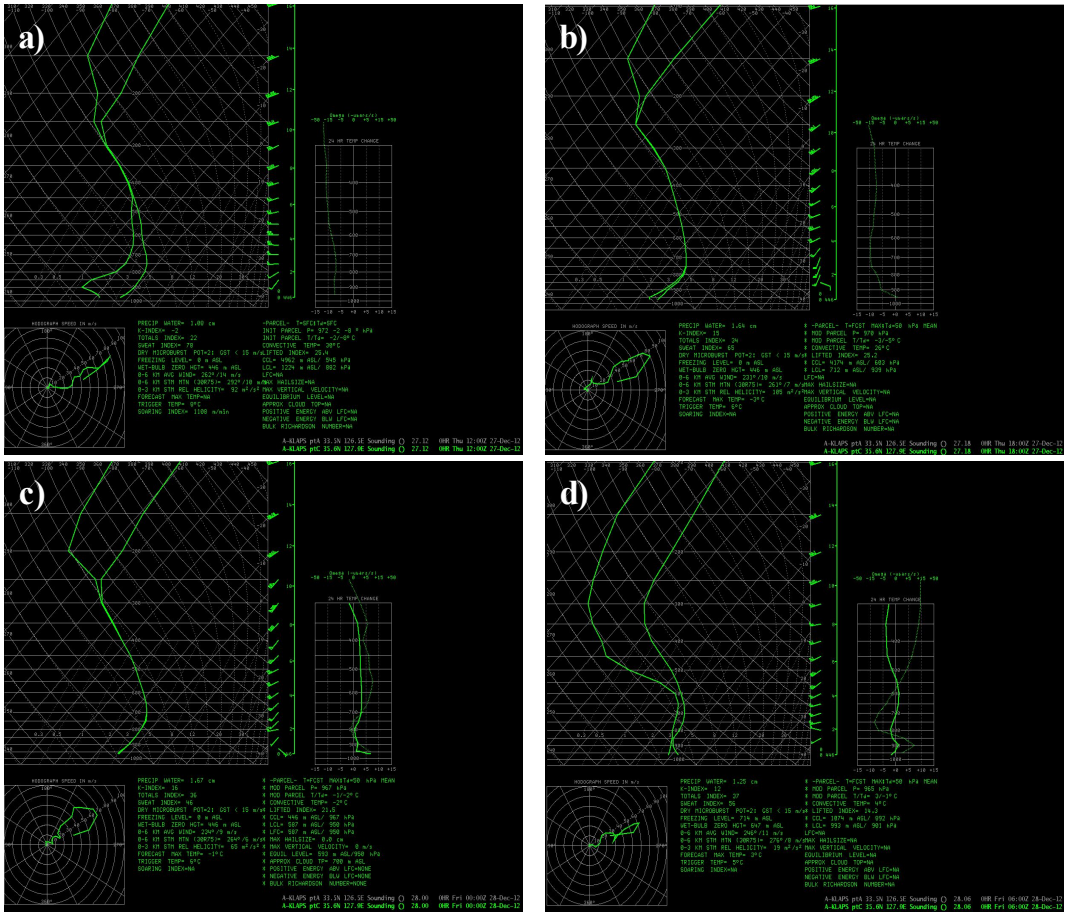

Fig. 4.36. Same as Fig. 4.35 but Geochang.

3. Model Results

a. Continental Anticyclone Case

(1) SST Difference

As we have surveyed in chapter 4, in the case 2010, a large scale of convective cloud develops in the west coast as the cold Siberian air mass expands, and when this convective cloud moved, a lot of snow fell in the west coast region. The relationship between the expansion of this Siberian air mass and the environment of west sea surface was surveyed. Fig. 4.37 shows the distribution of the sea surface temperature on the case day. It shows each sea surface temperature as of 30 December, 2010 when the heavy snowfall occurred.

According to the three sea surface temperature data, the climate value data (Default SST) is shows value depending on the latitude, and thus the value of the sea surface temperature is constant. In case of 2010-default, the distribution of sea surface distribution spreads horizontally by latitude. This distributional characteristic corresponds to the climatological distributional characteristics of general SST. The sea surface temperature of far south region of the west coast showed to be 298K.

For the case of RTG where the spatial resolution is much higher, the distribution shows to be similar to OSTIA, but the overall temperature shows to be higher than around 2K.

In the distribution of OSTIA, the mercury longitude is not that big by latitude indifferent from the climate value, and the sea surface temperature of Chungcheongnamdo region showed to be lower by around 5K maximum compared to the climate value. Also, the south coast of Honam showed to be low. It can be inferred that the distribution of the temperature of the sea surface temperature value of OSTIA is more minute and detailed compared to the climate value sea surface temperature. It is judged that this distribution characteristic are showed to be characteristic of the satellite and model.

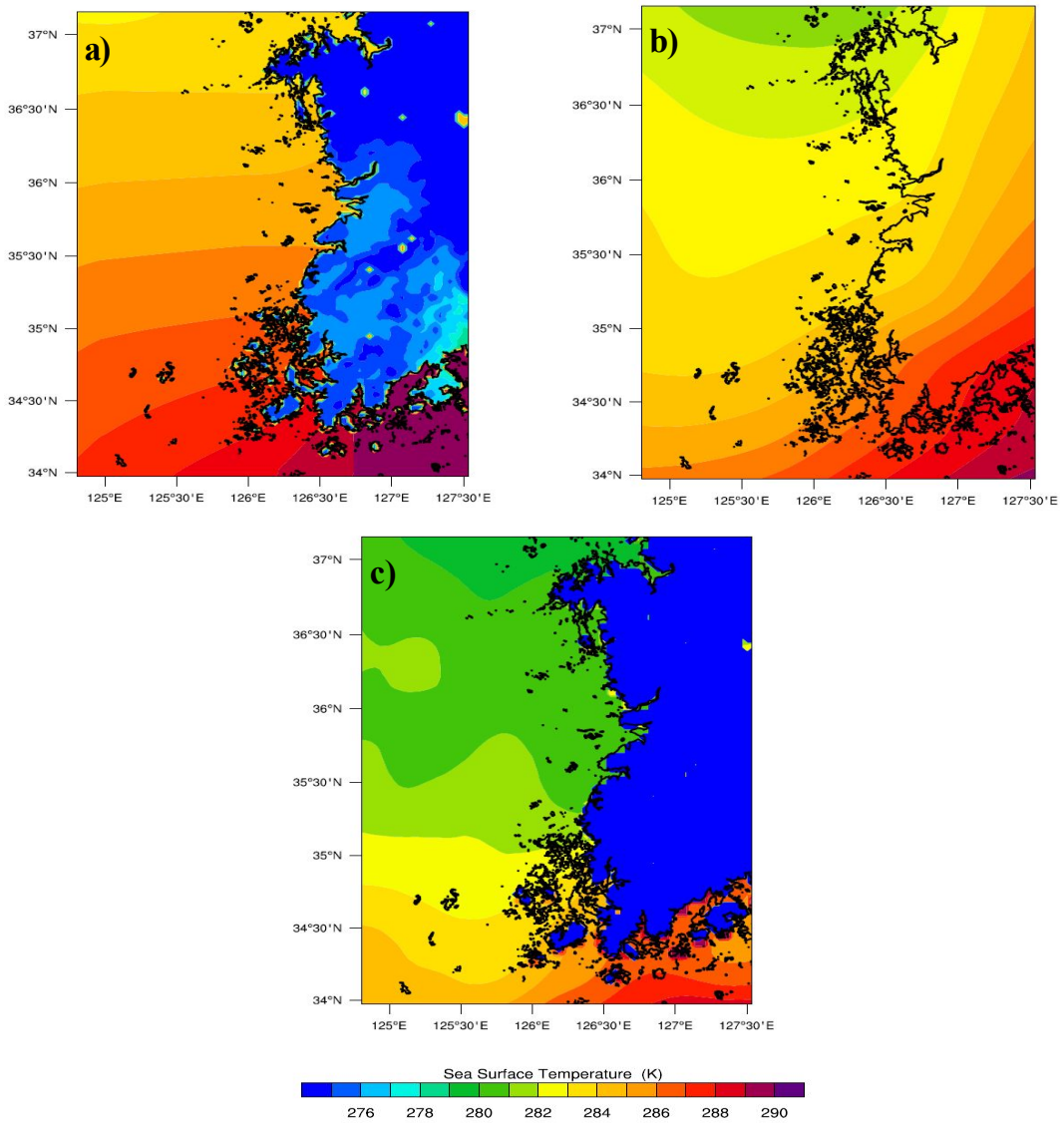

Fig. 4.37. Distribution of a) NCEP/NCAR SST, b) RTG SST, and c) OSTIA over West Sea.

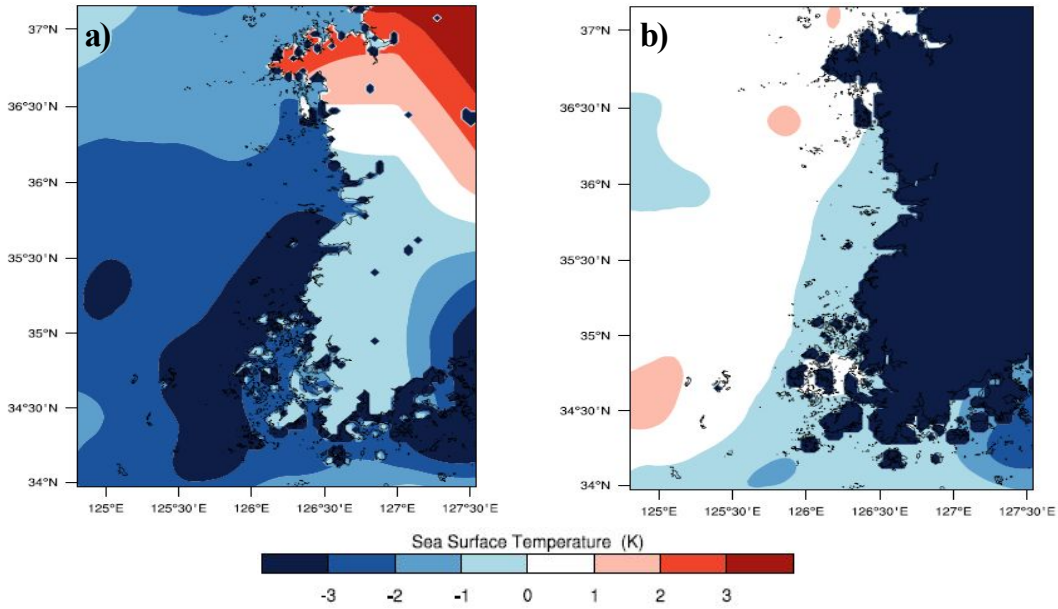

Fig. 4.38. Distribution of SST difference : a) OSTIA – NCEP/NCAR SST and b) OSTIA – RTG SST.

Fig. 4.38 shows the difference of each sea surface temperature. As proposed by Cha *et al.*(2011), this study shows that the correctiveness level of the coastal region has relatively high OSTIA and the spatial resolution also has high characteristic and thus, the difference of each sea surface temperature was proposed based on OSTIA.

First, when surveying on the difference between the SST of OSTIA and default, the OSTIA shows big difference along the west coast. This big difference of SST will show big difference in snowfall amount as well. On the other hand, as for the difference of SST between OSTIA and RTG, OSTIA showed to be low by 2K in some region of south coast and by 0.5K in south regions of west coast, but this difference was limited to the coastal regions. On the other hand, in most of ocean regions, OSTIA has the trend to be higher than RTG. Accordingly, it can be concluded that in the case where the snowfall develops passing by the west coast, the difference in amount of snowfall will not be that big.

(2) Temperature and Wind

From Fig. 4.39 to 4.41 are the analysis of the temperature and wind vector of the lowest layer calculated in the simulation where the 3 sea surfaces from 30 December, 2010, the case day of the numerical mock test were applied. Each figures show the expansion of the Siberia air mass at 6 hour interval from 1500UTC on 29 December.

The Fig. 4.39 is the case2010-default. As the west wind is infused continuously in 15UTC, and the cold air clearly is infused into the west coastal inland and this west wind gradually changes into a northwest wind.

In the north-west coastal region, the north wind is infused from the north, and a slight convergence occurs in the coastal region of Chungcheongnamdo. The temperature which showed to be as high as 10℃ at night falls by the effect of the cold Siberian High pressure which is coming from the north. It can be seen that a strong wind blows at 18m/s in the coast in day time.

On the other hand, in the Fig. 4.40, a wind distribution pattern that is similar to the case where the climate value was applied is showed in the numerical experiment where the RTG SST was applied, but in overall, the wind velocity is observed to be weak. Overall, the distribution of the temperature showed to be lower by 1℃ compared to the default, and especially, the temperature of the coast in the south coastal region showed to be low.

In the case of the interpolation of OSTIA SST in Fig. 4.41, the horizontal distribution showed to be of similar shape to the case where the RTG was interpolated and the numerical mock test was performed. The intensity of the wind that blows from the North and Northwest into 2100UTC showed to be strong, and the intensity of the wind and infuse of the wind into the Honam west coast region showed to be strong.

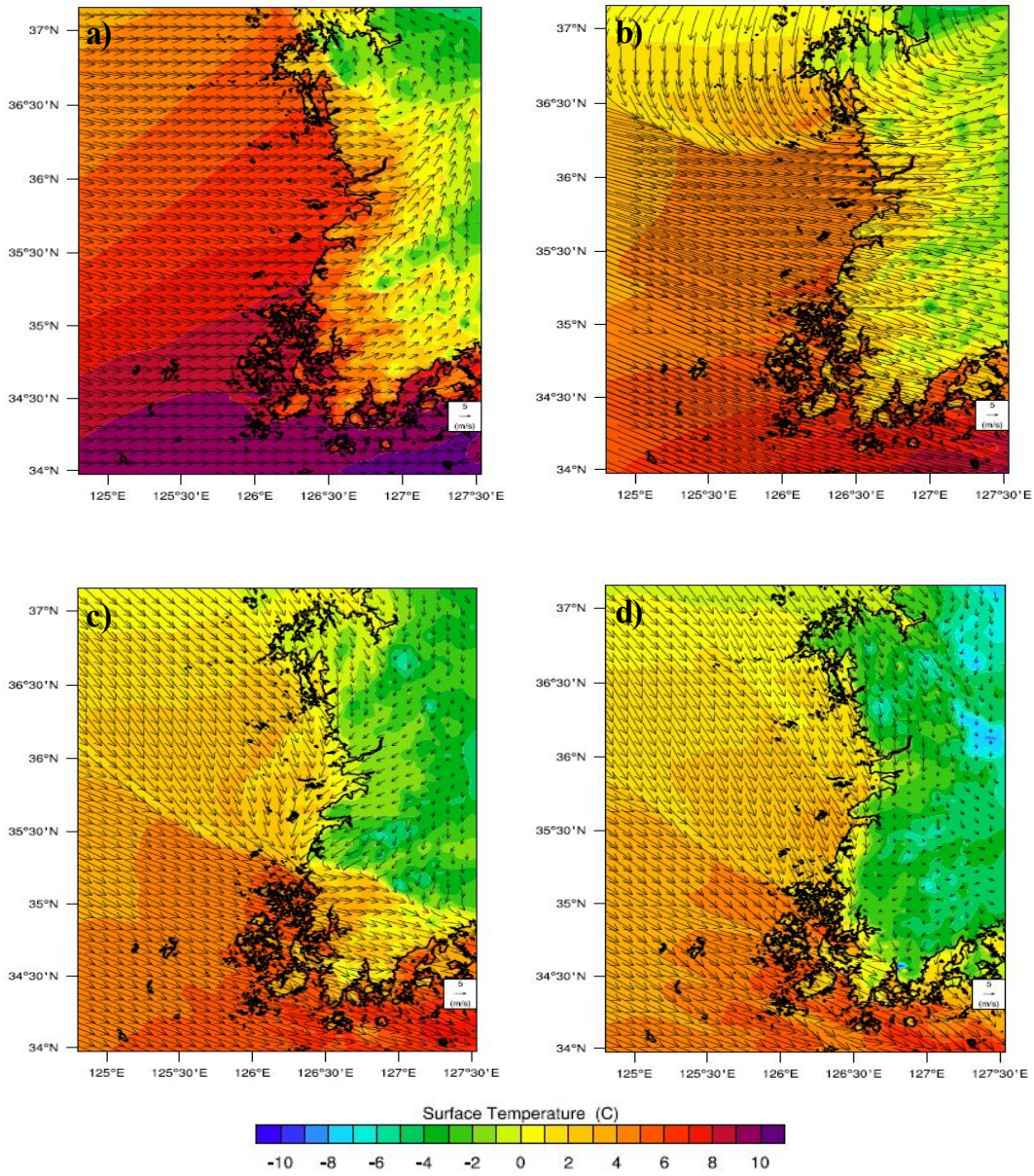

Fig. 4.39. Distribution of NCEP/NCAR SST and wind vector at a) 1500UTC, b) 2100UTC 29 December and c) 0300UTC and d) 0900UTC 30 December, 2010.

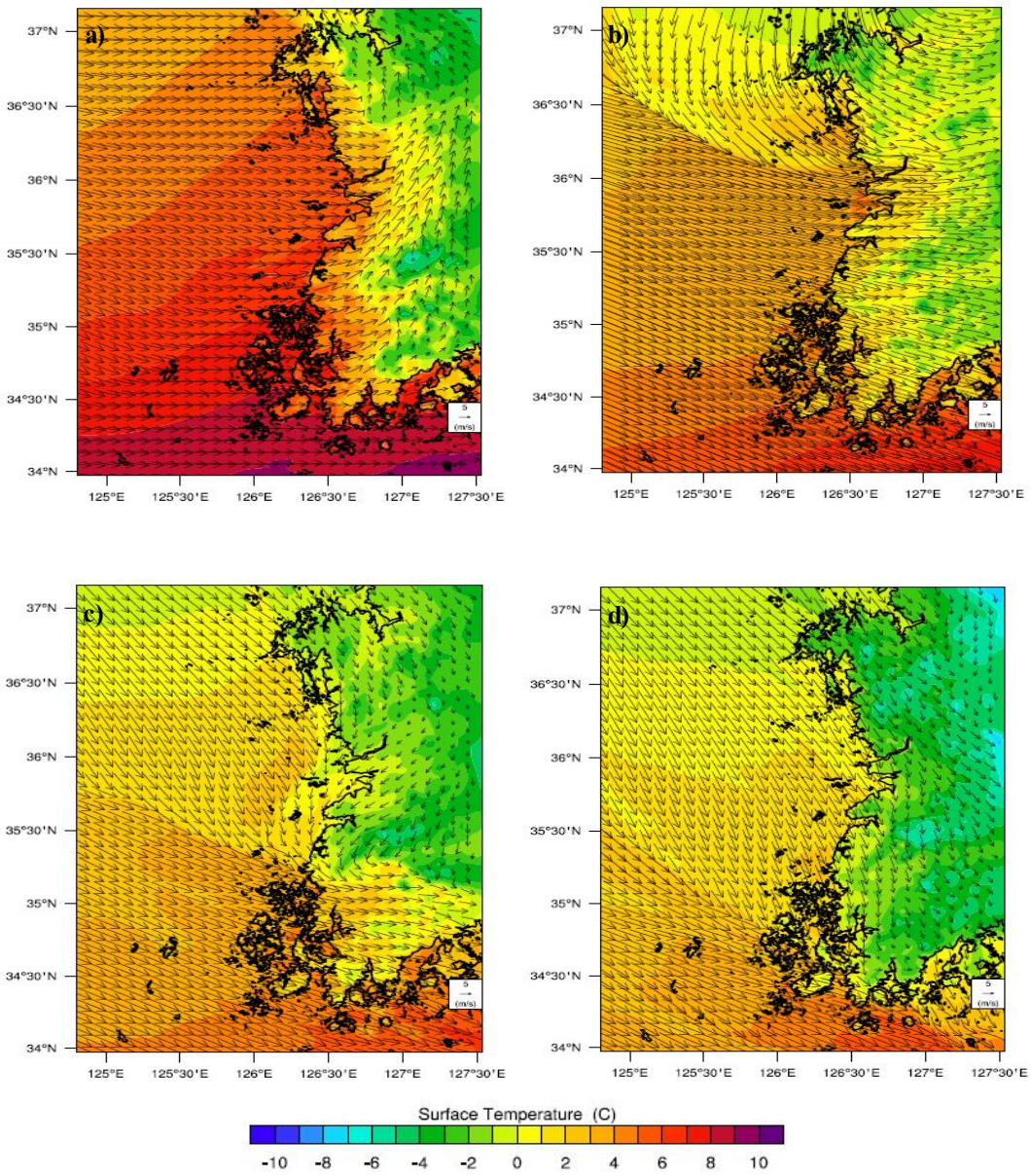

Fig. 4.40. Same as Fig. 4.39 but RTG SST.

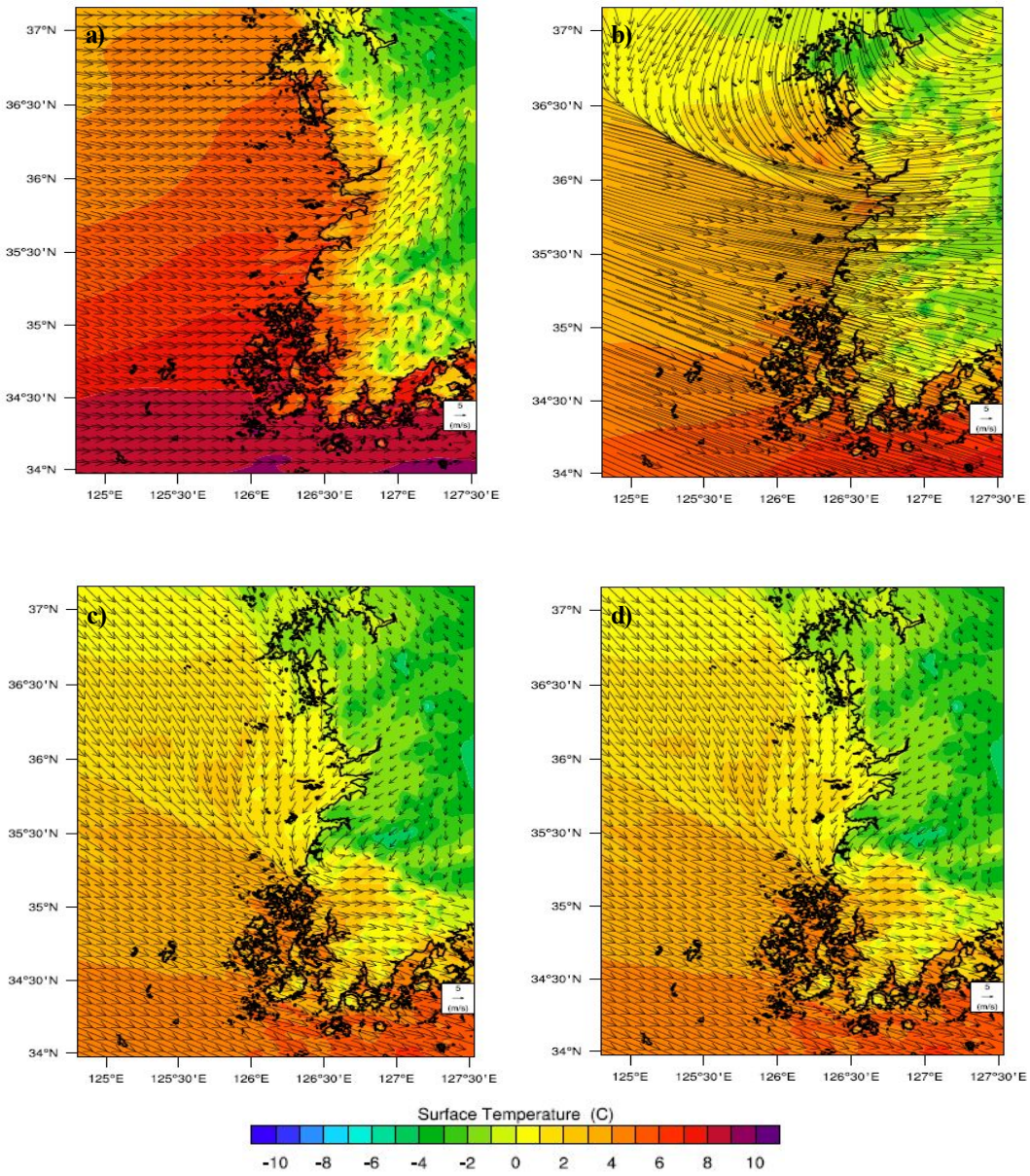

Fig. 4.41. Same as Fig. 4.39 but OSTIA.

(3) Total Snowfall and Precipitation

In order to assess the difference in the amount of snowfall, the difference of the result of simulation where the different sea surface temperatures were applied was surveyed. Fig. 4.42 show the difference in the amount of snowfall for the case day of numerical mock test where each sea surface information was applied. The difference of the amount of snowfall between the OSTIA where the difference of SST was biggest and the climate value was 20cm maximum.

This signifies that the amount of snowfall was smallest in the OSTIA case where the SST was lower than the default, and the largest amount of snowfall appeared in the west coastal region showing the biggest difference. As in the difference of SST of the amount of snowfall calculated in the numerical experiment where the OSTIA and RTG were applied, there were regional differences in the amount of snowfall, but the differences were not that big compared to the default. Overall, in the case of OSTIA, the value was smaller than the default and higher than the RTG case.

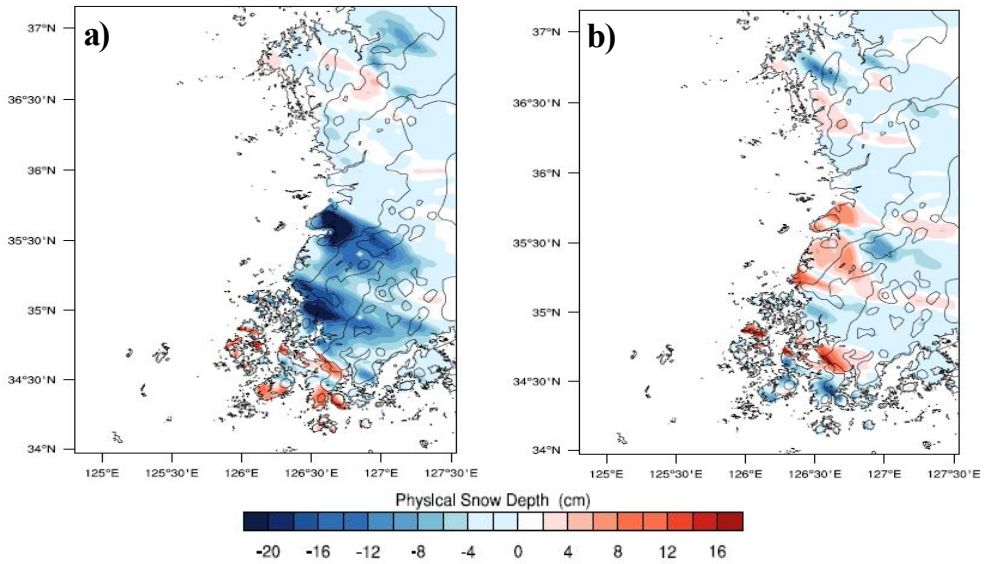

Fig. 4.42. Distribution of snowfall difference on 30 December, 2010 : a) OSTIA-NCEP/NCAR SST and b) OSTIA-RTG SST.

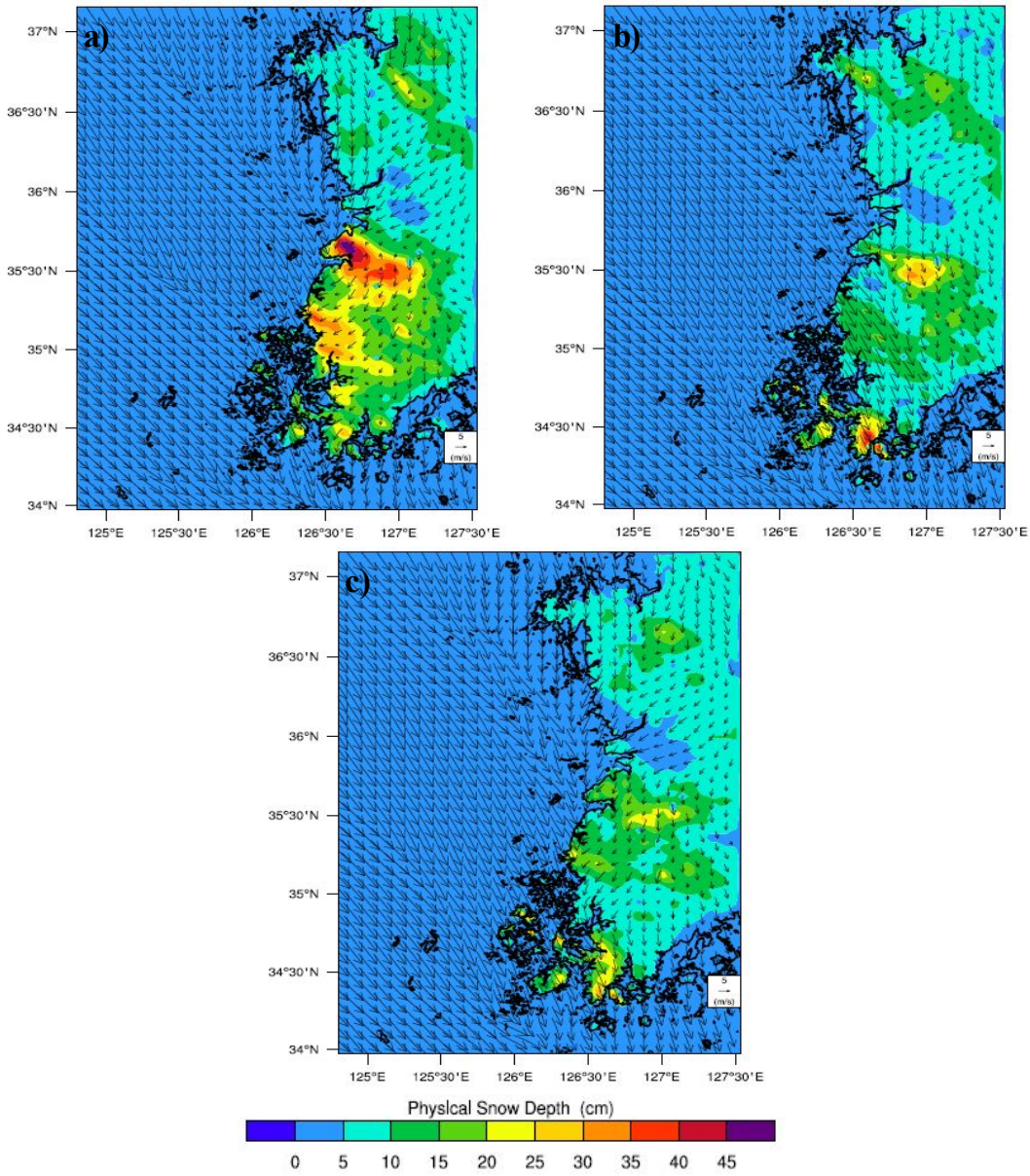

Fig. 4.43. Distribution of 24-hour accumulated snowfall on 30 December, 2010 : a) NCEP/NCAR SST, b) RTG SST, and c) OSTIA.

Fig. 4.43 shows the accumulated snowfall in 24 hours on 30 December, 2010, the case day of the numerical mock test. The distribution of the snowfall showed to be similar in all the three cases, but the quantitative amounts showed difference. For the case of the climate value (default), 45km of deep snow showed in Buan centered on Jeollabukdo west coast region, and 40cm of snowfall also appeared in the north coastal region of Jeonllanamdo. On the other hand, the RTS shows a maximum snowfall of 19cm and OSTIA around 27cm. This difference of amount of snowfall is directly related to the sea surface temperature.

When compared to the actually observed value proposed in Fig 4.2, the default case is over-mocking the snowfall. When considering the fact that the maximum observation value was 28cm of Jeoneup, the interpolation experiment of SST of OSTIA is seen to be similar to the actual observation value. Thus, sea surface temperature information of the west costal region becomes a very important element.

The snowfall is the presentation of the amount of snow fell on the ground, and it is needed that the total precipitation that exist in the air needs to be analyzed and the effect of the sea shall be analyzed practically.

Fig. 4.44 shows the distribution of the total precipitation calculated in the numerical experiment where each sea surface was applied. This total precipitation is the sum of the serve lattice precipitation that is generated by cumulus air current and the precipitation that is formed in the lattice point through the micro-physical process. Overall, in the default where the sea surface temperature found to be high, the total precipitation was observed to be high as well. In this case, it can be seen that a strong precipitation appeared not only in Buan region where the snowfall amount was high, but also in ocean region. This distribution of the precipitation is similar to the temperature distribution of 850 hPa that has been previously surveyed in the case analysis. On another hand, for the case of the RTG and OSTIA, it showed much at Jeonllanamdo west coast such as

Haenam and Muan than at Jeollabukdo region. This type of difference seems to be related to the convergence by way of wind direction.

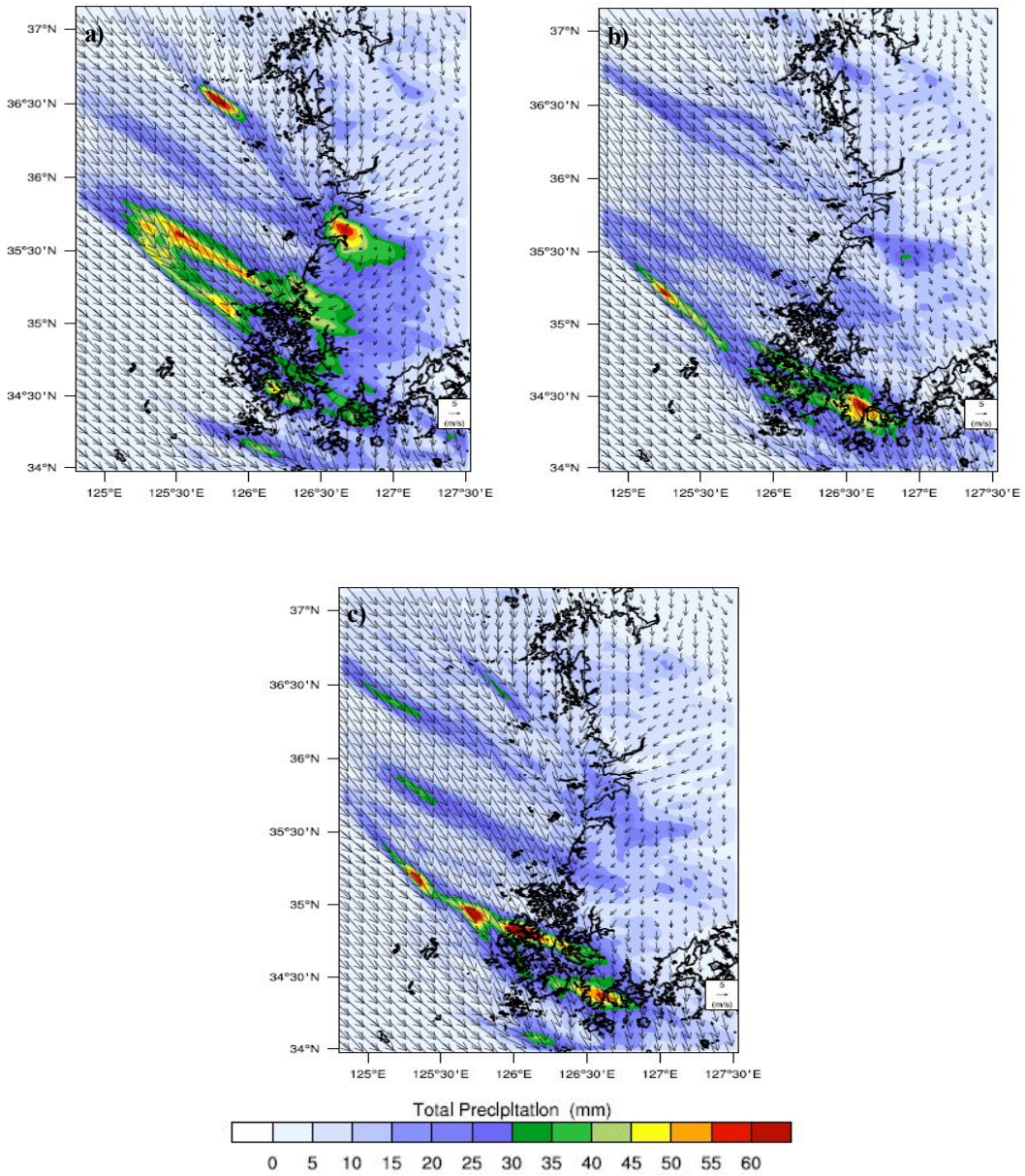

Fig. 4.44. Same as Fig. 4.43 but total precipitation.

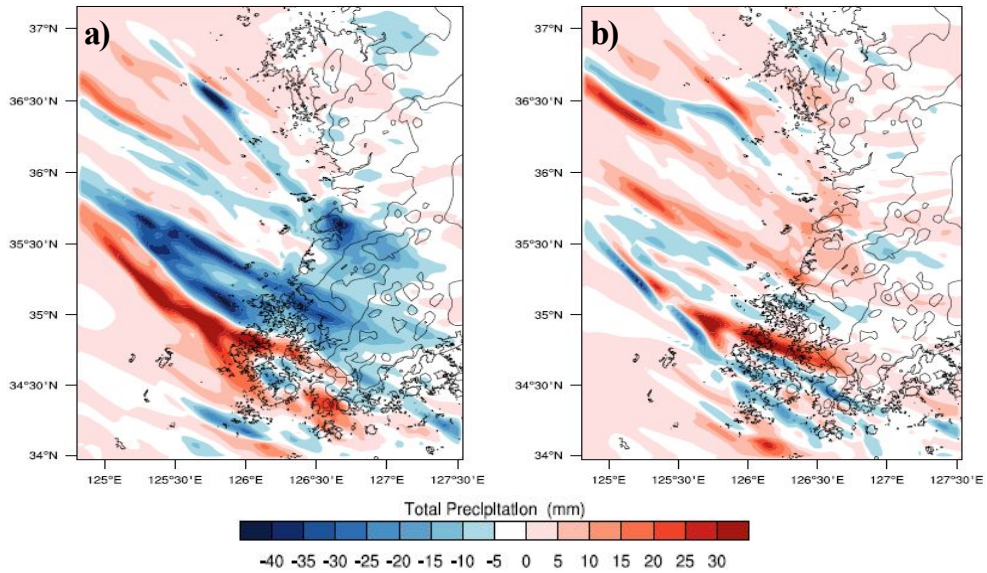

Fig. 4.45. Same as Fig. 4.42 but total precipitation.

In order to survey this quantitatively, the difference of the total precipitation of 1800UTC for the case day for numerical mock experiment, 30 December, 2010 is showed in Fig. 4.45. As for the difference of the total precipitation, there all showed big differences by each case.

As for the difference between the OSTIA and the default, the default was found to be higher by more than 40mm in Jeollabukdo Buan region and the OSTIA was found to be higher by more than 30mm in Jeonllanamdo Muan region. The difference of OSTIA and RTG was foung to be more than 20mm in Jeonllanamdo Muan region.

The difference of SST by each case contributes much to the formation of cumulus, and this shows big difference in the total precipitation. This clearly shows the location and intensity of the cumulus and the formation of the cumulus in the west coast caused by the High pressure of Siberia.

(4) Vertical cross-section

The cross-section is the west and east cross-section based on the points where the amount of snowfall is the largest, and the analysis elements are potential temperature and wind vector elements. Also, the effect of the temperature distribution on the sea surface on the heavy snowfall was quantitatively analyzed based on the difference between the each sea surface temperature and the cases.

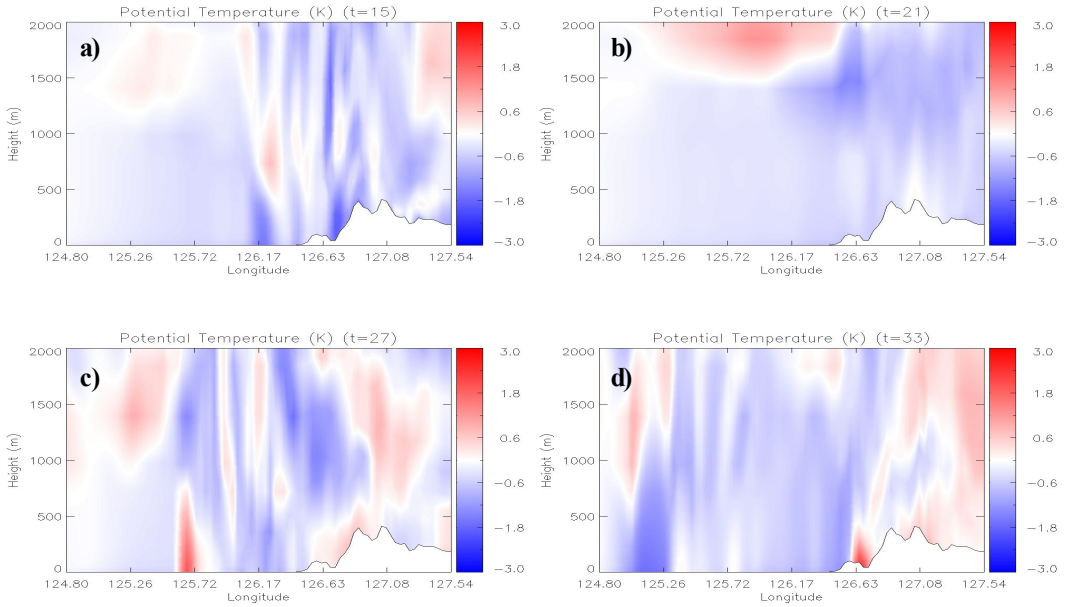

Fig. 4.46. Longitude-height distribution of potential temperature difference between OSTIA and NCEP/NCAR SST on 30 December, 2010.

Fig. 4.46 shows the difference of vertical potential temperature calculated in the OSTIA and the default. In the sky of the downwind region of the land, it showed a slight positive value in the 1500UTC and 21UTC, but in the 2100UTC and the 12UTC, there showed a positive value in the upper layer and a negative value in the lower layer. Overall, in the lower layer, a negative value appears at all time zones. This signifies that the lower atmosphere of under 2km is more unstable in the

default than in the OSTIA. In other words, it signifies that the heat is better transported upward by way of high SST of the sea in the lower layer. This type of upward transportation is occurring continuously during the day.

On the other hand, the difference between the OSTIA and RTG in Fig. 4.47 shows an opposite trend to the difference between the OSTIA and the default.

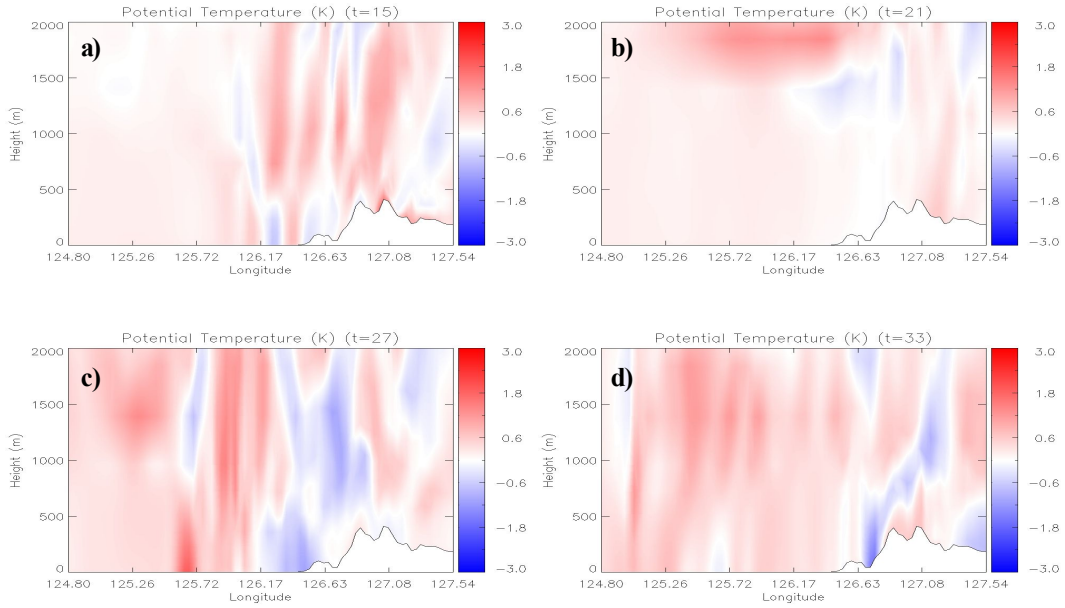

Fig. 4.47. Same as Fig. 4.46 but OSTIA and RTG SST.

In other words, except for certain regions, the overall potential temperature of the OSTIA shows to be high. This signifies that the atmosphere of the RTG case is more stable.

Fig. 4.48 shows the difference of the vertical velocity between OSTIA and default. It can be seen that there occurs a phase difference of vertical velocity in the two cases. This type of phase difference can be seen to occur by way of the parallel distribution of the sea surface temperature.

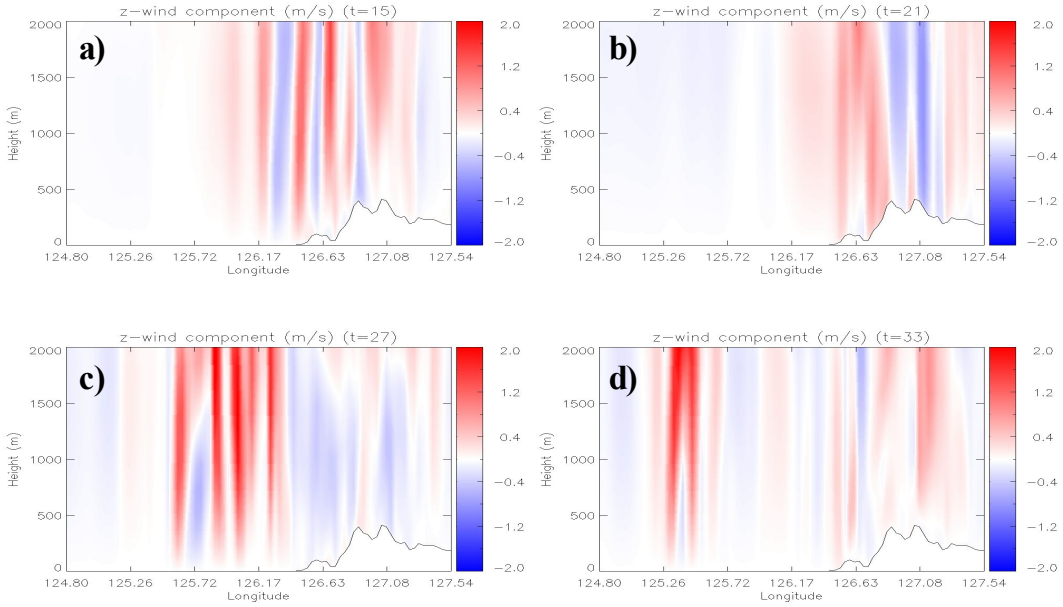

Fig. 4.48. Same as Fig. 4.46 but vertical velocity.

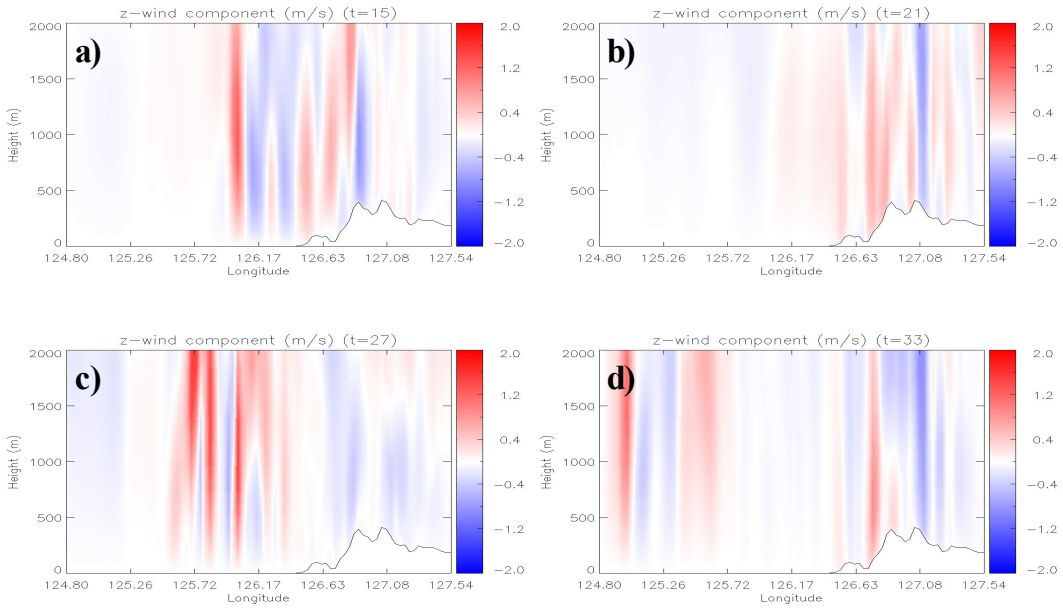

Fig. 4.49. Same as Fig. 4.47 but vertical velocity.

Also, it is expected that the 2-dimensional sea surface temperature distribution will induce the horizontal convergence and divergence of the atmosphere and thus, will be very complex. On the other hand, for the case of OSTIA and RTG in Fig. 4.49, there shows a phase difference as in the Fig. 4.48, but these distribution showed to be the opposite.

However, investigating through this difference of vertical velocity can be governed by many factors explained earlier such as the complexity of the sea surface distribution and thus precise comprehension is very hard.

(5) Heat Budget

Fig. 4.50 shows the distribution of latent heat flux for 31 December, 12UTC. This relates closely to the sea surface temperature and advection of the temperature, in other words the wind direction. The latent heat flux of the default shows to be higher than 700W/m^2 maximum in the west coast and the default of which the sea surface temperature is high overall shows the highest latent heat flux. On the other hand, for the case of RTG, the value is as low as 500W/m^2 and is very low in Chungcheongnamdo and Jeonllanamdo west coast regions.

For the case of upward heat, in the default, the value was found to be less compared to the two different SST. In other words, the higher the sea surface temperature, the more effective is the heat movement by way of latent heat flux and the movement heat by way of sensible heat is relatively limited to certain degree. Also, for the case of OSTIA and RTG, the sensible heat and latent heat flux showed in a similar size and although smaller sea surface temperature difference of 2~3K is noted, there is a probability that a very different result might be deducted in the heat balance phase.

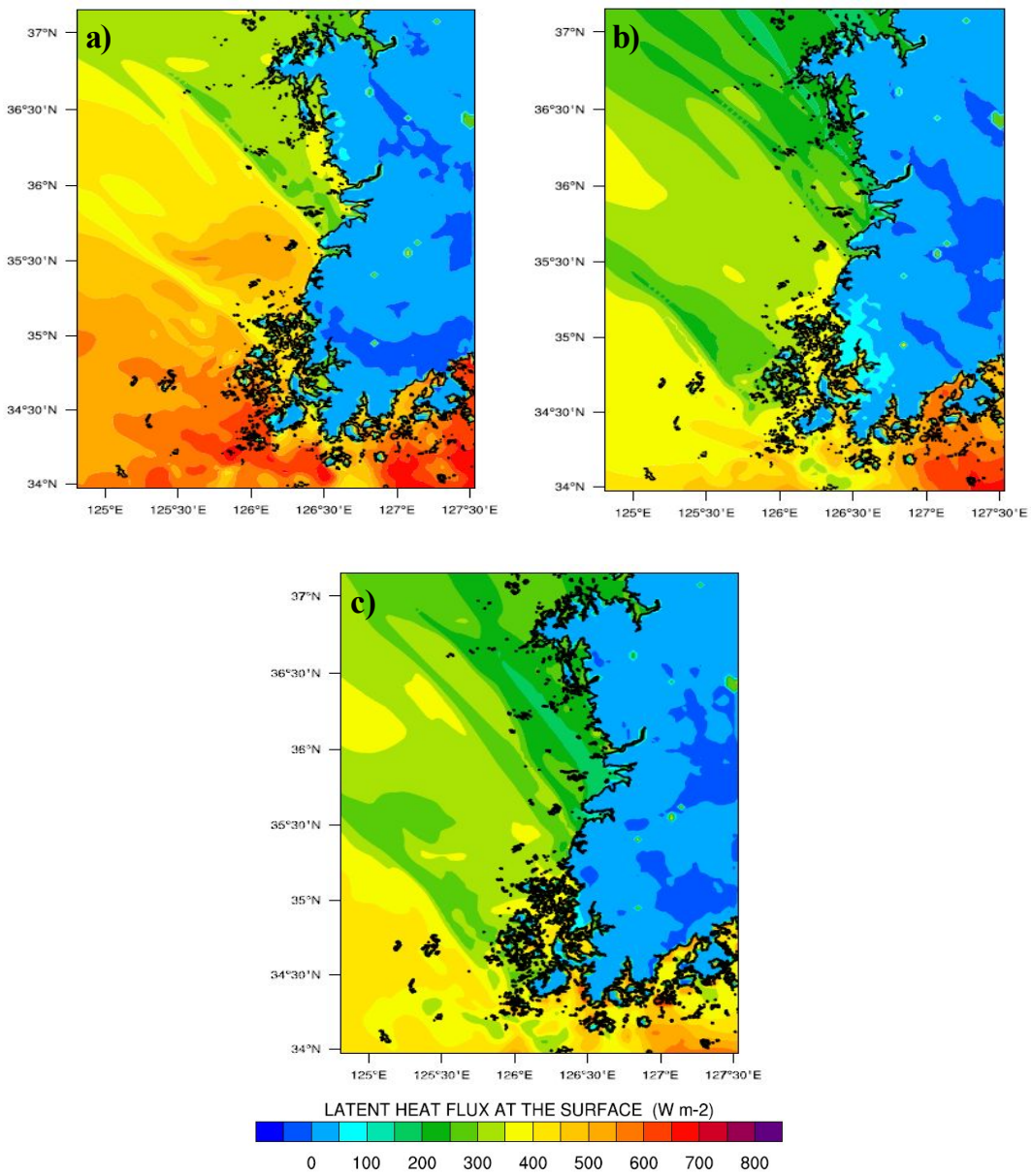

Fig. 4.50. Distribution of latent heat flux at 1800UTC 30 December, 2010 over Southwestern Sea.

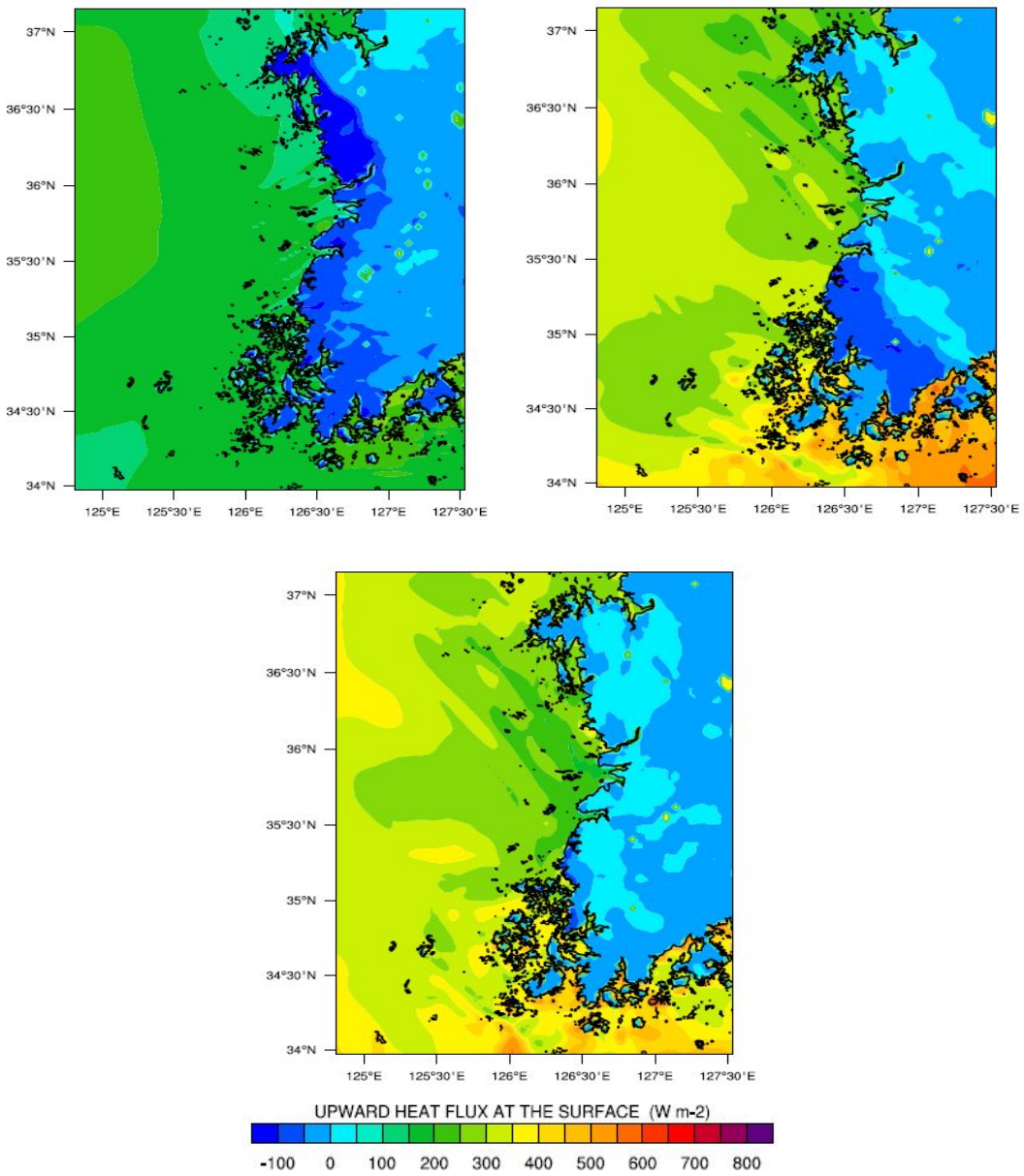

Fig. 4.51. Same as Fig. 4.50 but upward heat flux.

b. Extratropical Cyclone Case(Case2012)

(1) SST Difference

As we have surveyed in chapter 3, tthe case 2012 is the one where a lot of snow fell in Gyeongsangnambukdo as well as Jeollanambukdo, because of the cold High pressure located in the north of our country and the effect of the Low pressure that passes by south sea-side.

The relationship with the environment of southwest sea surface during migration of the Low pressure was surveyed.

Fig. 4.52 shows the distribution of the sea surface temperature of this case day. It shows each sea surface temperature of 28 December, 2012, when the heavy snowfall occurred as the starting point.

When the data for the three sea surface temperature is seen, the data of climate value (Default SST) is shows the value depending on the altitude, and thus the value of the sea surface temperature was found to be constant, and first, the distribution of the sea surface temperature in the case2012-default is distributed in a parallel way by each latitude.

This distribution characteristic corresponds to the climatological distribution characteristic of the SST. The sea surface temperature of the far south regions of the south coast showed to be 289K. For the case of the RTG of which the spacial resolution is higher, the distribution was similar as in OSTIA, but the temperature in the same location was lower by around 1K.

For the case of the distribution of OSTIA, the mercury longitude by each latitude was not that big indifferent from the climate value or the RTG, but is was distributed in a parallel way to the distribution of the mercury that occur in the south coast and the coastal line of west coast.

Also, the sea surface temperature of the OSTIA had the highest mercury in the low altitude of south coast. This signifies that it is the passage through which the Low pressure passes and thus the temperature was high.

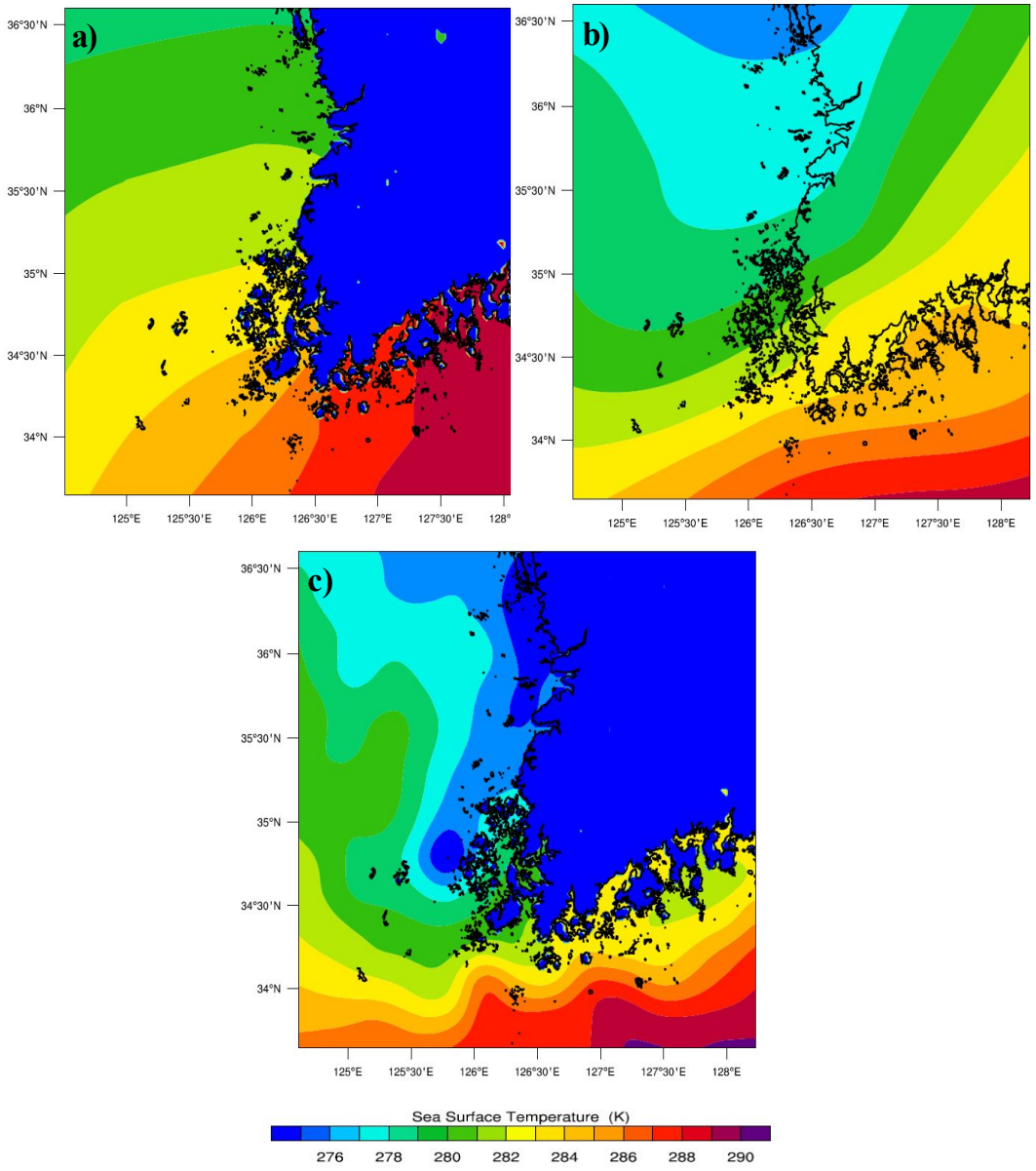

Fig. 4.52. Distribution of SST over West and South Sea : a) NCEP/NCAR SST, b) RTG SST, and c) OSTIA.

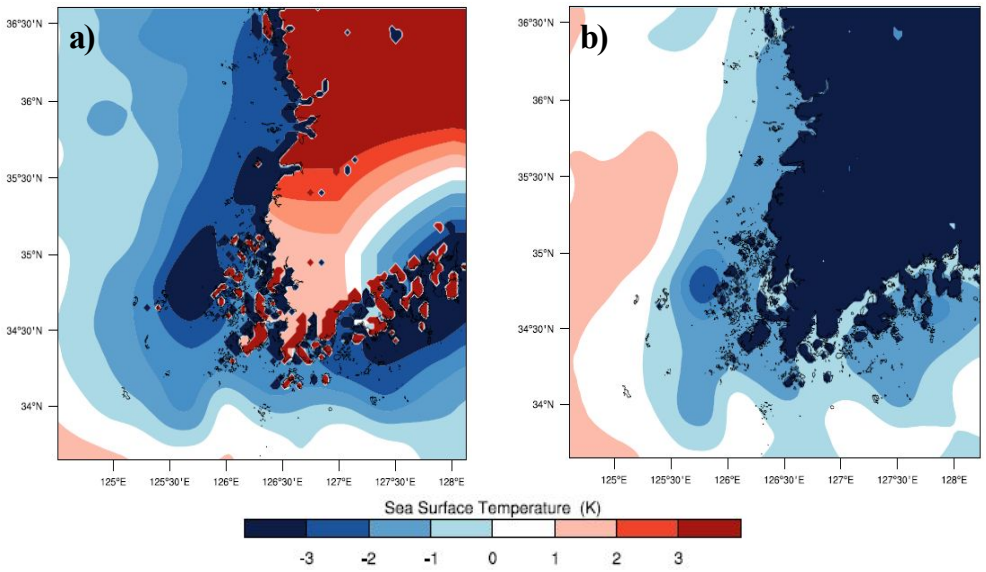

Fig. 4.53. Distribution of SST difference : a) OSTIA - NCEP/NCAR SST and b) OSTIA - RTG SST

It shows each sea surface temperature difference. As we have mentioned in the section 1 of this chapter, and as proposed by Cha *et al.* (2011), in this study, the correctiveness level of the coastal region showed relatively high in OSTIA and as the spatial resolution also has high characteristic, each sea surface temperature difference based on OSTIA was proposed.

Fig. 4.53 shows the difference between OSTIA and the default, OSTIA shows a distinct difference along the coastal line. But, as we go further from the coast, the temperature difference was not that big. The difference of SST between OSTIA and RTG did not show a very big value, but showed a similar pattern as above. This occurred limited to the coastal region. On the other hand, in most of the ocean regions, the OSTIA showed a high value than RTG. Thus, as we move along passing by the ocean and approach the coastal region, the temperature difference existed but the difference amount was not that big, and thus it is concluded that not a big difference of snowfall will occur in this case where the snowfall develops.

(2) Temperature and Wind

Fig. 4.54, 4.55 and, 4.56 are the analysis of the temperature and wind vector of the lowest layers calculated in the simulation where three sea surfaces were applied in 28 December, 2012, the case day for the numerical mock test.

The figures show the values at 6 hour interval starting from the 1500UTC of 28 December when the effect of the Low pressure started.

Fig. 4.54 is the case2012-default and as the northeast wind is infused continuously in 15UTC, the air in the inland becomes gradually warm , and the wind changes direction toward the north as the weekend comes and the wind becomes stronger.

The temperature dropped by the effect of the cold High pressure located in the north at night, but as the daytime approached, the temperature of over 0 degree showed. Especially, in the south coast of 21UTC, there was strong wind of 14m/s.

In Fig. 4.66, in the numerical experiment where the RTG SST was applied, the wind distribution pattern similar to the case where the climate value was applied is shown.

Overall, with respect to the temperature distribution, the temperature is not much different from the temperature of the ground and the wind vector compared to the default, but there is a 2℃ difference maximum in the south coast.

For the case of interpolation of the OSTIA SST in Fig. 4.55, the horizontal distribution showed to be similar shape as in the case of the numerical mock test which was done by interpolating the RTG.

It showed a strong wind intensity which blows from the north and northwest in 2100UTC and there showed a strong wind intensity and infuse showed toward Honam West coastal regions.

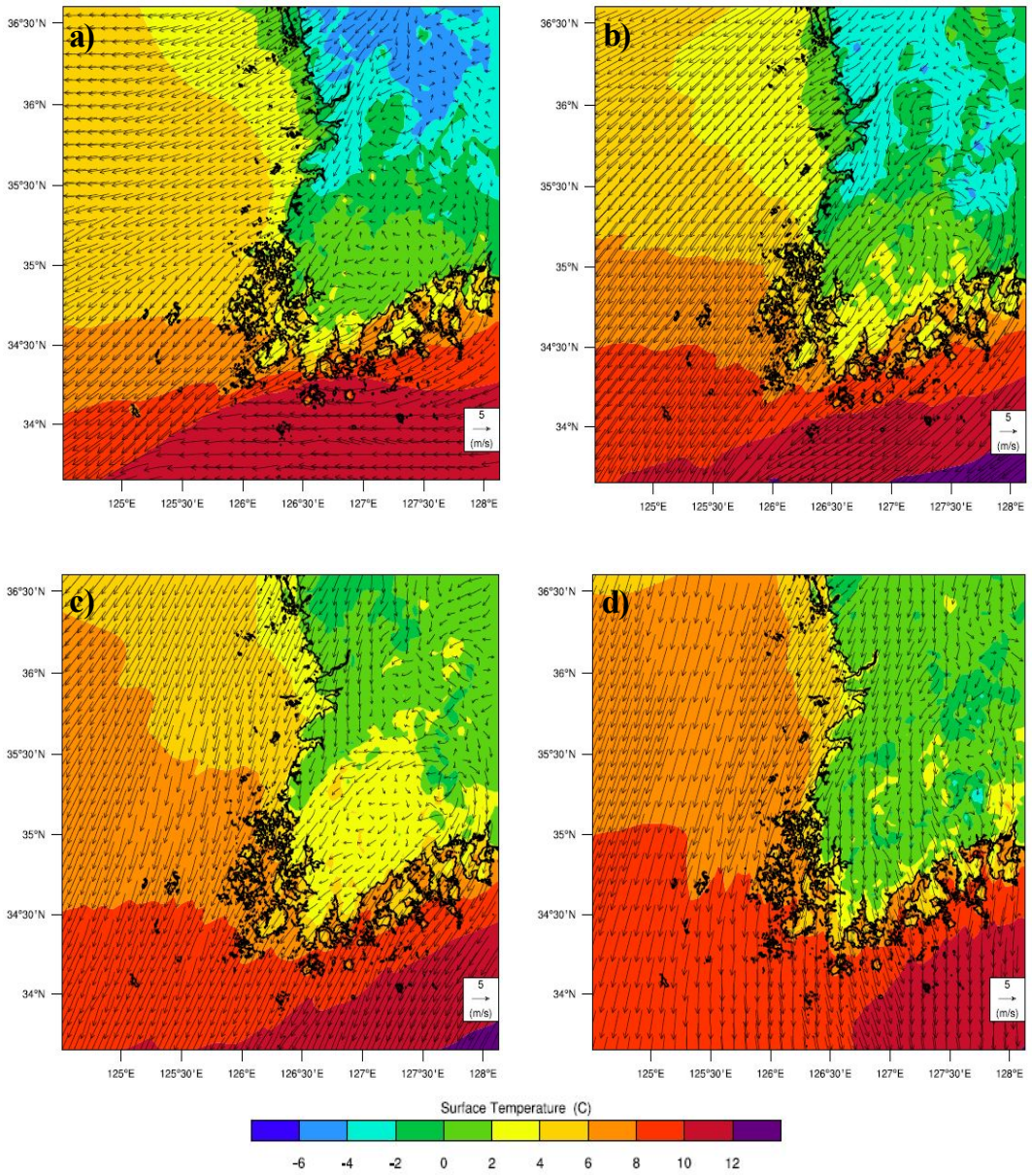

Fig. 4.54. Distribution of NCEP/NCAR SST and wind vector at a) 1500UTC and b) 2100UTC 27 December and c) 0300UTC and d) 0900UTC 28 December, 2012.

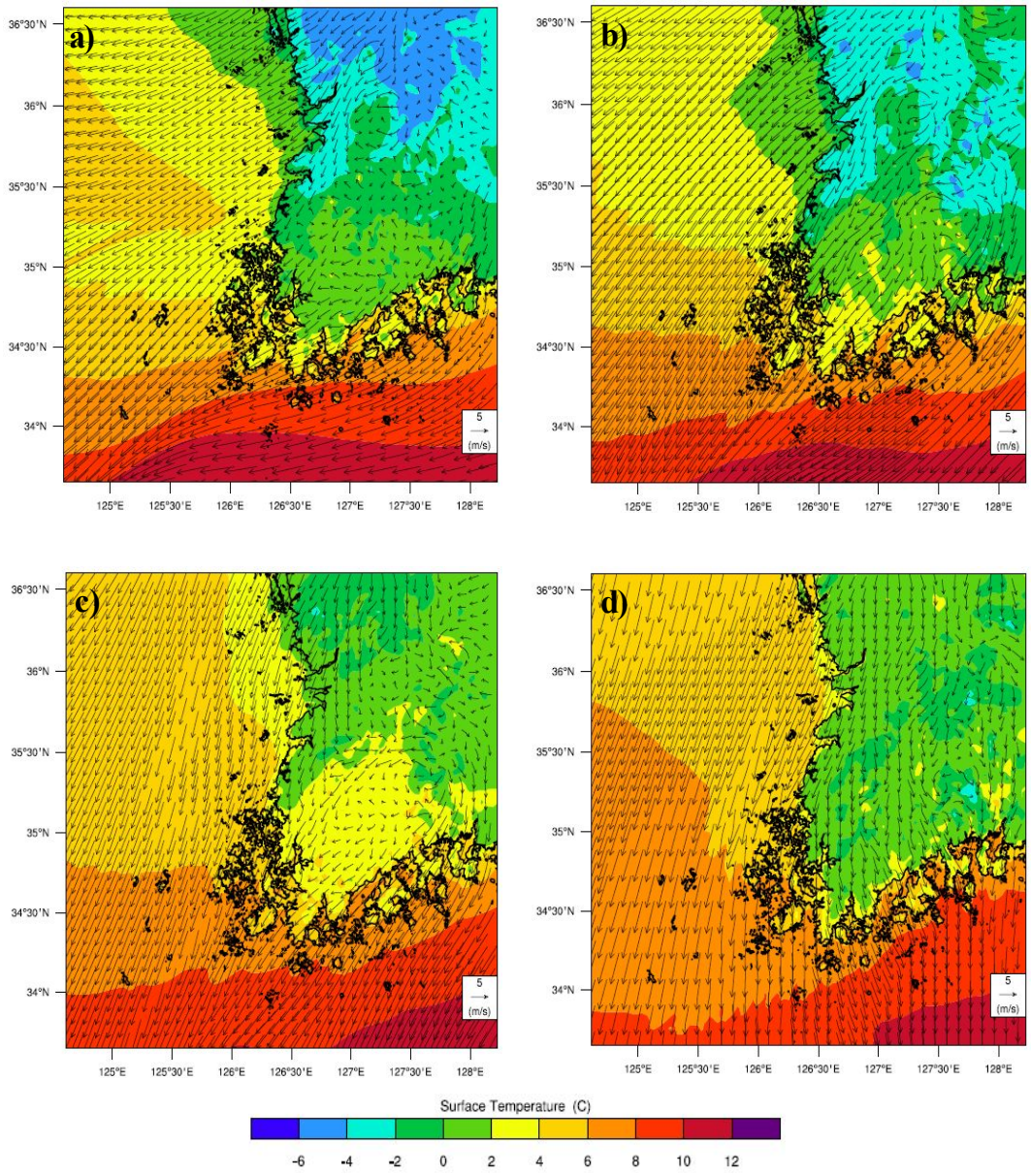

Fig. 4.55. Same as Fig. 4.54 but RTG SST.

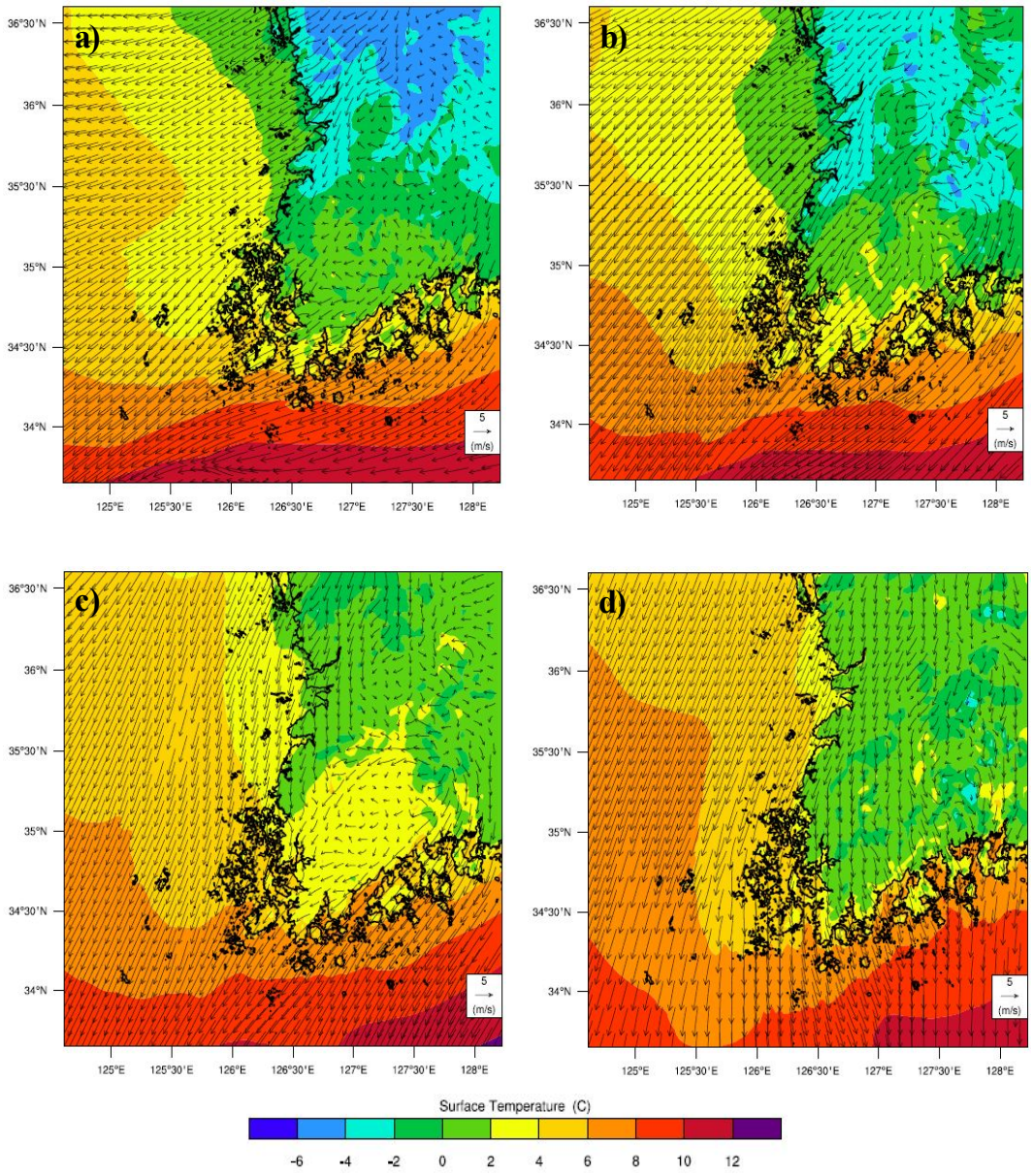

Fig. 4.56. Same as Fig. 4.54 but OSTIA.

(3) Total Snowfall and Precipitation

In order to assess the difference of the amount of snowfall, the difference of the result of the simulation where different sea surface temperatures were applied was surveyed. Fig. 4.57 shows the difference of the amount of snowfall in 1800UTC of the numerical mock case day where each sea surface information was applied. According to the amount of snowfall of OSTIA and the default, except for the Jiri Mountain regions where the deviation is big, the difference was very small of around 1~2cm overall. In other words, the difference of the snowfall depending on the difference of the sea surface is not big. However, these differences may be expressed in the topographical sense. (The snowfall of OSTIA is big in Jiri Mountain. The SST in the south coast's low latitude region which passes the Low pressure showed in the previous SST analysis is highest in OSTIA).

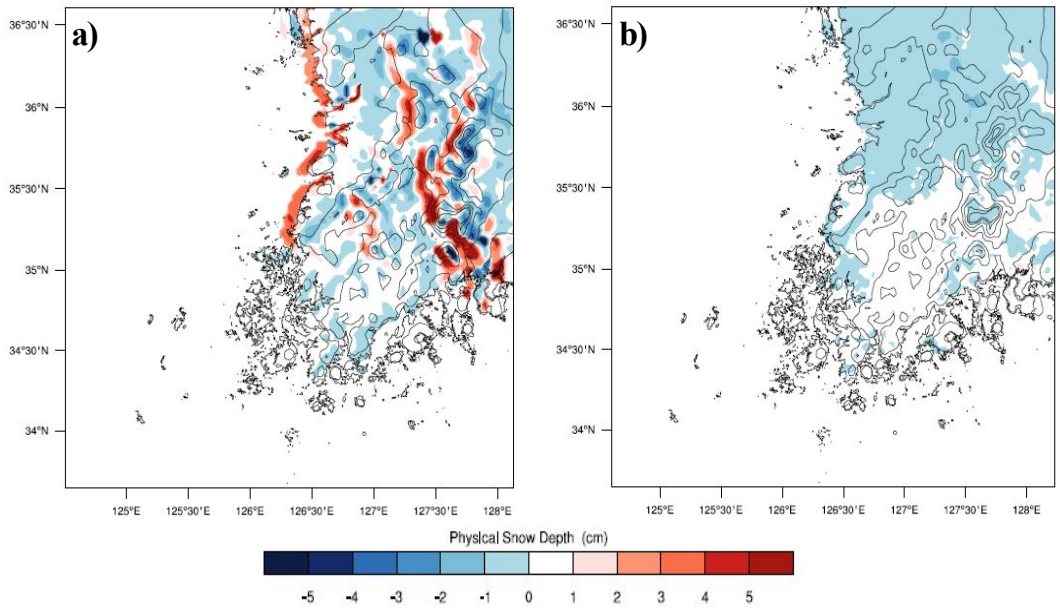

Fig. 4.57. Distribution of snowfall difference on 28 December, 2012 : a) OSTIA - NCEP/NCAR SST and b) OSTIA-RTG SST.

The difference between OSTIA and RTG is less than 1cm and thus shows a similar parallel distribution. Although the SST of each case showed a difference of a maximum of 3℃ in the west coastal line, when the Low pressure which was generated in the south sea side passes through the Korean peninsula, it passes relatively warm south coastal line and transforms itself into precipitation and thus when it reaches the inland, it does not affect much on the amount of the snowfall. The west coast also has some difference in the coastal lines, but this is limited to the coastal lines.

Fig. 4.58 shows the amount of snowfall at 1500UTC 28 December, 2012 the case day for the numerical mock test. It showed similar horizontality distribution in all the three cases.

When the Low pressure which was generated in the south sea side passes the Korean peninsula, the cumulus is developed due to the cold and dry Siberian high pressure, but the physical amount of rainfall shows to be little. The reason is that west Gyeongsangnamdo region where the snowfall occurs generally was because of the topographical element.

Also, the difference of SST mainly occurs in the west coast, and it is little in the south coast and is higher than in the west coast, and thus there is little difference in the amount of the snowfall that falls in the Korean peninsula.

In the previous section, it was discussed that the snowfall is the amount of snow that falls in the ground and thus there is need to analyze the effect of the ocean practically by analyzing the total snowfall amount that exist in the atmosphere. This shows the total precipitation during 24 hours on 28 December, 2012, the case day for the ground numerical mock test. The total precipitation is made by way of the cumulus and is the sum of the accumulated precipitation (RAINC) and precipitation accumulated in the total grid scale (RAINNC).

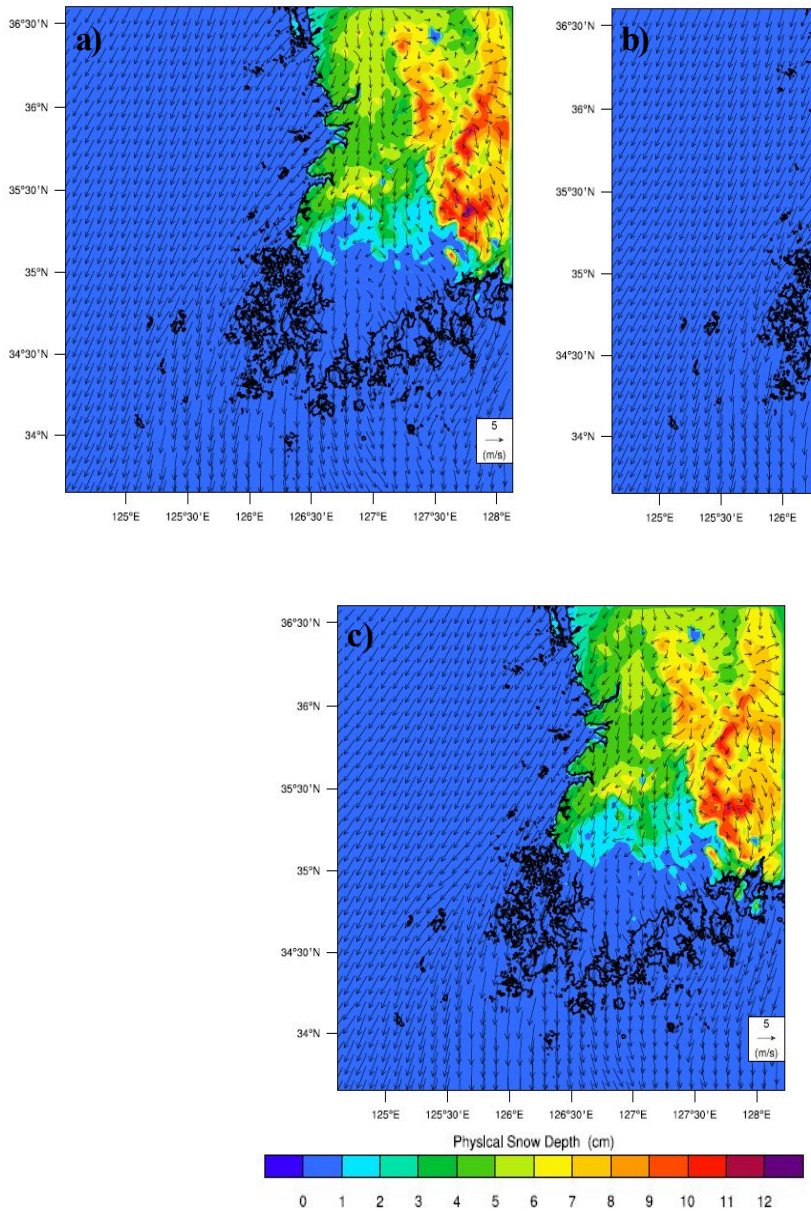

Fig. 4.58. Distribution of 24-hour accumulated snowfall on 28 December, 2012 : a) NCEP/NCAR SST, b) RTG SST, and c) OSTIA.

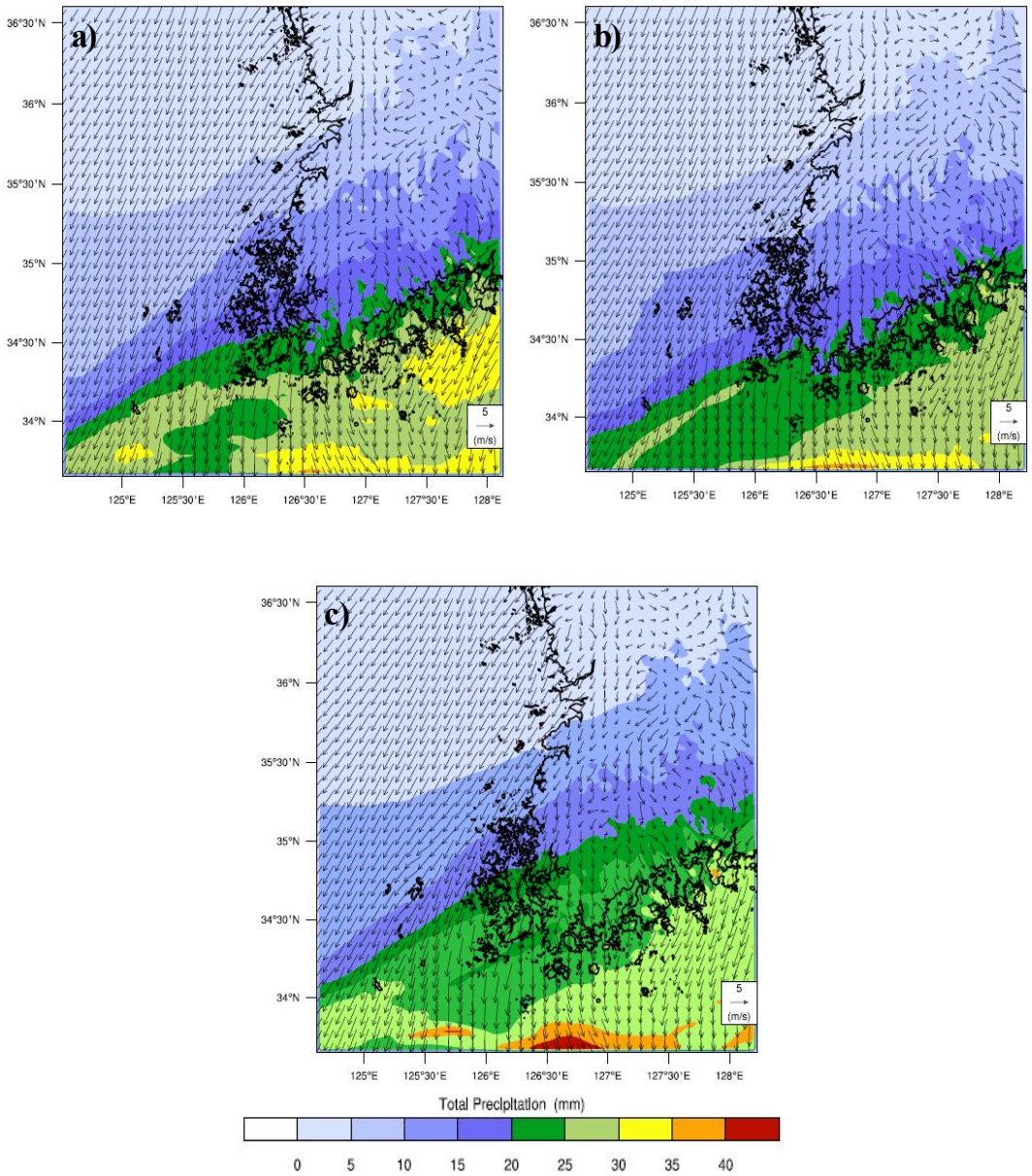

Fig. 4.59. Same as Fig. 4.58 but total precipitation on 28 December, 2012 : a) NCEP/NCAR SST, b) RTG SST, and c) OSTIA-RTG SST.

Fig. 4.59 shows the distribution of the total precipitation calculate in the numerical experiment where each sea surface was applied. This total precipitation is the sum of the serve grid precipitation generated by way of the cumulus current and the precipitation formed at the grid points through micro-physics process.

Overall, the total precipitation showed to be high in the default where the sea surface temperature was high. In this case, it was verified that strong precipitation occurred also in the ocean region along with the snowfall. On the other hand, there showed a bigger value in Jeonlanambukdo southwest coastal line and south coastal lines like Mokpo and Yeosu than in Jeonlabukdo west coast line for all the three cases. This difference seems to be related to the Low pressure that moves along the south coastal line.

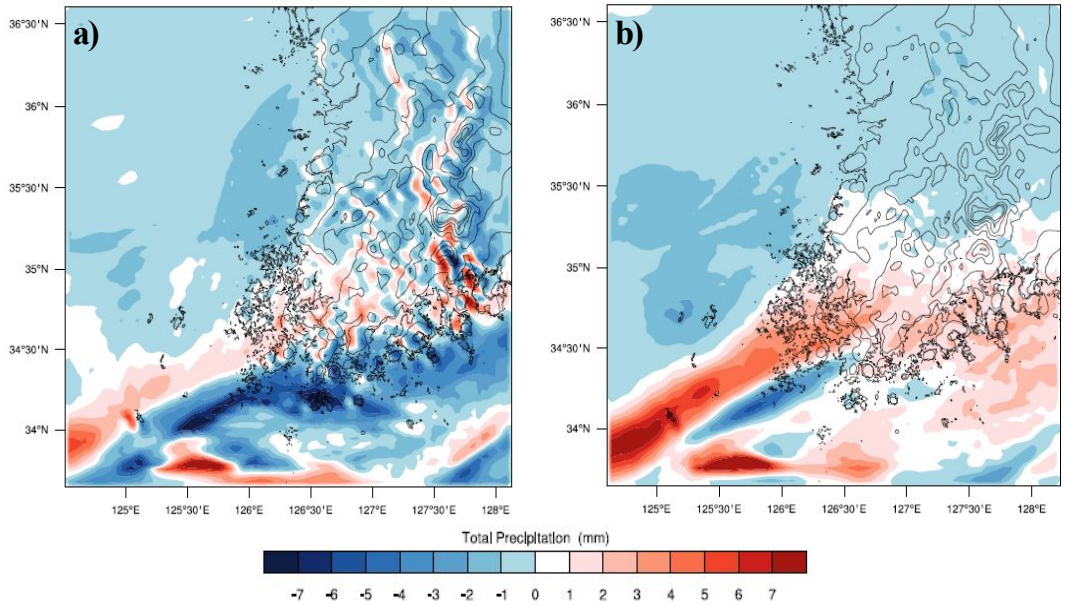

Fig. 4.60. Same as Fig. 4.58 but a) OSTIA - NCEP/NCAR SST and b) OSTIA - RTG SST.

In order to survey on this in a quantitative way, the difference of the total precipitation for the 24 hours of 31 December, 2010, the case day for the numerical test was showed in Fig. 4.60. It did not show big differences of total precipitation by each case. For the case of the total precipitation, it showed to be big in all the south coastal regions by each case and especially in the OSTIA case, it was 40mm maximum, the highest value. As mentioned above, this showed a very high total precipitation in the low altitude region of the south sea. Since the SST is relatively high in south coast than in west coast, it is judged that the Low pressure generated in the south passes the south coast and thus the total precipitation shows to be high.

(4) Vertical cross-section

Fig. 4.61 shows the difference of the vertical potential temperature calculated in the OSTIA and the default. The difference of the potential temperature of the high layer and low layers in the west coast was divided as of 500m and showed a weak but uniform value.

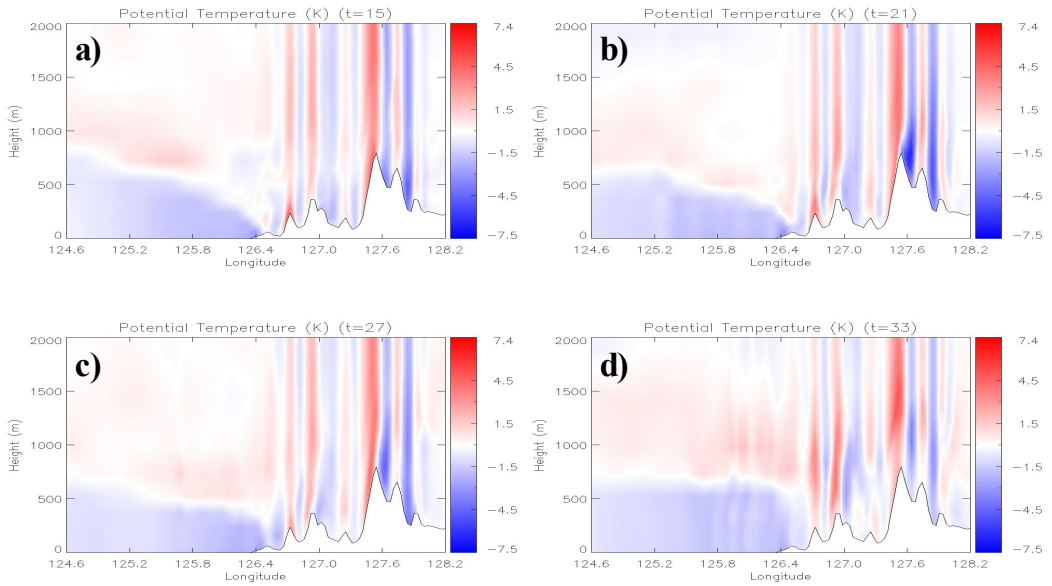

Fig. 4.61. Longitude-height distribution of potential temperature difference between OSTIA and NCEP/NCAR SST on 28 December, 2012.

This signifies that the low atmosphere of under 2km is more unstable in the default than in the OSTIA. In other words, the heat is being better transported upward by way of the high SST of the ocean in the low layer.

This continuous upward transportation occurs during the whole day continuously.

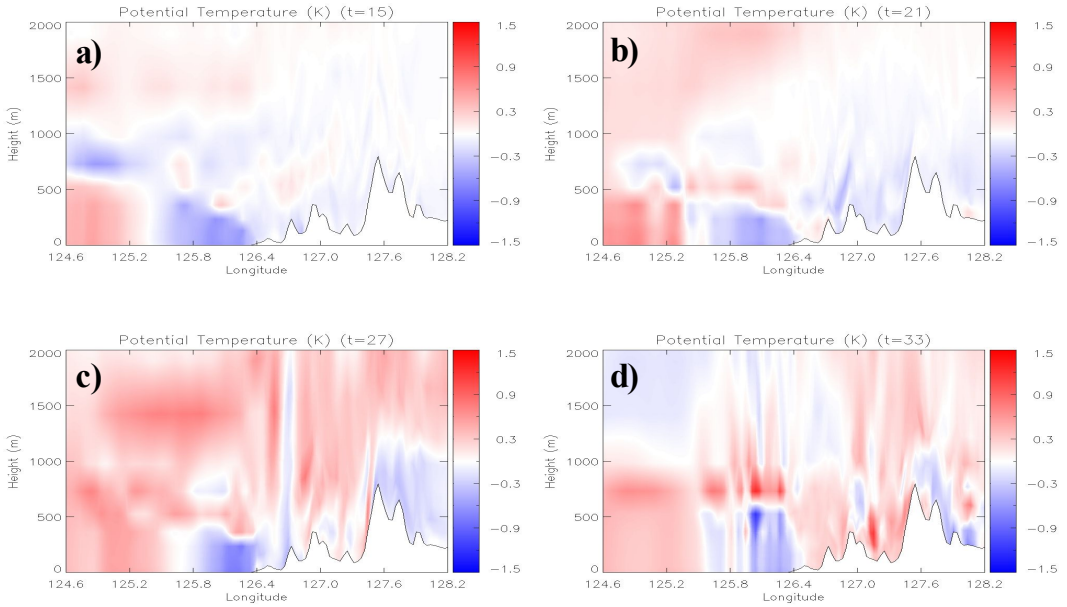

Fig. 4.62. Same as Fig. 4.61 but between OSTIA and RTG SST.

Fig. 4.63 shows the vertical velocity difference between OSTIA and RTG. Overall, it is seen that a very weak phase difference of vertical velocity occurs in the two cases.

It can be seen that this phase difference is very weak in the case where the heavy snowfall occurred when the parallel distribution of the sea surface temperature was affected by the Low pressure. Also, it is expected that the 2-dimensional sea surface temperature distribution induces the horizontal convergence and divergence of the atmosphere and it shall appear to be very complex.

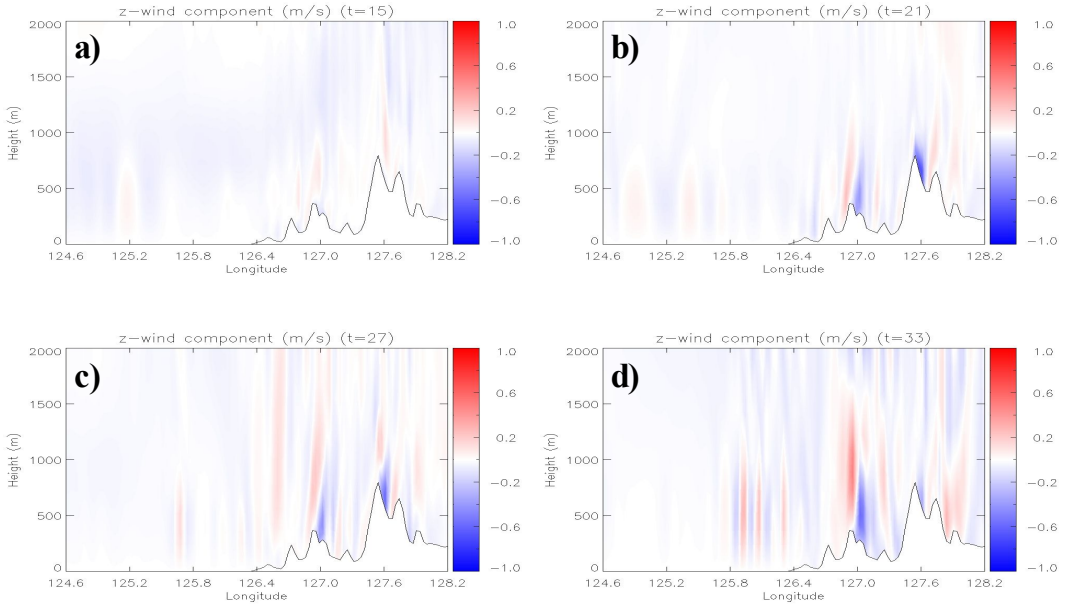

Fig. 4.63. Same as Fig. 4.61 but vertical velocity.

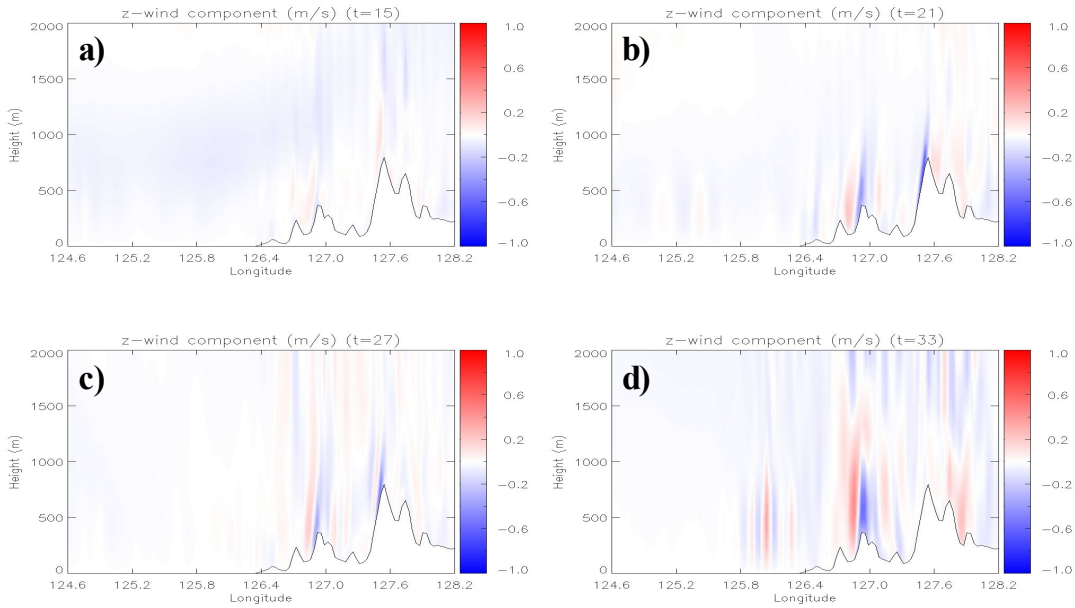

Fig. 4.64. Same as Fig. 4.63 but between OSTIA and RTG SST.

On the other hand, for the case of OSTIA and RTG in Fig. 4.64, phase difference also appears as in the Fig. 4.63, but it is a little different. For the case of the snowfall that appears by being affected by the low pressure, investigating on the difference of the vertical velocity through the 2-dimensional distribution of the sea surface temperature is difficult to be judged.

(5) Heat Budget

Fig. 4.65 shows the distribution of the latent heat flux for 1200UTC, 28 December. This closely related to the sea surface temperature and the migration of the temperature, in other words, the wind direction. The latent heat flux of default is found to be very low in the west sea and in overall the OSTIA shows a high latent heat flux in the south regions. This is located in the Low pressure route, and it can appear in a very big size by effects of the topographical reasons such as Jiri Mountain after it moves to the land.

The difference of the upward heat flux (Fig. 4.66) was not observed except for very few regions in west coast for the 3 cases. The latent heat flux that occurs due to the effect of SST when the Low pressure moves is not that big.

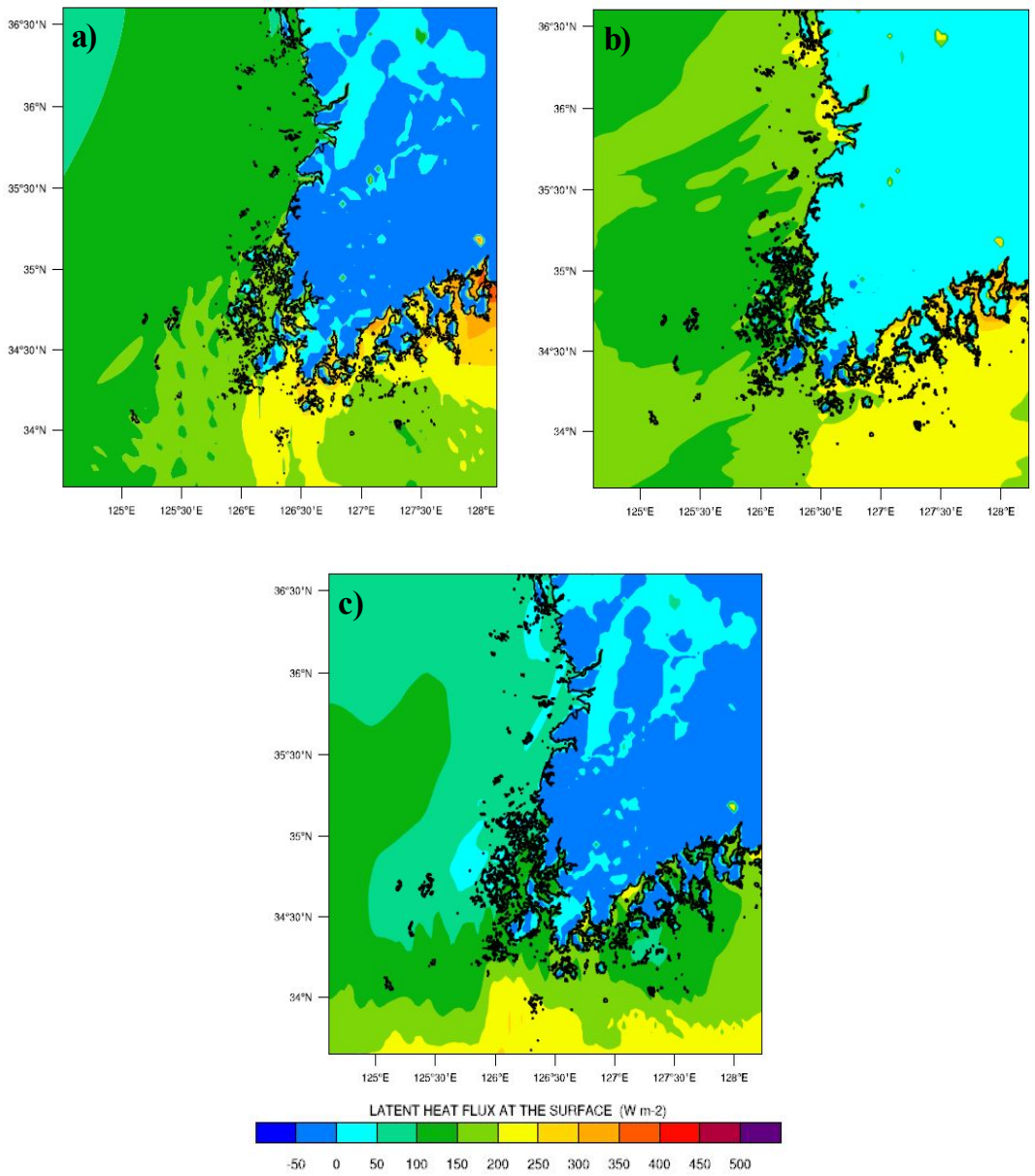

Fig. 4.65. Distribution of latent heat flux at 1800UTC 28 December, 2012 : a) NCEP/NCAR SST, b) RTG SST, and c) OSTIA..

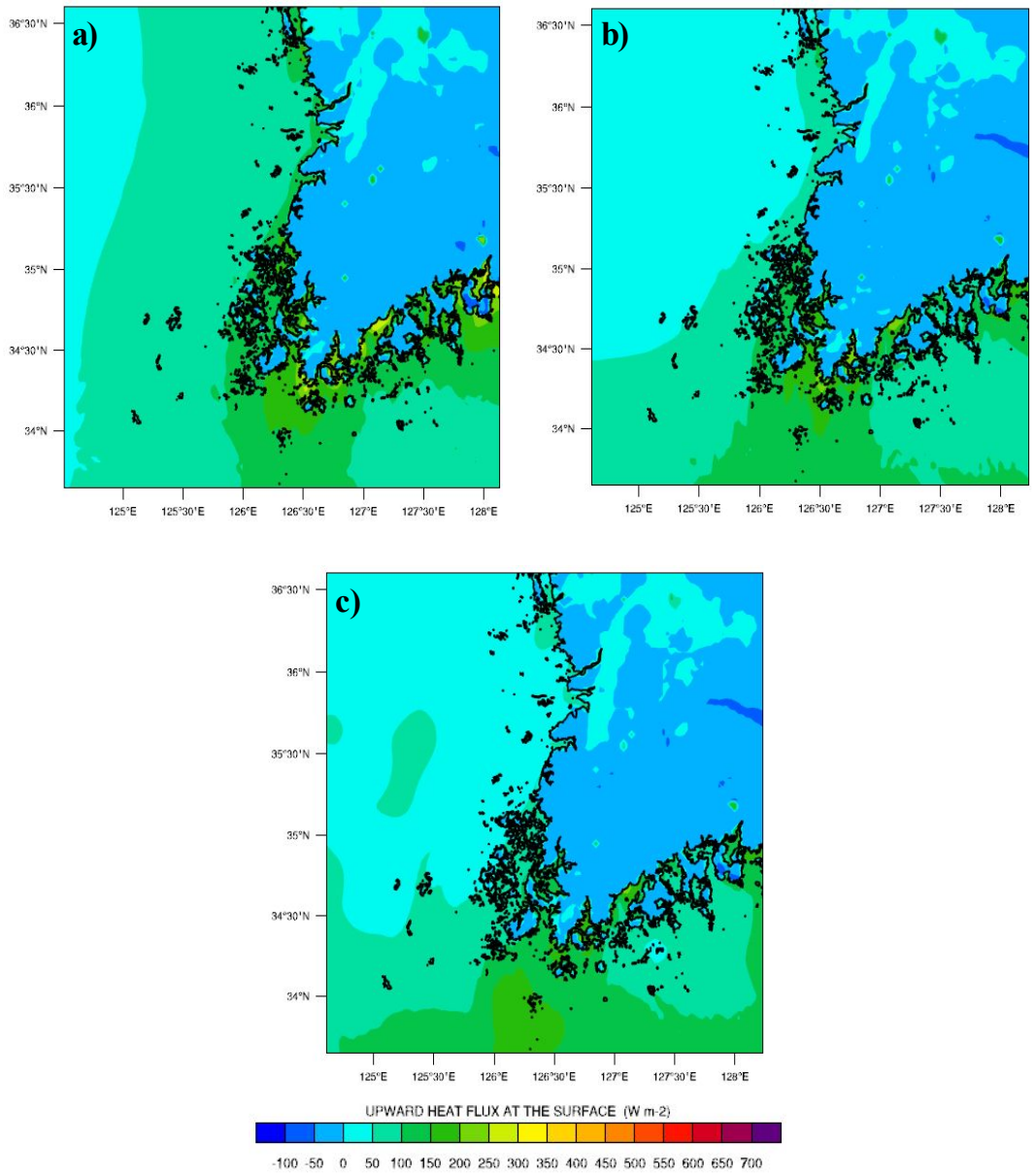

Fig. 4.66. Same as Fig. 4.65 but upward heat flux.

CHAPTER Ⅴ. SUMMARY AND CONCLUSION

This study has surveyed on the heavy snowfall occurrence factors through the case days when the heavy snowfall occurred in the south coast and southwest coast of Korean peninsula and especially on the meteorological phenomena of middle size on the heavy snowfall. Based on the conventional study data and the data used in this study, among the representative 2 cases of heavy snowfall that affect our country, what type of change the heavy snowfall intensity has brought into our country's coastal line by way of SST was surveyed through numerical experiment. This study intends to be an aid to enhance the correctiveness of the heavy snowfall forecast through the comparison and analysis by way of SST data.

Recently, the intensity and frequency of the snowfall is increasing in the west coast due to the sea air difference. The cases which affect much on the winter season of our country have been selected. The cases where the cold and dry cold High pressure passes through the west sea and is offered a lot of vapor and induced a lot of heavy snowfall in the west coast were selected. Another case that was selected was the one where the cold High pressure is situated in the north of our country, the Low pressure moves toward the southwest coast and is affected and caused a heavy snowfall.

The two cases selected were when a lot of snowfall recently was observed in our country. The effect of the meteorological elements and the effect on the heavy snowfall in the southwest regions were analyzed using the synoptic data and non-synoptic data based on the cases of 2010(cP expansion) and 2010(effect of Low pressure) on what type of effect they have on the heavy snowfall by way of increase of SST by selecting the recent cases of heavy snowfall. The 3 different sea surface temperatures were mock sampled and the effect on the occurrence of

heavy snowfall was quantitatively analyzed through the temperature, wind vector, amount of snowfall, total precipitation, cross section (potential temperature and wind velocity), and heat balance analysis.

1) It is the case where the effect of the Low pressure which was coming from the northwest on 29th starting from the west coast region was gradually given, and then with the expansion of the cold continent high pressure, the nation was generally cloudy and the snowfall occured based on the middle region (except for Gangwon and Yeongdong) like Seoul and Jeonlanambukdo regions during the 2 days of 29 and 31 of December 2010. On the 31, the Low pressure in the east coast of Japan was developed was going eastward slowly and the Low pressure near the gulf of Pohai was slowly moving southward and east ward. The continental High pressure near Baikal Lake was slowly moving southeastward, and after being affected by the Low pressure and the cold continental High pressure that was expanding in the northwest, the whole country was cloudy and snowfall was observed. With the resistance of the High pressure located in the East Siberia, the pressure band current of high latitude was slow, but as the Low pressure cut-off which accompanied the cold air of mid region of Manchuria circulate in a reverse manner, the short wave trough was penetrated and the pressure trough penetrated from the continent etc. and the middle latitude was periodically affected by the pressure trough like this.

The pressure trough near the gulf of Pohai was developed with an aid of the chill (-44℃) and was continuously moving southeastward, inducing the development of the ground Low pressure, has affected our country until the morning of the 31. On the other hand, since the shortwave trough that is accompanied by the Low pressure cut-off near Manchuria is situated in middle of Manchuria and in the Littoral province, and as this short wave trough reverse-circulates, the trough of Manchuria penetrated south regions on dawn of the 31th and the trough of littoral province in the first half of the 31st, moving the chill and thus developed strong snow

cloud in the west coast.

Along with much wind since the dawn of the 31, in some parts of Honam southwest coast, the strong-wind warning and heavy snowfall warning was released and when afternoon of the 31 approached, heavy snowfall warning was released in most of the Honam inland region and a lot of snowfall occurred. Snowfall occurred in the afternoon in Middle region and in the middle of the night in Gangwondo east coast with the infuse of the east wind current. A lot of snowfall occurred in the Honam inland west coast region and the whole country became sunny with the effect of the cold continent High pressure in the afternoon, and as the Low region High pressure located in Siberia gradually becomes weak and goes southward, the developed Low pressure cut-off located in Manchuria also gradually became weak and went eastward. It was the case day where the Low pressure cut-off developed in Machuria region nearly stagnates and makes short wave trough goes southward periodically, and pulled down the chill continuously and showed a strong cold for a certain period of time. The sea water temperature of this west coast is relatively high and thus worked as the Convergence Zone formation condition.

In Honam west coast region, the synoptic meteorological characteristic that occur through the past case analysis that happens during cP expansion happen much in West coast region including Gwangu and for the case by trough, it happens much in Jeollabukdo inland region. As the pressure trough developed in the upper layer and low layer passes our country, and the cold continental pressure expands toward our country, the pressure gradient becomes big, and thus the ground wind velocity increases to as big as around 25kts ~ 30kts. As the cold and dry air mass of winter season passes by the west coast and is provided with the vapor and heat, the air mass gets spoiled. As for the sea air difference during the heavy snowfall occurrence of this case day, the difference with the ground temperature was over 10℃ and the difference of 850hPa was over 20℃이상 and the heavy snowfall occurred. In addition to this, as the

convective cloud is formed and moves in the west coast, the orographic snowfall affected on the west coast region by way of the friction with the ground.

2) For the case of the heavy snowfall that occurs during expansion of cP, the three sea surface temperatures of default, RTG, and OSTIA where the climate value SST data was applied were applied. For the case of the temperature and wind vector, in the case of the default, it showed parallel by the altitude and 289K in the far lowest part. On the other hand, for the case of the OSTIA and RTG, the SST is distributed along the coastal line and the value shows as low as 5K in Chungcheongnamdo coastal region.

This type of temperature distribution affects the mesoscale meteorological model, and when the OSTIA and RTG SST was applied, the temperature of the coastal region is sampled lower by 1~2K in the 2100UTC compared to the default, and the wind velocity had the trend of being sampled weak because of the vertical pressure pattern.

The snowfall is being over-sampled in the case of the default. When considering the maximum observation value being 28cm of Jeongeup, the interpolation test of SST of OSTIA seems to be similar to the actual observation value. TThis difference depends upon the sea surface temperature distribution of the west coast and it seems to be because the SST of the default was over-sampled than actual. Also, this over-estimation of the SST relates directly to the over-sampling of the snowfall. Thus, the sea surface temperature information of the west coastal line becomes a very important element.

For the case of rainfall as well, it could be verified that strong snowfall occurred not only in Buan where the amount of snowfall was largest but also in the ocean region. The difference of SST by the case contributes much to the formation of the cumulus and this showed big in the difference of the total precipitation, and showed clearly the formation of the cumulus in the west coast and developed location and intensity caused

by the Siberian high pressure.

The cross section is the west and east cross section based on the points with highest snowfall and the analysis factors are the potential temperature and wind vector factor. The quantitative analysis result of the effect of the temperature distribution of the sea surface on the heavy snowfall by analyzing the difference among each sea surface temperature cases deducts the fact that the heat was transported better upward by way of the high SST of the ocean in the low layers.

For the case of heat balance analysis, the higher the sea surface temperature is, the more effective the vertical movement by latent heat flux is and for the case of the default, it is around 600 W/m2 in Jeongeup coastal region but for the case of the RTG and OSTIA, it is not more than 400 W/m2 . On the other hand, the movement of heat by sensible heat is limited to a large degree and thus for the case of default it is under 200 W/m2. Also, for the case of the OSTIA and RTG, the sensible heat flux showed to be similar to the latent heat flux, although there is a small difference in sea surface temperature of 2~3K, the probability is that a very different result might be deducted in the heat balance level.

3) The characteristic that shows through the case analysis of the past that occurs during expansion of the Low pressure based on the south region showed that the layer with high humidity is formed thick in the upper layer and thus there showed a lot of precipitation near the Low pressure. According to the observation data of the case day, the precipitation occurred as much as 35mm in Jeju island region between dawn and morning. Most regions except Jeju was under 0 degrees and snowfall occurred and accumulated much, and it occurred as the wet tongue form and a lot of snowfall as much as 5~10cm was observed in Jeonllanamdo region and as much as 10~17cm in Gyeongsangnamdo inland region.

According to the analysis result of the ground air pressure, with the

effect of the pressure trough that approaches from the north and the Low pressure which develops in the Jeju south sea and approaches, snowfall or rainfall was observed in all the regions in the country since late afternoon. With the effect of the Low pressure which develops in Taiwan region and approaches, the wind of southward kind which accompanies vapor blew strongly especially in the Gyeongsangnamdo coast region, and the current of low and moist waters showed to be similar to 700hPa. 0 degree of isothermal line will stay in south coast, the 1297gpm line comes toward the south coast in the thickness level of 1000-850hPa, and thus the south inland region had rain and the rain changes into snow and snowfall occurred in some regions. The low and moist waters located in Jeonllanamdo coast region expanded gradually to the whole country, and went away swiftly toward the east. According to the analysis result of the upper layer's meteorology, since the pressure tomb in Caspian west through Middle Siberia, the Blocking high in the arctic ocean, low region pressure tomb in east pacific and north america east coast are located, the flow of the pressure band of the middle and high latitude region is being stagnated but there is smooth circulation in our country.

As the short wave trough located in middle south region of China passes by our country since dawn until afternoon, it affected on the south and middle region. Especially, the trough which approaches toward the south coast became more active than the north trough as the temperature trough deepens. Also, until the Low pressure which develops in Mongol approaches, a weak altitude decrease showed in our country, but a very big altitude decrease showed in all around the country. The polar jet was flowing from the Baikal Lake through northwest, north of china and north korea and the tropical jet was flowing from the china's south-middle inland toward Japanese inland region, and thus a strong divergence region is located and supported the development of ground Low pressure.

4) For the case of the heavy snowfall that occurs during expansion of

Low pressure, three types of sea surface temperatures of SST (default), RTG, and OSTIA were applied through the numerical experiment. According to the difference of SST between the OSTIA were applied through the numerical experiment. According to the difference of SST between the OSTIA and the default, similarly to the case of 2010, for the case of the default, the form showed to follow the altitude and the RTG also followed the altitude. However, as we go farther from the coast line, the difference of the temperature was not that big. The difference of SST between OSTIA and RTG is not such a big value but showed a similar form as above. This showed limited to the coastal region. On the other hand, in most of the ocean region, the OSTIA had the trend of being higher than the RTG. Although this distributional difference is very big, the overall sea surface temperature difference in coastal region is not that big, and thus there showed a temperature difference of around 2K in Jindo, Jeonllanamdo. Accordingly, as it approaches the coastal line after passing through the ocean, there showed temperature difference, but the value was not that big and thus it is thought that there will not be big difference of the amount of the snowfall in this case where snowfall develops.

As for the temperature and wind vector, the difference of the temperature of the default with the ground surface temperature and wind vector is small, but there is a maximum difference of 2℃ in the south coast. For the case of the interpolation of the SST of OSTIA, the parallel distribution was seen to be in the shape similar to the case where the RTG is interpolated and numerically sampled.

As for the amount of snowfall in the OSTIA and default, except for the case where the deviation is big around Jiri Mountain, in overall the difference was small as 1~2cm. In other words, it is analyzed that the difference of the snowfall by way of the difference of the sea surface is not that big.

The total precipitation showed to be high in default where the sea

surface temperature of the snowfall is high. It could be verified that not only strong snowfall but also strong precipitation occurs in ocean region in this case. On the other hand, the strong precipitation showed more in Jeonllanamdo southwest coast and south coast like Mokpo and Yeosu than in Jeollanamdo and Jeollabukdo west coast in all the 3 cases.

The potential temperature difference and difference of vertical velocity of the cross section showed to be weak when affected by Low pressure. Also, the 2-dimensional sea surface temperature distribution will induce the parallel convergence and divergence and will show to be very complex.

As for the heat balance analysis, the latent heat flux is shown to be very low in the west coast and in overall the OSTIA shows a high latent heat flux in south regions. This can happen because it is located on the route of the Low pressure and due to the topographical effect such as Jiri Mountain after movement toward the inland.

To summarize the above results, the Low pressures which move along the south sea of our country and effect was interpreted differently. Unlike in the expansion of the cP, it did not show a big difference of snowfall by way of SST. For the case of the snowfall which occurred by being affected by pressure as showed in various analysis data and numerical mock teat result, it was judged that it is difficult to investigate on it through the 2-dimensional distribution of the sea surface temperature. It was concluded that for the case of the accumulation of snowfall by way of Low pressure, the judgement on the snow and rain depending on the temperature distribution of the low layer is important rather than the strength of the chill of the continental high pressure.

Especially, since there shows a lot of snowfall during a short period of time. If the possibility of precipitation exist and low layer of the atmosphere is under 0 degree, it can be thought that the temperature structure and humidity due to the saturation in the low layer are

important elements. Accordingly, it is judged that the quantitative analysis on the relationship between the specific humidity, humidity and temperature of ground ~925hPa will be necessary.

As the cold and dry High pressure passes by the west coast of our country, the air mass spoils due to the vapor and heat, there shows a very big difference in the heavy snowfall in the southwest coast. According to the survey result based on SST among all the other complex elements, when the observation values of SST(default), RTG SST, OSTIA were applied, what sampled the best value numerically in various atmosphere conditions was OSTIA. It is expected that the use of appropriate sea surface temperature data can contribute to the assessment of the correct heavy snowfall forecast.

REFERENCES

Barros, A. P., and R. J. Kuligowski, 1997:Orographic effects during a severe wintertime rainstorm in the Appalachian mountain. Mon. Wea. Rev., 126, 2648-2672.

Byun, D. S.,and Y. K. Cho, 2006; Double peak-flood current asymmetry in a shallow-water constituent dominated embayment with a macro-tidal flat. Geophysical Research Letter. VOL. 33, doi:10.1029/2006GL026967.

Carruthers, D. J.,T. W. Choularton, 1983:A model of the feeder-seeder mechanism of orgraphics rain including stratification and wind-drift effects. Quart. J. R. Meteor. Soc., 109, 575-588.

Cheong, S.-H., K.-Y. Byun, and T.-Y. Lee, 2006; Classification of snowfall over the Korean Peninsula based on development mechanism. Atmosphere, 16 (1), 33-48. (in Korean)

Choi, G.-Y., and Kwon, W.-T., 2008, Current and Future Changes in the Type of Wintertime Precipitation in South Korea, The Korean Geographical Society, 43(1), 1-19.

Donlon, C., Robinson, I., Casey, K. S., Vazquez- Cuervo, J., Armstrong, E., Arino, O., Gentemann, C., May, D., LeBorgne, P., Piolle, J., Barton, I., Beggs, H., Poulter, D. J. S., Merchant, C. J., Bingham, A., Heinz, S., Harris, A., Wick, G., Emery, B., Minnett, P., Evans, R., Llewellyn-Jones, D., Mutlow, C., Reynolds, R. W., Kawamura , H., Rayner, N., 2007, The Global Ocean Data Assimilation Experiment High-resolution Sea Surface Temperature Pilot Project, Bulletin of the American Meteorological Society, 88(8), 1197-1213.

Dudhia, J., 1993; A nonhydrostatic version of the Penn State/NCAR mesoscale model: Validation tests and simulation of an Atlantic cyclone and cloud front. Mon. Wea. Rev., 121, 1493-1513.

Dudhia, J., and J. F. Bresch, 2002; A global version of the PSU-NCAR

mesoscale model. Mon. Wea. Rev., 130, 2989-3007.

Gwangju Regional Meteorological Administration, 2000; Guidelines of Honam predictive analytics, 36-69.

Grell, G. A., L. Schade, R. Knoche, A. Pfeiffer, and J. Egger, 2000; Nonhydrostatic climate simulations of precipitation over complex terrain. Journal of Geophysical Research, Washington, DC, 105(D24): 29595-29608.

Grell,G., J. Dudhia, and D. Stauffer, 1995;A description of the fifth-generation

Guan, L.,and H. Kawamura, 2004; Merging satellite infrared and microwave SSTs: Methodology and evaluation of the new SST. J. Oceanogr., 60, 905-912.

Guo, Z., D. H. Bromwich, and J. J. Cassano, 2003; Evaluation of polar MM5 simulations of Antarctic atmospheric circulation. Mon. Wea. Rev., 131, 384-411.

Hong, S.-Y., and H.-L. Pan, 1996; Nonlocal boundary layer vertical diffusion in a medium-range forecast model, Mon. Wea. Rev., 124, 2322-2339.

Hosoda, K.,and H. Kawamura, 2004; Global space-time statistics of sea surface temperature estimated from AMSR-E data. Geophys. Res. Letter., 31 (17): Art. No. L17202.

http://www.mmm.ucar.edu/wrf/users/

http://www.mmm.ucar.edu/wrf/users/docs/wrf-phy.html

http://www.wrf-model.org/index.php

Hwang, Y.-H., 2005; A study for the Case that the Snowfall in Gwangju Chonnam Provice when Continental Polar is Expanded, 1-52.

Im, E.-H. and Lee, T.-Y., 1994; Two-Dimensional Numerical Study of the Terrain Effects on the Development of Cloud and Precipitation for the Middle Part of Korea, Atmosphere, 30(4), 565-582.

IPCC, 2007 ; Bindoff, N.L., J. Willebrand, V. Artale, A, Cazenave, J.

Gregory, S. Gulev, K. Hanawa, C. Le Qu□r□, S. Levitus, Y. Nojiri, C.K. Shum, L.D. Talley and A. Unnikrishnan, 2007: Observations: Oceanic Climate Change and Sea Level. In: Climate Change 2007: The Physical Science Basis . Contribution of Working Group I to the Fourth Assessment Report of the Intergovernmental Panel on Climate Change [Solomon, S., D. Qin, M. Manning, Z. Chen, M. Marquis, K.B. Averyt, M.Tignor and H.L. Miller(eds.)]. Cambridge University Press, Cambridge, United Kingdom and New York, NY, USA.

Janjic, Z. I., 1990: The step-mountain coordinate: physical package. Mon. Wea. Rev., 118, 1429-1443.

Janjic, Z. I., 1996a: The surface layer in the NCEP Eta Model. Eleventh Conference on Numerical Weather Prediction, Norfolk, VA, 19-23 August 1996; Amer. Meteor. Soc., Boston, MA, 354-355.

Janjic, Z. I., 2002: Nonsingular Implementation of the Mellor-Yamada Level 2.5 Scheme in the NCEP Meso model. NCEP Office Note No. 437, 61 pp.

Jun, J.-G., Lee, D.-G., and Lee, H.-A., 1994; A Study on the heavy Snowfalls Occurred in South Korea, Atmosphere, 30(1), 97-117.

Jo, I.-H., you, H.-D., Lee, W.-J. and Shin, G.-S., 2004; Analyses of the heavy Snowfall Event Occurred over the Middle Part of the Korean Peninsula on March 4, 2004 and Suggestions for the Future Forecast, Atmosphere, 14(3), 3-18.

Ju. H.-D., 2001; Honam Province fresh snow Prediction Analysis, 219-237.

Jung, B.-J., Hong, S.-Y., Seo, M,-S., and Na, D.-G., 2005; A Numerical Study of Dynamical and Thermodynamical Characteristics Associated with a heavy Snowfall Event over the Korean Peninsula on 4-5 March 2004, Atmosphere, 41(3), 387-399.

Jung, B.-J., S.-Y. Hong, M.-S. Suh, and D.-K. Rha, 2005; A numerical study of dynamic and thermodynamical characteristics associated

with a heavy snowfall event over the Korean Peninsula on 4-5 March 2004. J. Korean Meteor. Soc., 41(3), 387-399. (in Korean)

Jung, G.-B., Kim, J.-U, and Kwon, T.-Y. 2004; Characteristics of Lower-Tropospheric Wind Related with Winter Precipitation in the Yeongdong Region, Atmosphere, 40(4), 369-380.

Jung, Y.-G. 1999, Synoptic Environment Associated with the heavy Snowfall in the Southwestern Region of Korean peninsula, Jour. Korean Earth Science Society, 20(4), 398-410.

Kawai, Y.,and H. Kawamura, 2003; Validation of daily amplitude of sea surface temperature evaluated with a parametric model using satellite data. J. Oceanogr., 59, 637-644.

Kim, J.-A., 2013; A Study on Climatological Characteristics of Snowfall Occurrence over the Gwangju and Jeonllanamdo Region, 9-17.

K.M.A, 1997, Case Analysis heavy snowfall - 97 Forecast technology presentation, 87-104.

K.M.A, 2006; Deveelopment of Prediction Technic for Local Weather/ Severe rainfall and snowfall in Honam District(2002M-001-01), 236-257.

Lacis, A. A., and J. E. Hansen, 1974: A parameterization for the absorption of solar radiation in the earth's atmosphere. J. Atmos. Sci., 31, 118-133.

Laprise R., 1992: The Euler Equations of motion with hydrostatic pressure as as independent

Lee, H., and T. Y. Lee, 1994; The govering factors for heavy snowfall in Youngdong area. J. Korean Meteor. Soc., 30, 197-218. (in Korean)

Lee, J.-G. 1999; Synoptic Structure Causing the Difference in Observed Snowfall Amount at Taegwallyong and Kangnung: Case Study, Asia-Pacific Journal of Atmospheric Sciences, 35(2), 319-334.

Lee, J.-G. and Kim. U.-J. 2008; A Numerical Simulation Study Using WRF of a heavy Snowfall Event in the Yeongdong Coastal Area in Relation to the Northeasterly, Atmosphere, 18(4), 339-354, 35(2),

319-334.

Lee, J.-G., and J.-S. Lee, 2003; A numerical study of Yeongdong heavy snowfall events associated with easterly. J. Korean Meteor. Soc., 39, 475-490. (in Korean)

Lee, J.-J., Jang, J.-Y. and Kwak, C.-J., 2010; An Analysis of Temporal Characteristic Change for Various Hydrologic Weather Parameters (II) - On the Variability, Periodicity -, Journal of Korea Water Resources Association, 43(3), 483-493.

Lee, S.-H., D.-H. Kim, and H.-W. Lee, 2007b; Satellite-based assessment of the impact of sea-surface winds on regional atmospheric circulations over the Korean Peninsula. International Journal of Remote Sensing (in print).

Lee, S.-H., Y.-K. Kim, H.-S. Kim, and H.-W. Lee, 2007a; Influence of dense surface meteorological data assimilation on the prediction accuracy of ozone pollution in the southeastern coastal area of the Korean Peninsula. Atmospheric Environment, 41(21), 4451-4465.

Lee, T.-Y., and Y.-Y. Park, 1996; Formation of a mesoscale trough over the Korean Peninsula during an excursion of Siberian high, J. Meteor. Soc. Japan, 299-323.

Lee. S.-H. and Won, H.-S., 2005; Characters of Mesoscale Convective Complex Development in Korean Peninsula, Jour. Korean Earth Science Society, 26(7), 698-705.

Lee. S.-H., and Chun. J.-H.., 2003; The Distribution of Snowfall by Siberian High in the Honam Region - Emphasized on the Westward Region of the Noryung mountain ranges -, The Korean Geographical Society, 38(2), 173-178.

Lee. S.-H., Park. G.-Y., and Ryu, C.-S., 2006; Numerical Study on the Sensitivity of Meteorological Field Variation due to Radar Data Assimilation, Journal of the Environmental Sciences, 15(1), 9-19.

Levitus, S., J.I. Antonov, and T.P. Boyer, 2005a: Warming of the World Ocean, 1955-2003. Geophys. Res. Lett. , 32, L02604, doi:10.1029/

2004GL021592.

NIMR, 2006; A Study on the Regional Characteristics of heavy Snowfall Occurred in Honam Area.

NIMR, 2006; The Application of Regional Climate Change Scenario for the National Climate Change Report(II), 2006, 611 pp.

NIMR, 2009 ; To understand climate change, pp. 20.

NIMR, 2012 ; 『2012 Global climate change report』 in order to respond to IPCC5 Assessment Report, 46-47.

Mlawer, E. J., S. J. Taubman, P. D. Brown, M. J. Iacono, and S. A. Clough, 1997: Radiative trans-fer for inhomogeneous atmosphere: RRTM, a validated correlated-k model for the long-wave. J. Geophys. Res., 102(D14), 16663-16682.

Na, C.-H., and Kim, B.-S., 1990; "National phenomenon heavy snowfall in late January 1990" Forecast technology - Mar -, 1-8.

Nagata, M., 1993; Meso-β-scale vortices developing along the Japan-Sea polar-airmass convergence zone cloud band: Numerical simulation. J. Meteor. Soc. Japan, 71, 43-57.

Nikerson, E. C. E. R. Richard., Rosset, and D.R Smith, 1985 : The numerical simulation of cloud, rain, and airflow over the Vosges and Black forest mountains: AMeso-β model with parameterized microphysics. Mon. Wea. Rev., 114, 398-414

Ninomiya, K., J. Fujimori, and T. Akiyama, 1996; Multiscale feature of the cold air outbreak over Japan Sea and the northwestern Pacific. J. Meteor. Soc. Japan, 74, 745-761.

Ninomiya, K., T. Nishimura, T. Suzuki, and S. Matsumura, 2006; Polar-Air outbreak and air mass transformation over the east coast of Asia as simulated by an AGCM. J. Meteor. Soc. Japan, 84(1), 47-68.

Olson, D. A., N. W. Junker, and B. Korty, 1995; Evaluation of 33 years of quantitative precipitation forecasting at NMC. Wea. Forecasting, 10, 498-511.

Park. J.-H., Kim, K.-I., Lee, H.-L., 2006; Development framework and

mesoscale cyclone occurrence of East Sea brought heavy snowfallfall on the East Coast, Proceedings of Korean Meteorological Society, 290-291.

Penn State/NCAR Mesoscale Model (MM5)NCAR/TN-398+STR.

Richard, E. N. Chaumerliac, and J. F. Mahfouf, 1986: Numerical Simulation of orographic enhancement of rain with a mesoscale model. j. Climate Appl. Meteor., 26, 661-669.

Romero, R., C. A. Doswell, III, and C. Ramis, 2000; Mesoscale numerical study of two cases of long-lived quasi-stationary convective systems over eastern Spain. Monthly Weather Review, Boston, MA, 128(11), 3731-3751.

Romero, R., C. A. Doswell, III, and R. Riosalido, 2001; Observations and fine-grid simulations of a convective outbreak in Northeastern Spain: Importance of diurnal forcing and convective cold pools. Monthly Weather Review, Boston, MA, 129(9), 2157-2182.

Rutunno, R., and R. Ferretti, 2001; Mechanisms of intense Alpine rainfall. J. Atmos. Sci., 58, 1732-1749.

Ryu, C.-S., Sin, Y.-M., and Lee, S.-H., 2004, Numerical Studies for the Effects of Complicate Coastal Area on Variation of Mesoscale Circulation, Asia-Pacific Journal of Atmospheric Sciences, 40(1), 71-86.

Ryu, C.-S., Won, H.-S., and Lee, S.-H., 2005; A Study on the Influence of Aerological Observation Data Assimilation at Honam Area on Numerical Weather Prediction, 26(1), 66-77.

Ryu. C.-S., and Lee, S.-H, 2002; Numerical simulation on the flow of the sea surface and Louis wind formation whether the east coast of the using the coupled ocean system of mesoscale, Jour. Korean Earth Science Society, 42-43.

Seo, Y.-S. 2007; Climate change research of impact on marine resources and marine ecosystems, Expert seminar materials to respond to national land Research Institute climate change.

Shin, D.-B. 1988; Effect of terrain on the Heryukupun circulation in the central part of the Korean peninsula.

Smolarkiewicz, P. K., R. M. Rasmussen, and T. L. Clark, 1987: On the dynamics of Hwaiian cloud band: Island forcing. J.Atmos. Sci., 45, 1872-1905.

Song. B.-H., 1993; A comparative study for snowfalls between east coast and west coast region in South Korea, 1-30.

Stark, J. D., Donlon, C. J., Martin, M. J., McCulloch, M. E., 2007, OSTIA : An operational, high resolution, real time, global sea surface temperature analysis system, OCEANS 2007 - Europe, 1-4.

Stark, J. D., Donlon, C. J., O' arroll, A., 2008, Determination of AATSR Biases Using the OSTIA SST Analysis System and a Matchup Database, Journal of Atmospheric and Oceanic Technology, 25(7), 1208- 1217.

Stephens, G. L., 1978: Radiation profiles in extended water clouds. Part II: Parameterization schemes. J. Atmos. Sci., 35, 2123-2132.

Thiebaux, J., Rogers, E., Wang, W., Katz, B., 2003, A new high-resolution blended real-time global sea surface temperature analysis, Bulletin of the American Meteorological Society, 84(5), 645-656

Torrence, C. and G. P. Compo, 1998: A Practical Guide to Wavelet Analysis. Bull. Amer. Meteor. Soc., 79, 61-78.

variable, Mon. Wea. Rev., 120, 197-207.

Yoshizaki, M., T. Kato, H. Eito, S. Hayashi, and W.-K. Tao, 2004; An overview of the field experiment "Winter Mesoscale Convective Systems over the Japan Sea in 2001," and comparisons of the cold-air outbreak case (14 January) between analysis and a non-hydrostatic cloud-resolving model. J. Meteor. Soc. Japan, 82, 1365-1387.

ABSTRACT(in KOREAN)

대기-해양 상호작용과 관련된 대설강도에 관한 연구

박 근 영
지도교수 : 류 찬 수
조선대학교 대학원 대기과학과

최근 전 지구 및 한반도 주변 해수면온도의 증가에 따라 겨울철 대기-해양상호작용의 강화로 우리나라의 서해안과 남해안에 대설이 빈번히 발생하고 있다. 이러한 겨울철 위험기상현상에 따른 재해의 저감을 위하여 종관기상학적 분석 및 중규모수치모델 기반 예측기술 개발이 요구된다.

본 연구에서는 최근에 서해안과 남해안에 발생한 대설의 3사례(대륙성 고기압 장출, 이동성 고기압 으로 전이, 중위도 저기압)를 종관기상학적 분석을 하였고, WRF(Weather Research and Forecasting)를 기반으로 하여 대설에 미치는 3가지 종류의 SST(NCEP/NCAR SST, RTG SST, OSTIA) 민감도실험을 실시하여, 대기-해양 상호작용이 이들 지역의 강설 강도에 미치는 영향을 해석하였다.

대설 사례에 대한 종관기상학적 분석 결과, 차고 건조한 대륙성 고기압이 장출하는 경우, 대설은 상층 대기의 냉각이 뚜렷하게 나타나는 새벽시간에 많이 발생하였다. 특히, 대륙성 고기압 확장 시 상층 기압골이 지나면서 대설이 서해안 지역에 형성된 수렴역의 영향으로 발생하였고, 가끔씩 호남지방의 내륙까지 나타났다. 또한, 상·하층의 습수 변화는 대설 가능성 및 시작과 종료, 강도를 판단하는데 중요한 자료로 활용될 수 있음을 밝혔다. 그러나, 중위도 저기압의 영향을 받는 경우, 대설은 하층(925hPa와 850hPa)의 바람, 상당온위, 수렴장, 수분수렴과 지형의 효과의 영향을 크게 받았다.

한편, 우리나라의 서해안과 남해안에 각각 대설을 초래한 두 사례(2010년 12월 30일, 대륙성 고기압의 장출, Case 2010 ; 2012년 12월 28일, 이동성 저기압의 영향, Case 2012)에 대한 SST 민감도 실험을 실시한 결과, 일반적으로 NCEP/NCAR SST는 위도별로 평형한 반면, OSTIA와 RTG SST는 해안선을

따라 분포하는 특징이 있다. SST 민감도에 앞서 NCEP/NCAR SST가 서해 연안지역의 과대 모의된 SST의 영향으로 강설량도 과대 모의하였다.

2010년 12월 30일 사례(Case 2010)의 경우, 다양한 대기환경 조건에서 가장 좋은 수치모의를 보인 것은 OSTIA이었으며, 특히, NCEP/NCAR SST와 OSTIA간의 수치모의된 강설량의 차이가 최대 20cm로 나타났다. OSTIA와 RTG SST를 적용한 수치실험에서도 SST의 차이에 따른 강설량의 지역적 차이가 나타났지만, 이전의 경우에 비하여 그 차이가 크지 않았다. 이러한 결과는 SST가 높을수록 많은 강설량을 수치모의하는 경향을 보였으며, 지역적으로는 서해안 지역의 부안 근처에서 가장 큰 차이를 보였다.

2012년 12월 28일의 사례(Case 2012)는 Case2010에 비하여 SST에 따른 강설량의 변화가 크지 않았다. 다만, NCEP/NCAR SST와 OSTIA를 적용하여 수치모의된 강설량은 지형효과에 기인하여 지리산 주변에서 큰 차이가 나타났고, 그 밖의 지역에서는 대체적으로 1~2cm의 차이가 나타났다. 또한, 강설 강도에 미치는 OSTIA와 RTG SST간의 민감도 실험에서는 강설의 공간적 차이는 1cm 미만으로 나타났다. 한편, 남쪽 해상에서 발달한 저기압이 한반도를 통과하는 경우, 상대적으로 따뜻한 남해안을 통과하면서 강설보다는 강수의 형태를 보였고, 육지에 도달 후 내리는 강설량에는 크게 영향을 주지 않았으며, 서해안에서도 해안선에 국한되어 차이가 나타났다.

이처럼, 우리나라의 서해안과 남해안의 대설 발생에 있어서 서해와 남해의 SST는 매우 중요한 요소가 됨을 알 수 있었다. 그러나, 저기압의 영향에 의한 강설의 경우 2차원적 SST 분포뿐만 아니라 지형적 요인, 강수형태의 판별 등을 고려하여 강설발생 기구를 규명할 수 있으리라 판단된다.

APPENDIX

Ⅰ. Introduction to WRF Modeling

A. Numerical model WRF

WRF is a model used for the numerical simulation of weather field (Weather Research and Forecasting), is a community model that has been developed at the center (NCAR, National Center for Atmospheric Research) the U.S. National Atmospheric Environment Institute, and field research it is the atmospheric simulation system that is designed to be in use.

The Weather Research and Forecasting (WRF) Model is a next-generation mesoscale numerical weather prediction system designed to serve both atmospheric research and operational forecasting needs. It features two dynamical cores, a data assimilation system, and a software architecture allowing for parallel computation and system extensibility. The model serves a wide range of meteorological applications across scales ranging from meters to thousands of kilometers. The effort to develop WRF began in the latter part of the 1990's and was a collaborative partnership principally among the National Center for Atmospheric Research (NCAR), the National Oceanic and Atmospheric Administration (represented by the National Centers for Environmental Prediction (NCEP) and the (then) Forecast Systems Laboratory (FSL)), the Air Force Weather Agency (AFWA), the Naval Research Laboratory, the University of Oklahoma, and the Federal Aviation Administration (FAA).

WRF allows researchers the ability to produce simulations reflecting either real data (observations, analyses) or idealized atmospheric conditions. WRF provides operational forecasting a flexible and computationally efficient platform, while offering advances in physics, numerics, and data assimilation contributed by the many research community developers. WRF is currently in operational use at NCEP, AFWA, and other centers.

Ⅱ. Overview of WRF Modeling System

A. Introduction

The Advanced Research WRF (ARW) modeling system has been in development for the past few years. The current release is Version 3, available since April 2008. The ARW is designed to be a flexible, state of the art atmospheric simulation system that is portable and efficient on available parallel computing platforms. The ARW is suitable for use in a broad range of applications across scales ranging from meters to thousands of kilometers, including Idealized simulations, Parameterization research, Data assimilation research, Forecast research, Real-time NWP Hurricane research, Regional climate research, Coupled-model applications Teaching.

The Mesoscale and Microscale Meteorology Division of NCAR is currently maintaining and supporting a subset of the overall WRF code (Version 3) that includes WRF Software Framework (WSF), Advanced Research WRF (ARW) dynamic solver, including one-way, two-way nesting and moving nest. The WRF Preprocessing System (WPS), WRF Data Assimilation (WRF-DA) system which currently, supports 3DVAR 4DVAR, and hybrid data assimilation capabilities, Numerous physics packages contributed by WRF partners and the research community, Several graphics programs and conversion programs for other, graphics tools, The WRF modeling system software is in the public domain and is freely available for community use.

B. WRF Modeling System Program Components

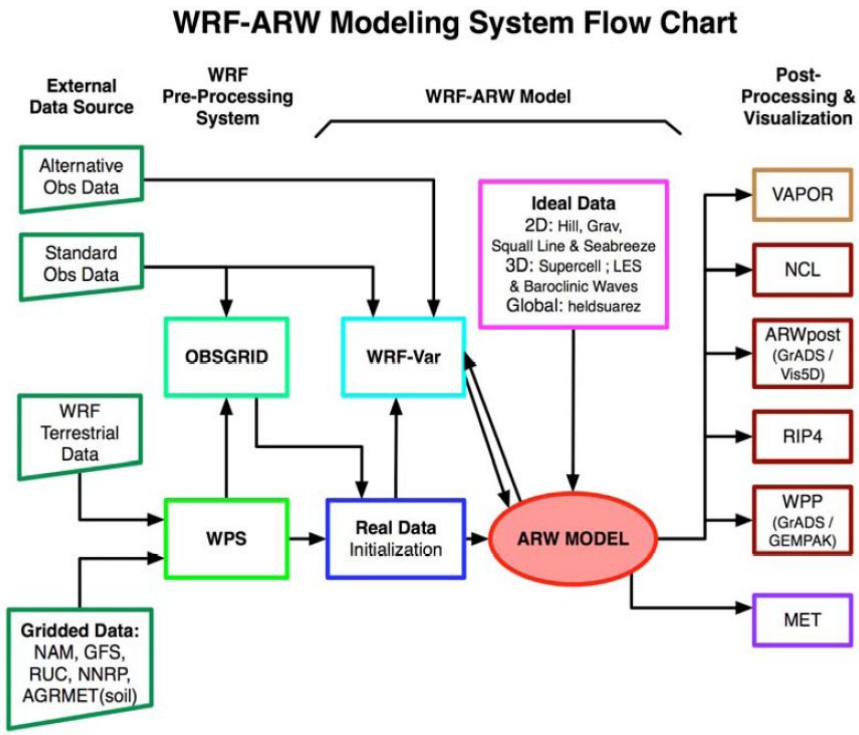

Fig. B.1. WRF Modeling System flow chart

As showed in the diagram, the WRF Modeling System consists of these major programs: The WRF Preprocessing System (WPS), WRF-Var, ARW solver, Post-processing & Visualization tools.

1. WPS

The function of the WRF Preprocessing System (WPS) is to define WRF grid, generate map, elevation and land information for WRF, take real-data analyses/forecasts from another model, and interpolate the data to the WRF grid. The time-dependent (analysis) fields consist of 3d wind, potential temperature, and water vapor, and a number of 2d fields.

This program is used primarily for real-data simulations.

Its functions include 1) defining simulation domains; 2) interpolating terrestrial data (such as terrain, land use, and soil types) to the simulation domain; and 3) degribbing and interpolating meteorological data from another model to this simulation domain. Its main features includeGRIB 1/2 meteorological data from various centers around the world, USGS 24 category and MODIS 20 category land data sets, Map projections for a) polar stereo graphic, b) Lambert-Conformal, c) Mercator and d) latitude-longitude, Nesting, User-interfaces to input other static data as well as met data.

2. WRF-Var

This program is optional, but can be used to ingest observations into the interpolated analyses created by WPS. It can also be used to update WRF model's initial conditions when the WRF model is run in cycling mode. Its main features are as follows. It is based on an incremental variational data assimilation technique, and has both 3D-Var and 4D-Var capabilities, It also includes the capability of hybrid data assimilation (Variational + Ensemble), The conjugate gradient method is utilized to minimize the cost function in the analysis control variable space, Analysis is performed on an un-staggered Arakawa A-grid, Analysis increments are interpolated to staggered Arakawa C-grid and it gets added to the background (first guess) to get the final analysis of the WRF-model grid, Conventional observation data input may be supplied either in ASCII format via the "obsproc" utility or "PREPBUFR" format, Multiple satellite observation data input may be supplied in BUFR format, Multiple radar data (reflectivity & radial velocity) input is supplied through ASCII format, Multiple outer loop to address the non linearity Capability to compute adjoint sensitivity Horizontal component of the background (first guess) error is represented via a recursive filter (for regional) or power spectrum

(for global), Horizontal and vertical background errors are non-separable. Each eigenvector has its own horizontal climatologically-determined length scale Preconditioning of the background part of the cost function is done via the control variable transform U defined as B= UUT, It includes the "gen_be" utility to generate the climatological background error covariance estimate via the NMC-method or ensemble perturbations, A utility program to update WRF boundary condition file after WRF-DA.

3. ARW Solver

The equation set for ARW is fully compressible, Eulerian and nonhydrostatic with a run-time hydrostatic option. It is conservative for scalar variables. The model uses terrain-following, hydrostatic-pressure vertical coordinate with the top of the model being a constant pressure surface.

a. Vertical Coordinate and Variables

The ARW equations are formulated using a terrain-following hydrostatic-pressure vertical co- ordinate denoted by η and defined as

$$\eta = (p_h - p_{ht})/\mu \qquad \text{where } \mu = p_{hs} - p_{ht}. \quad \text{(B.1)}$$

p_h is the hydrostatic component of the pressure, and p_{hs} and p_{ht} refer to values along the surface and top boundaries, respectively. The coordinate definition (4.1), proposed by Laprise (1992), is the traditional σ coordinate used in many hydro- static atmospheric models. η varies from a value of 1 at the surface to 0 at the upper boundary of the model domain (Fig. B.1). This vertical coor- dinate is also called a mass vertical coordinate.

Since $\mu(x, y)$ represents the mass per unit region within the column in the model domain at (x, y), the appropriate flux form variables are

$$\mathbf{V} = \mu\mathbf{v} = (U, V, W), \qquad \Omega = \mu\dot{\eta}, \qquad \Theta = \mu\theta. \quad \text{(B.2)}$$

$\mathbf{v} = (u, v, w)$ are the covariant velocities in the two horizontal and vertical directions, respec-tively, while $\omega = \dot{\eta}$ is the contravariant 'vertical' velocity. θ is the potential temperature. Also appearing in the governing equations of the ARW are the non-conserved variables $\varphi = gz$ (the geopotential), p (pressure), and $\alpha = 1/\rho$ (the inverse density).

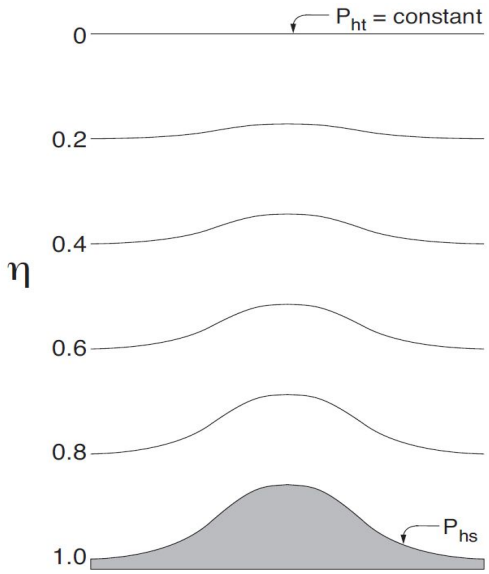

Fig. B.2. ARW η coordinate.

b. Euler Equations

Using the variables defined above, the flux-form Eulere equations can be written as

$$\partial_t U + (\nabla \cdot \mathbf{V}u) - \partial_x(p\varphi_\eta) + \partial_\eta(p\varphi_x) = F_U \quad \text{(B.3)}$$

$$\partial_t V + (\nabla \cdot \mathbf{V}v) - \partial_y(p\varphi_\eta) + \partial_\eta(p\varphi_y) = F_V \quad \text{(B.4)}$$

$$\partial_t W + (\nabla \cdot \mathbf{V}w) - g(\partial_\eta p - \mu) = F_W \quad \text{(B.5)}$$

$$\partial_t \Theta + (\nabla \cdot \mathbf{V}\theta) = F_\Theta \quad \text{(B.6)}$$

$$\partial_t \square + (\nabla \cdot \mathbf{V}) = 0 \quad \text{(B.7)}$$

$$\partial_t \varphi + \square^{-1}[(\mathbf{V} \cdot \nabla\varphi) - gW] = 0 \quad \text{(B.8)}$$

along with the diagnostic relation for the inverse density

$$\partial_\eta \varphi = -\alpha\mu, \quad (2.9)$$

and the equation of state

$$p = p_0(R_d\theta/p_0\alpha)^\gamma . \quad \text{(B.10)}$$

In (4.3) - (4.10), the subscripts x, y and η denote differentiation,

$\nabla \cdot \mathbf{V}a = \partial_x(Ua) + \partial_y(Va) + \partial_\eta(\Omega a)$, and

$$\mathbf{V} \cdot \nabla a = U\partial_x a + V\partial_y a + \Omega\partial_\eta a,$$

where a represents a generic variable. $\gamma = c_p/c_V = 1.4$ is the ratio of the heat capacities for dry air, R_d is the gas constant for dry air, and p_0 is a reference pressure (typically 10^5 Pascals). The right-hand-side (RHS) terms F_U, F_V, F_W, and F_Θ represent forcing terms arising from model physics, turbulent mixing, spherical projections, and the earth's rotation.

The horizontal grid is the Arakawa-C grid. Arakawa-C grid staggering for a portion of a parent domain and an imbedded nest domain with a 3:1 grid size ratio. The solid lines denote coarse grid cell boundaries, and the

dashed lines are the boundaries for each fine grid cell. The horizontal components of velocity ("U" and "V") are defined along the normal cell face, and the thermodynamic variables ("θ") are defined at the center of the grid cell (each square). The bold typeface variables along the interface between the coarse and the fine grid define the locations where the specified lateral boundaries for the nest are in effect.

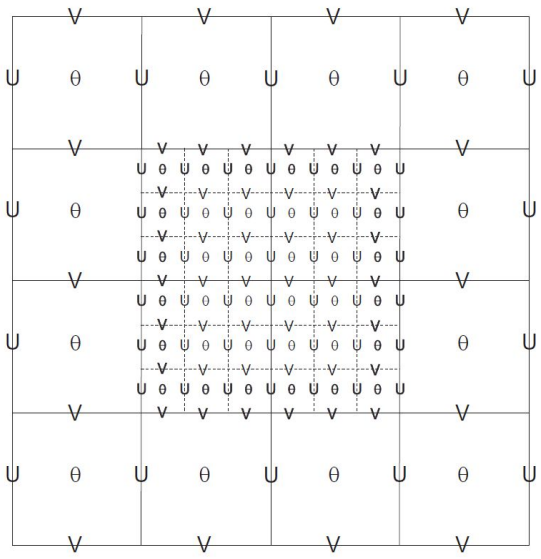

Fig. B.3. Arakawa-C grid staggering for a portion of a parent domain and an imbedded nest domain with a 3:1 grid size ratio.

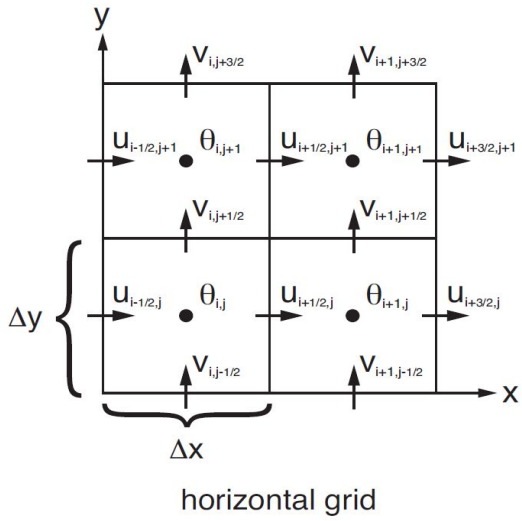

Fig. B.4. WRF Modeling System flow chart

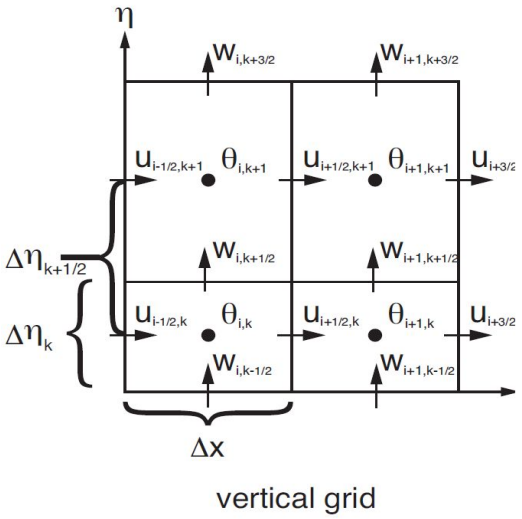

Fig. B.5. WRF Modeling System flow chart

The time integration scheme in the model uses the third-order Runge-Kutta scheme, and the spatial discretization employs 2nd to 6th order schemes. The model supports both idealized and real-data applications with various lateral boundary condition options. The model also supports one-way, two-way and moving nest options. It runs on

single-processor, shared- and distributed-memory computers.

The WRF model can be run with either idealized initialization or real-data initialization. In the current release (release 3.0, April 2008), the WRF model supports the Eulerian mass solver, referred to as the advanced research WRF (ARW) dynamical solver. The purpose of the ideal.F (pink) and real_em.F (blue) programs is to generate input and (if necessary) boundary files for the WRF model. This involves a hydrostatic balance adjustment in addition to setting up the initial 3d and 2d fields of the WRF variables. The WRF model supports full physics, two-way, one-way and two-way moving nests, analysis and observation nudging.

4. Initial conditions

The ARW may be run with user-defined initial conditions for idealized simulations, or it may be run using interpolated data from either an external analysis or forecast for real-data cases. Both

2D and 3D tests cases for idealized simulations are provided. Several sample cases for real-data simulations are provided, which rely on pre-processing from an external package (usually the WRF Preprocessor System, referred to as WPS) that converts the large-scale GriB data into a format suitable for ingest by the ARW's real-data processor.

The programs that generate the specific initial conditions for the selected idealized or real- data case function similarly. They provide the ARW with, input data that is on the correct horizontal and vertical staggering, hydrostatically balanced reference state and perturbation fields and metadata specifying such information as the date, grid physical characteristics, and projection details.

For neither the idealized nor the real-data cases are the initial conditions strengthened with observations. However, output from the ARW system initial condition programs is suitable as input to the WRF variational assimilation package.

5. Physics

To simulate real weather and to do simulations with coarse resolutions, a minimum set of physics components is required, namely radiation, boundary layer and land-surface parameterization, convective parameterization, sub grid eddy diffusion, and microphysics. Since the model is developed for both research and operational groups, sophisticated physics schemes and simple physics schemes are needed in the model. The objectives of the WRF physics development are to implement a basic set of physics into the WRF model and to design a user friendly physics interface.

Currently, several physics components have been included in WRF: microphysics, cumulus parameterization, long wave radiation, short wave radiation, boundary layer turbulence (PBL), surface layer, land-surface parameterization, and sub-grid scale diffusion.

Long wave radiation is (a) RRTM (rrtmscheme) [module_ra_rrtm.F This RRTM, which is taken from MM5, is based on Mlawer *et al.* (1997), and it is a spectral-band scheme using the correlated-k method. It uses pre-set tables to accurately represent longwave processes due to water vapor, ozone, CO2, and trace gases (if present) as well as accounting for cloud optical depth. (b) ETA GFDL long wave (gfdllwscheme) [module_ra_gfdleta.F] This long wave radiation is from GFDL. It follows the simplified exchange method of Fels and Schwarzkopf (1975) and Schwarzkopf and Fels (1991), with calculation over spectral bands associated with carbon dioxide, water vapor, and ozone. Schwarzkopf and Fels (1985) transmission coefficients for carbon dioxide, a Roberts *et al.* (1976) water vapor continuum, and the effects of water vapor-carbon dioxide overlap and of a Voigt line-shape correction are included. The Rodgers (1968) formulation is adopted for ozone absorption. Clouds are randomly overlapped. (This paragraph was provided by Kenneth Campana.) This scheme is

implemented to conduct tests with old Eta model.

Short wave radiation is (a) Simple short wave (swscheme) [module_ra_sw.F] The scheme is base on Dudhia (1989) and taken from MM5. It is a simple downward integration of solar flux, accounting for clear-air scattering, water vapor absorption (Lacis and Hansen 1974), and cloud albedo and absorption. It uses look-up tables for clouds from Stephens (1978). (b) Goddard short wave (gsfcswscheme) [module_ra_gsfcsw.F] This scheme is base on Chou and Suarez (1994). (c) ETA GFDL short wave (gfdlswscheme) [module_ra_gfdleta.F]

This shortwave radiation is a GFDL version of the Lacis and Hansen (1974) parameterization. Effects of atmospheric water vapor, ozone (both from Lacis and Hansen, 1974) and carbon dioxide (Sasamori, *et al.*, 1972) are employed. Clouds are randomly overlapped. SW calculations are made using a daylight-mean cosine solar zenith angle over the time interval (given in name list.input). The diurnal cycle is approximated during the hour by weighting SW heating rates and fluxes with the actual cosine zenith angle at each model time-step. (This paragraph was provided by Kenneth Campana.) This scheme is implemented to conduct tests with old Eta model.

6. Boundary layer parameterization

(a) MRF (mrfscheme) [module_bl_mrf.F] is The scheme is described by Hong and Pan (1996). This uses a so-called countergradient flux for heat and moisture in unstable conditions. It uses strengthened vertical flux coefficients in the PBL, and the PBL height is determined from a critical bulk Richardson number. It handles vertical diffusion with an implicit local scheme, and it is based on local Ri in the free atmosphere.

(b) MYJ (myjpblscheme) [module_bl_myjpbl.F] is The parameterization of turbulence in the PBL and in the free atmosphere

(Janjic, 1990, 1996b, 2002) represents a nonsingular implementation of the Mellor–Yamada Level 2.5 turbulence closure model (Mellor and Yamada, 1982) through the full range of atmospheric turbulent regimes. In this implementation, an upper limit is imposed on the master length scale. This upper limit depends on TKE and the buoyancy and shear of the driving flow. In the unstable range the functional form of the upper limit is derived from the requirement that the TKE production be nonsingular in the case of growing turbulence. In the stable range the upper limit is derived from the requirement that the ratio of the variance of the vertical velocity deviation and TKE cannot be smaller than that corresponding to the regime of vanishing turbulence. The TKE production/dissipation differential equation is solved iteratively The empirical constants have been revised as well (Janjic, 1996b, 2002). (This paragraph was provided by Zavisa Janjic)

감사의 글

‘지식을 배웠음에도 불구하고 그것을 활용하지 않는 사람은 밭을 열심히 갈아 놓고도 씨앗을 뿌리지 않는 사람과 같다’ – Lev Nikolayevich Tolstoy

라는 말처럼 박사과정을 수료 한 채로 졸업의 결실을 맺지 못하여 한동안 아쉬움이 남는 시간들의 연속 이였습니다. 이제야 졸업논문을 마치면서 도움을 주신 많은 분들에게 감사의 인사를 전하고자 합니다.

먼저 10여년 넘도록 지금까지 많이 부족한 저를 학문의 길로 이끌어 주시고, 자식처럼 격려와 배려를 해주시며, 학문뿐만 아니라 세상을 살아가는데 필요한 많은 지식을 가르쳐 주신 류찬수 교수님께 진심으로 감사드립니다. 교수님의 따뜻한 가르침을 잊어버리지 않고, 감사하는 마음을 지니며 끊임없이 정진하도록 노력하겠습니다.

저의 학위논문 심사위원장님으로 논문의 부족한 부분에 대해 도움을 주신 이종호 센터장님, 가까이 있으면서 세심한 배려와 조언을 아끼지 않으시며 밝은 미소와 다정한 말씀으로 지도해주신 정효상 교수님, 올해 교수로 부임하시면서 너무나도 바쁘신 가운데 많은 도움을 주신 이순환 교수님, 논문의 완성도를 높일 수 있도록 제 논문에 애정을 가지시고 세심하게 지도해주신 김백조 과장님께 깊은 감사드립니다.

학부 때부터 지금까지 오랜 시간동안 지도와 격려를 해주시며 많은 도움을 주신 신인현 교수님, 세월이 흘러도 학부 때나 지금이나 따뜻한 눈길로 바라봐주시며 격려해주시며 항상 도움을 주려하시는 안건상 교수님께도 깊은 감사를 드립니다.

논문이 완성되기까지 친구의 졸업을 기원하며 용기를 북돋아준 임용재와 심재욱, 자료제공에 힘써주고 대학원생활을 같이하며 많은 도움을 준 친형 같은 원효성 선배, 몇 년을 같이 동고동락하며 많은 도움을 받았던 국립기상연구소 모선진, 행정적인 일처리와 논문작성에 많은 도움을 준 황성은, 광주지방기상청을 오가며 자료를 제공해준 김창모, 같은 해에 졸업하며 늦게까지 같이 학교에 남아 공부하며 도움을 요청해도 마다하지 않았던 박진우, 항상 밝은 미소로 대해준 이혜민등 대기과학실험실 모든 분들께 감사드립니다.

항상 아들이 잘되길 바라며 노심초사 마음 써주시며 오랜 시간동안 묵묵히 바라봐 주신 아버지와 어머니, 두 아이를 보살펴 주시고 논문에 집중할 수 있도록 항상 격려해주신 장인어른과 장모님께 감사드리며, 앞으로 더 열심히 사는 아들, 사위의 모습을 보여드리며 노력하고 효도하며 살겠습니다. 남동생을 걱정해주고 이해해주는 누나내외분과 오빠가 해야 할 일을 많이 신경써준 동생내외에게도 미안함과 고마움을 전합니다. 가까이 살면서 항상 친형제처럼 조언을 아끼지 않고 졸업을 하기까지 많은 용기와 격려를 북돋아준 큰형님 내외분에게 고마움을 전하고, 둘째형님 내외분, 막내처제 내외에게도 고마움을 전합니다.

마지막으로, 아빠가 지치고 힘들 때 활력소가 되어 웃음을 잃지 않게 해준 예쁜 우리 딸 희연이와 작년에 귀한 아들로 태어나 아빠의 든든한 지원군이 되어줄 아들 승찬에게도 자랑스러운 아빠가 될 것을 약속합니다. 직장생활과 육아에 신경쓰며 논문준비에 집중 할 수 있도록 도와주고, 결혼 전부터 지금까지 13년여의 긴 시간동안 용기를 잃고 힘들어 할 때 항상 곁에서 응원해주고 격려를 아껴주지 않았던 사랑스런 아내 미연에게 항상 미안하고 고맙게 생각하며, 사랑한다는 말을 전하며 이 글을 마칩니다.